

**NONLINEAR DYNAMICS AND SYSTEMS THEORY**

An International Journal of Research and Surveys

Volume 23                      Number 2                      2023

**CONTENTS**

A DC Algorithm for Solving non-Uniquely Solvable Absolute Value Equations ..... 119  
*N. Anane, Z. Kebaili and M. Achache*

Forecasting of Occupied Rooms in the Hotel Using Linear Support Vector Machine ..... 129  
*M. Y. Anshori, I. H. Santoso, T. Herlambang, D. Rahmalia, K. Oktafanto and P. Katias*

Contact Problem for Thermo-Elasto-Viscoplastic Material with Friction ..... 141  
*N. Bensebaa and N. Lebri*

Implementation of Infeasible Interior-Point Methods Based on a New Search Direction ..... 157  
*L. Derbal*

A Frictional Contact Problem with Wear for Two Electro-Viscoelastic Bodies..... 167  
*A. Djabi*

Global Optimization Method of Multivariate non-Lipschitz Functions Using Tangent Minorants ..... 183  
*Djaouida Guettal, Chahinez Chenouf and Mohamed Rahal*

Analysis of Solutions to Equations with a Generalized Derivative and Delay ..... 195  
*O. D. Kichmarenko, I. V. Chepovskyi, Y. Platonova and S. Dashkovskiy*

Chaos Anti-Synchronization between Fractional-Order Lesser Date Moth Chaotic System and Integer-Order Chaotic System by Nonlinear Control ..... 207  
*M. Labid and N. Hamri*

A New Hidden Attractor Hyperchaotic System and Its Circuit Implementation, Adaptive Synchronization and FPGA Implementation ..... 214  
*R. Rameshbabu, K. Kavitha, P. S. Gomathi and K. Kalaichelvi*

Nonlinear Damped Oscillator with Varying Coefcients and Periodic External Forces..... 227  
*M. Alhaz Uddin, Mahmuda Akhter Nishu and M. Wali Ullah*

NONLINEAR DYNAMICS & SYSTEMS THEORY

Volume 23, No. 2, 2023

# Nonlinear Dynamics and Systems Theory

**An International Journal of Research and Surveys**

**EDITOR-IN-CHIEF A.A.MARTYNYUK**

*S.P.Timoshenko Institute of Mechanics  
National Academy of Sciences of Ukraine, Kiev, Ukraine*

**MANAGING EDITOR I.P.STAVROULAKIS**

*Department of Mathematics, University of Ioannina, Greece*

**REGIONAL EDITORS**

P.BORNE, Lille, France  
 A.OKNIŃSKI, Kielce, Poland  
*Europe*

M.BOHNER, Rolla, USA  
 HAO WANG, Edmonton, Canada  
*USA and Canada*

T.A.BURTON, Port Angeles, USA  
 C.CRUZ-HERNANDEZ, Ensenada, Mexico  
*USA and Latin America*

M.ALQURAN, Irbid, Jordan  
*Jordan and Middle East*

T.HERLAMBANG, Surabaya, Indonesia  
*Indonesia and New Zealand*

Nonlinear Dynamics and Systems Theory  
An International Journal of Research and Surveys

**EDITOR-IN-CHIEF A.A.MARTYNYUK**

The S.P.Timoshenko Institute of Mechanics, National Academy of Sciences of Ukraine,  
Nesterov Str. 3, 03680 MSP, Kiev-57, UKRAINE / e-mail: journalndst@gmail.com

**MANAGING EDITOR I.P.STAVROULAKIS**

Department of Mathematics, University of Ioannina  
451 10 Ioannina, HELLAS (GREECE) / e-mail: ipstav@cc.uoi.gr

**ADVISORY EDITOR A.G.MAZKO,**

Institute of Mathematics of NAS of Ukraine, Kiev (Ukraine)  
e-mail: mazko@imath.kiev.ua

**REGIONAL EDITORS**

M.ALQURAN (Jordan), e-mail: marwan04@just.edu.jo  
P.BORNE (France), e-mail: Pierre.Borne@ec-lille.fr  
M.BOHNER (USA), e-mail: bohner@mst.edu  
T.A.BURTON (USA), e-mail: taburton@olypen.com  
C.CRUZ-HERNANDEZ (Mexico), e-mail: ccruz@cicese.mx  
T.HERLAMBANG (Indonesia), e-mail: teguh@unusa.ac.id  
A.OKNINSKI (Poland), e-mail: fizao@tu.kielce.pl  
HAO WANG (Canada), e-mail: hao8@ualberta.ca

**EDITORIAL BOARD**

Adzkiya, D. (Indonesia)	Kloedon, P. (Germany)
Artstein, Z. (Israel)	Kokologiannaki, C. (Greece)
Awrejcewicz, J. (Poland)	Kouzou, A. (Algeria)
Braiek, N.B. (Tunisia)	Krishnan, E.V. (Oman)
Chen Ye-Hwa (USA)	Limarchenko, O.S. (Ukraine)
De Angelis, M. (Italy)	Lopez Gutierrez R.M. (Mexico)
Denton, Z. (USA)	Peterson, A. (USA)
Djemai, M. (France)	Radziszewski, B. (Poland)
Dshalalow, J.H. (USA)	Shi Yan (Japan)
Gajic Z. (USA)	Sivasundaram, S. (USA)
Georgiev, S.G. (France)	Sree Hari Rao, V. (India)
Georgiou, G. (Cyprus)	Staicu V. (Portugal)
Honglei Xu (Australia)	Vatsala, A. (USA)
Jafari, H. (South African Republic)	Zuyev, A.L. (Germany)
Khusainov, D.Ya. (Ukraine)	

**ADVISORY COMPUTER SCIENCE EDITORS**

A.N.CHERNIENKO and A.S.KHOROSHUN, Kiev, Ukraine

**ADVISORY LINGUISTIC EDITOR**

S.N.RASSHYVALOVA, Kiev, Ukraine

© 2023, InforMath Publishing Group, ISSN 1562-8353 print, ISSN 1813-7385 online, Printed in Ukraine  
No part of this Journal may be reproduced or transmitted in any form or by any means without  
permission from InforMath Publishing Group.

**INSTRUCTIONS FOR CONTRIBUTORS**

**(1) General.** Nonlinear Dynamics and Systems Theory (ND&ST) is an international journal devoted to publishing peer-refereed, high quality, original papers, brief notes and review articles focusing on nonlinear dynamics and systems theory and their practical applications in engineering, physical and life sciences. Submission of a manuscript is a representation that the submission has been approved by all of the authors and by the institution where the work was carried out. It also represents that the manuscript has not been previously published, has not been copyrighted, is not being submitted for publication elsewhere, and that the authors have agreed that the copyright in the article shall be assigned exclusively to InforMath Publishing Group by signing a transfer of copyright form. Before submission, the authors should visit the website:

<http://www.e-ndst.kiev.ua>

for information on the preparation of accepted manuscripts. Please download the archive Sample\_NDST.zip containing example of article file (you can edit only the file Samplefilename.tex).

**(2) Manuscript and Correspondence.** Manuscripts should be in English and must meet common standards of usage and grammar. To submit a paper, send by e-mail a file in PDF format directly to

*Professor A.A. Martynyuk, Institute of Mechanics,  
Nesterov str.3, 03057, MSP 680, Kiev-57, Ukraine  
e-mail: journalndst@gmail.com*

or to one of the Regional Editors or to a member of the Editorial Board. Final version of the manuscript must typeset using LaTeX program which is prepared in accordance with the style file of the Journal. Manuscript texts should contain the title of the article, name(s) of the author(s) and complete affiliations. Each article requires an abstract not exceeding 150 words. Formulas and citations should not be included in the abstract. AMS subject classifications and key words must be included in all accepted papers. Each article requires a running head (abbreviated form of the title) of no more than 30 characters. The sizes for regular papers, survey articles, brief notes, letters to editors and book reviews are: (i) 10-14 pages for regular papers, (ii) up to 24 pages for survey articles, and (iii) 2-3 pages for brief notes, letters to the editor and book reviews.

**(3) Tables, Graphs and Illustrations.** Each figure must be of a quality suitable for direct reproduction and must include a caption. Drawings should include all relevant details and should be drawn professionally in black ink on plain white drawing paper. In addition to a hard copy of the artwork, it is necessary to attach the electronic file of the artwork (preferably in PCX format).

**(4) References.** Each entry must be cited in the text by author(s) and number or by number alone. All references should be listed in their alphabetic order. Use please the following style:

Journal: [1] H. Poincare, Title of the article. *Title of the Journal* **volume**  
(issue) (year) pages. [Language]

Book: [2] A.M. Lyapunov, *Title of the Book*. Name of the Publishers, Town, year.

Proceeding: [3] R. Bellman, Title of the article. In: *Title of the Book*. (Eds.).  
Name of the Publishers, Town, year, pages. [Language]

**(5) Proofs and Sample Copy.** Proofs sent to authors should be returned to the Editorial Office with corrections within three days after receipt. The corresponding author will receive a sample copy of the issue of the Journal for which his/her paper is published.

**(6) Editorial Policy.** Every submission will undergo a stringent peer review process. An editor will be assigned to handle the review process of the paper. He/she will secure at least two reviewers' reports. The decision on acceptance, rejection or acceptance subject to revision will be made based on these reviewers' reports and the editor's own reading of the paper.

# NONLINEAR DYNAMICS AND SYSTEMS THEORY

An International Journal of Research and Surveys  
Published by InforMath Publishing Group since 2001

Volume 23

Number 2

2023

## CONTENTS

A DC Algorithm for Solving non-Uniquely Solvable Absolute Value Equations .....	119
<i>N. Anane, Z. Kebaili and M. Achache</i>	
Forecasting of Occupied Rooms in the Hotel Using Linear Support Vector Machine .....	129
<i>M. Y. Anshori, I. H. Santoso, T. Herlambang, D. Rahmalia, K. Oktafianto and P. Katias</i>	
Contact Problem for Thermo-Elasto-Viscoplastic Material with Friction .....	141
<i>N. Bensebaa and N. Lebri</i>	
Implementation of Infeasible Interior-Point Methods Based on a New Search Direction ...	157
<i>L. Derbal</i>	
A Frictional Contact Problem with Wear for Two Electro-Viscoelastic Bodies .....	167
<i>A. Djabi</i>	
Global Optimization Method of Multivariate non-Lipschitz Functions Using Tangent Minorants .....	183
<i>Djaouida Guettal, Chahinez Chenouf and Mohamed Rahal</i>	
Analysis of Solutions to Equations with a Generalized Derivative and Delay .....	195
<i>O. D. Kichmarenko, I. V. Chepovskyi, Y. Platonova and S. Dashkovskiy</i>	
Chaos Anti-Synchronization between Fractional-Order Lesser Date Moth Chaotic System and Integer-Order Chaotic System by Nonlinear Control .....	207
<i>M. Labid and N. Hamri</i>	
A New Hidden Attractor Hyperchaotic System and Its Circuit Implementation, Adaptive Synchronization and FPGA Implementation .....	214
<i>R. Rameshbabu, K. Kavitha, P. S. Gomathi and K. Kalaichelvi</i>	
Nonlinear Damped Oscillator with Varying Coefficients and Periodic External Forces .....	227
<i>M. Alhaz Uddin, Mahmuda Akhter Nishu and M. Wali Ullah</i>	

*Founded by A.A. Martynyuk in 2001.*

*Registered in Ukraine Number: KB No 5267 / 04.07.2001.*

# NONLINEAR DYNAMICS AND SYSTEMS THEORY

An International Journal of Research and Surveys

*Impact Factor from SCOPUS for 2021: SJR – 0.326, SNIP – 0.601 and CiteScore – 1.5*

**Nonlinear Dynamics and Systems Theory** (ISSN 1562–8353 (Print), ISSN 1813–7385 (Online)) is an international journal published under the auspices of the S.P. Timoshenko Institute of Mechanics of National Academy of Sciences of Ukraine and Curtin University of Technology (Perth, Australia). It aims to publish high quality original scientific papers and surveys in areas of nonlinear dynamics and systems theory and their real world applications.

## AIMS AND SCOPE

**Nonlinear Dynamics and Systems Theory** is a multidisciplinary journal. It publishes papers focusing on proofs of important theorems as well as papers presenting new ideas and new theory, conjectures, numerical algorithms and physical experiments in areas related to nonlinear dynamics and systems theory. Papers that deal with theoretical aspects of nonlinear dynamics and/or systems theory should contain significant mathematical results with an indication of their possible applications. Papers that emphasize applications should contain new mathematical models of real world phenomena and/or description of engineering problems. They should include rigorous analysis of data used and results obtained. Papers that integrate and interrelate ideas and methods of nonlinear dynamics and systems theory will be particularly welcomed. This journal and the individual contributions published therein are protected under the copyright by International InforMath Publishing Group.

## PUBLICATION AND SUBSCRIPTION INFORMATION

**Nonlinear Dynamics and Systems Theory** will have 5 issues in 2023, printed in hard copy (ISSN 1562–8353) and available online (ISSN 1813–7385), by InforMath Publishing Group, Nesterov str., 3, Institute of Mechanics, Kiev, MSP 680, Ukraine, 03057. Subscription prices are available upon request from the Publisher, EBSCO Information Services (<mailto:journals@ebSCO.com>), or website of the Journal: <http://e-ndst.kiev.ua>. Subscriptions are accepted on a calendar year basis. Issues are sent by airmail to all countries of the world. Claims for missing issues should be made within six months of the date of dispatch.

## ABSTRACTING AND INDEXING SERVICES

Papers published in this journal are indexed or abstracted in: Mathematical Reviews / MathSciNet, Zentralblatt MATH / Mathematics Abstracts, PASCAL database (INIST–CNRS) and SCOPUS.



# A DC Algorithm for Solving non-Uniquely Solvable Absolute Value Equations

N. Anane\*, Z. Kebaili and M. Achache

*Fundamental and Numerical Mathematics Laboratory, Ferhat Abbas University,  
Setif 1, Setif 19000, Algeria.*

Received: January 19, 2023; Revised: March 20, 2023

**Abstract:** In this paper, we deal with the solution of non-uniquely solvable absolute value equations (AVE) of the form  $Ax - B|x| = b$ , where  $A, B \in \mathbb{R}^{n \times n}$  and  $b \in \mathbb{R}^n$ . To do so, a non-convex quadratic optimization is considered, where its first-order optimality conditions are reduced to AVEs. Therefore, solving the AVE is equivalent to computing the local minimum of the non-convex quadratic optimization. Next, by exploiting the technique of DC programming, a reformulation of the latter as a DC program is presented. The resulting DC algorithm (DCA) is simple and consists of solving a successive linear system of equations. Numerical experiments on some non-uniquely solvable AVE problems are given to illustrate the efficiency of this approach.

**Keywords:** *absolute value equations; DC programming; linear system; nonlinear modes; nonlinear systems in control theory.*

**Mathematics Subject Classification (2010):** 90C50, 90C33, 14C20, 70K75, 93C10.

## 1 Introduction

In this paper, we consider the absolute value equation (AVE) of the form

$$Ax - B|x| = b, \quad (1)$$

where  $A, B \in \mathbb{R}^{n \times n}$ ,  $b, x \in \mathbb{R}^n$  and  $|x|$  denotes the component-wise absolute value of the vector  $x$ . When  $B = I$ , the AVE (1) reduces to a special form

$$Ax - |x| = b. \quad (2)$$

---

\* Corresponding author: <mailto:nasimaannan@gmail.com>.

In the last years, the AVEs have become an interesting topic of research in the domain of mathematical programming and applied sciences. For instance, linear complementarity problems, bi-matrix games and equilibrium problems, and the hydrodynamic equation can be reformulated as AVE (1) [4, 7, 9]. For the existence and uniqueness of solutions of AVE (1) and (2), many results are stated based on different assumptions most of which are made on matrices  $A$  and  $B$ . Besides, various numerical methods have been developed for solving efficiently the uniquely solvable AVEs (see eg. [1, 2, 5, 8, 10, 13, 17] and the references therein).

The present work deals with AVE (1) that is not necessarily uniquely solvable, i.e., it has more than one solution. For that, a non-convex quadratic optimization is considered and its first-order optimality conditions are reduced to AVE (1). Therefore, finding a solution of AVE (1) is equivalent to computing a local minimum of the corresponding non-convex quadratic optimization. Next, by exploiting the idea of DC programming and DC Algorithm (DCA) for non-convex optimization [11, 14, 15], we propose a simple and efficient iterative method for solving the AVE (1) by its non-convex quadratic optimization. Hence, a suitable DC decomposition of the DC program is proposed for which the DC algorithm is applied. Numerical results are reported by some examples of solvable AVE (1) that can have either a unique solution or many solutions.

At the end of this section, some notations used in the paper are as follows. The scalar product of two vectors  $x$  and  $y$  in  $\mathbb{R}^n$  is denoted by  $\langle x, y \rangle = x^T y$ . For  $x \in \mathbb{R}^n$ , the norm  $\|x\|$  will denote the Euclidean norm  $(x^T x)^{1/2}$  and  $sign(x)$  will denote a vector with components equal to  $+1, 0$  or  $-1$ , depending on whether the corresponding component of  $x$  is positive, zero or negative, respectively. In addition,  $D := \partial|x| = \text{Diag}(sign(x))$  ( $D$  is a diagonal matrix corresponding to  $sign(x)$ ), where  $\partial|x|$  represents the generalized Jacobian of  $|x|$  based on the sub-gradient.  $\lambda_{\max}(A)$  stands for the maximal eigenvalue of a matrix  $A$ . The vector of one is denoted by  $e$  and the matrix  $A$  is positive semi-definite if  $x^T A x \geq 0$  for any  $x \in \mathbb{R}^n$ . Finally,  $\|A\| := \max \{\|Ax\| : x \in \mathbb{R}^n, \|x\| = 1\}$  denotes the induced norm of  $A$ .

The paper is organized as follows. In Section 2, a quadratic formulation of the AVE (1) is presented. The equivalence of its first optimality conditions to AVE (1) is shown, where any local minimum of the latter is a solution of the AVE. In Section 3, a brief outline of DC programming and the DCA is given. The DCA for this formulation is discussed. In Section 4, some numerical results are reported. A conclusion and future work outlook end Section 5.

## 2 Quadratic Formulation of AVE

In this section, we present a quadratic formulation of the AVE (1). It states that when  $A$  and  $B$  are given arbitrary matrices, the AVE (1) is equivalent to the first-order optimality conditions of the following unconstrained quadratic optimization problem:

$$\min_{x \in \mathbb{R}^n} q(x) = \frac{1}{2} \langle Ax - B|x|, x \rangle - \langle b, x \rangle \quad (3)$$

or, equivalently,

$$\min_{x \in \mathbb{R}^n} q(x) = \frac{1}{2} \langle Cx - F|x|, x \rangle - \langle b, x \rangle,$$

where  $C = A^T + A$ ,  $F = B^T + B$  are symmetric matrices, and  $q(x)$  is the quadratic objective function of (3). Indeed, if  $x$  satisfies the first-order optimality conditions of

problem (3), then we have  $\nabla q(x) = Ax - B|x| - b = 0$ . It follows that any local minimum of (3) is a solution of the AVE (1). In the case where  $q$  is convex, any local minimum is global. Consequently, any unique solution of AVE (1) is a global minimum of (3).

### 3 Outline of DC Programming and DCA (Algorithm)

In general, a DC program takes the form

$$\alpha = \inf_{x \in \mathbb{R}^n} (q(x) = g(x) - h(x)) (P_{dc}),$$

where  $g, h$  are proper lower semi-continuous and convex functions on  $\mathbb{R}^n$ . The function  $q$  is called a DC function, and  $g - h$  is a DC decomposition of  $q$ , while  $g$  and  $h$  are the DC components of  $q$ .

A point  $x^*$  is called a critical point of  $g - h$  or a generalized Karush-Kuhn-Tucker (KKT) point of  $P_{dc}$  (3) if

$$\partial h(x^*) \cap \partial g(x^*) = \emptyset,$$

where  $\partial\phi(x)$  denotes the sub-differential of  $\phi(x)$  at the point  $x$ . Based on local optimality conditions and duality in DC programming, the DCA generates two sequences  $\{x^k\}$  and  $\{y^k\}$  in the primal and its dual, respectively. Each iteration  $k$  of DCA approximates the concave part of  $-g$  by its affine majorization (that corresponds to taking  $y^k \in \partial h(x^k)$ ) and minimizing the resulting convex function (that is equivalent to determining a point  $x^{k+1} \in \partial g^*(y^k)$  (or  $y^k \in \partial g(x^{k+1})$ )) with  $g^*$  being the conjugate function of  $g$ . The generic form of a DC algorithm is stated as follows.

#### 3.1 Generic DCA scheme

Initialization: Let  $x^0 \in \mathbb{R}^n$  be a starting point,  $k := 0$ ;  
 Repeat.  
 Calculate  $y^k \in \partial h(x^k)$ ;  
 Calculate  $x^{k+1} \in \partial g^*(y^k) \Rightarrow y^k \in \partial g(x^{k+1})$ ;  
 $k := k + 1$ ;  
 Until convergence of  $\{x^k\}$ .

We note that the convergence properties of DCA (Algorithm) can be found in details in [14].

### 4 Proposed DC Decompositions

Let  $\rho > 0$  be such that  $g$  and  $h$  are convex. In this paper, we adopt the following DC decomposition of  $q(x)$ :

$$q(x) = g(x) - h(x). \tag{4}$$

#### 4.1 DCA for AVE

The DC decomposition of the objective function  $q(x)$  is given by

$$g(x) = \frac{1}{2}x^T(A + \rho I)x \text{ and } h(x) = \frac{1}{2}(x^T(BD + \rho I)x) + x^T b$$

with  $D(x)x = |x|$ . Then the problem (4) is a DC program in the standard form

$$\min_{x \in \mathbb{R}^n} \{g(x) - h(x)\}.$$

Following the generic DCA scheme and its properties, we detail the ingredients of the DC algorithm for solving AVE (1).

- An initial point  $x^0 \in \mathbb{R}^n$ .
- Computation of  $y^k$ . We have

$$y^k \in \partial h(x^k) = \{\nabla h(x^k)\} = \{(\rho I + BD(x^k))x^k + b\}.$$

Then

$$y^k = (\rho I + BD(x^k))x^k + b. \quad (5)$$

- Computation of  $x^{k+1}$ . We have

$$x^{k+1} \in \partial g^*(y^k) \Rightarrow y^k \in \partial g(x^{k+1}) = \{\nabla g(x^{k+1})\} = \{(A + \rho I)x^{k+1}\}.$$

Hence

$$y^k = (A + \rho I)x^{k+1}. \quad (6)$$

Consequently, due to (5) and (6), we deduce that the DC algorithm is based only on solving the following linear system to obtain at each iteration  $k$ ,  $x^{k+1}$ :

$$(A + \rho I)x^{k+1} = (\rho I + BD(x^k))x^k + b. \quad (7)$$

- Choice of  $\rho$ . The choice of the parameter  $\rho$  is based on the fact that  $g$  and  $h$  in (4) are convex functions. This is equivalent to obtaining for what suitable values of  $\rho$ , the Hessian matrices

$$\nabla^2 g(x) = A + \rho I \text{ and } \nabla^2 h(x) = \rho I + BD$$

are positive semi-definite (PSD) for any matrix  $D$  whose elements are  $\pm 1$  or  $0$ . The matrix  $\nabla^2 h(x)$  is a generalized Hessian caused by the non-differentiability of the absolute value function  $|x|$ . We have  $\nabla^2 g(x)$  is PSD if  $v^T(A + \rho I)v \geq 0$  for any vector  $v \in \mathbb{R}^n$ . By the Cauchy-Schwartz inequality, it follows that

$$v^T(A + \rho I)v \geq \rho v^T v - \|A\| \|v\|^2 = (\rho - \|A\|) \|v\|^2.$$

Hence  $(A + \rho I)$  is PSD if  $(\rho - \|A\|) \geq 0$ . Therefore, it suffices to take  $\rho \geq \|A\|$  such that  $\nabla^2 g(x)$  is PSD and so  $g$  is convex. Now, according to the linear system (7), the matrix  $(A + \rho I)$  must be invertible to ensure the uniqueness of solution of the latter. Therefore, we require only the values of  $\rho$  which provide the positive definiteness of this matrix, i.e.,  $\rho > \|A\|$ .

In a similar way,  $\nabla^2 h(x)$  is PSD for any diagonal matrix  $D$  whose elements are  $\pm 1$  or  $0$  if  $v^T(\rho I + BD)v \geq 0$  for any  $v \in \mathbb{R}^n$ . Also, by the Cauchy-Schwartz inequality, we get

$$v^T(\rho I + BD)v \geq \rho v^T v - \|B\| \|D\| \|v\|^2 \geq (\rho - \|B\|) \|v\|^2, \quad \forall v \in \mathbb{R}^n.$$

Hence,  $(\rho I + BD)$  is PSD for all diagonal matrix  $D$  whose elements are  $\pm 1$  or  $0$  if  $(\rho - \|B\|) \geq 0$ . So, it suffices to take  $\rho \geq \|B\|$  such that  $(\rho I + BD)$  is PSD. Finally, to guarantee that  $g$  and  $h$  are convex, we take  $\rho$  as follows:

$$\rho \geq \rho_{\min} = \max(\|A\|, \|B\|).$$

**Remark 4.1** When  $A$  and  $B$  are symmetric matrices,  $\rho$  is taken as follows:

$$\rho \geq \rho_{\min} = \max(|\lambda_{\max}(A)|, |\lambda_{\max}(B)|).$$

Now, according to (7), the DCA for solving AVE (1) is presented in Figure 1 as follows.

**Step 0.**  
 A precision  $\epsilon > 0$ ;  
 a starting point  $x^0 \in \mathbb{R}^n$ , a parameter  $\rho \geq \rho_{\min}$ , set  $k := 0$ ;  
 for  $k = 0, 1, \dots$   
**Step 1.** Compute  $x^{k+1}$  the unique solution of the system (7);  
 If the relative residue  $\text{RSD} := \frac{\|x^{k+1} - x^k\|}{1 + \|b\|} \leq \epsilon$ ,  
 then stop and  $x^{k+1}$  is an approximated solution;  
 If not, set  $k := k + 1$  and go to **Step 1**.

Figure 1. DC Algorithm for the AVE (1).

### 4.2 Numerical experiments

In this section, we implement the DC algorithm on **MATLAB** and run it on three examples of solvable AVE (1). We denote by  $x^0$  the initial point in the algorithm and  $x^*$  is the true solution of the AVE (1). In the tables of the obtained numerical results, (Iter) represents the number of iterations produced by the algorithm and CPU(s) is the elapsed time. In all our implementation, we set  $\epsilon = 10^{-6}$ . However, the value of  $\rho > 0$  is taken such that  $\rho \geq \rho_{\min}$ , which ensures the convexity of functions  $g$  and  $h$  as well the uniqueness of solution of system (7). Our stopping criterion is the residual relative error  $\text{RSD} := \frac{\|x^{k+1} - x^k\|}{1 + \|b\|}$ .

**Problem 1.** Consider the AVE, where  $A$  and  $B$  are symmetric matrices:

$$A = \begin{bmatrix} 0 & 1 & 2 \\ 1 & 3 & 1 \\ 2 & 1 & 0 \end{bmatrix}, \quad B = \begin{bmatrix} 2 & -1 & -2 \\ -1 & -1 & -1 \\ -2 & -1 & 2 \end{bmatrix}, \quad b = [-1, 2, -1]^T.$$

In this example, two initial points are taken as  $x_1^0 = [0, 0, 0]^T$  and  $x_2^0 = [0.8, 0.8, 0.8]^T$ . The iterations number, the CPU(s) times and the RSD for our obtained numerical results are stated in Table 1.

$\rho \downarrow$	$x_1^0$			$x_2^0$		
	Iter	CPU(s)	RSD	Iter	CPU(s)	RSD
0.8	18	0.006220	$6.2374e - 007$	18	0.005908	$7.4684e - 007$
2.5	20	0.006584	$4.5457e - 007$	20	0.005955	$8.3400e - 007$
3	22	0.005967	$6.5456e - 007$	23	0.005950	$5.5641e - 007$
$\rho_{\min}$	25	0.010668	$5.6823e - 007$	26	0.010063	$4.6759e - 007$
10	45	0.006927	$8.1837e - 007$	55	0.008193	$8.7384e - 007$

Table 1.

This example of the AVE has at least two solutions, namely,

$$x_1^* = [-1, 0.5, -1]^T \text{ and } x_2^* = \left[ \frac{2}{3}, \frac{1}{6}, -2 \right]^T.$$

**Problem 2.** In this example of AVEs, the matrices  $A$  and  $B$  are not symmetric and sparse, where

$$A = \begin{bmatrix} -5 & 0 & 0 & \cdots & 0 & 0 \\ 0 & 10 & 0 & \cdots & 0 & 0 \\ 0 & 0 & 10 & \cdots & 0 & \vdots \\ \vdots & \vdots & \ddots & \ddots & 0 & 0 \\ 0 & 0 & 0 & \cdots & 10 & 0 \\ 0 & 0 & \cdots & 0 & 1 & 10 \end{bmatrix}$$

and

$$B = \begin{bmatrix} 10 & 0 & 0 & \cdots & 0 & 0 \\ 0 & 10 & 0 & \cdots & 0 & 0 \\ 0 & 0 & 10 & \cdots & 0 & \vdots \\ \vdots & \vdots & \ddots & \ddots & 0 & 0 \\ 0 & 0 & 0 & \cdots & 10 & 0 \\ 0 & 0 & \cdots & 0 & 12 & 3 \end{bmatrix}.$$

For  $b = [-15, -20, \dots, -20, -26]^T$ , this example of the AVE admits at least two solutions, namely,

$$x_1^* = [1, -1, \dots, -1]^T \text{ and } x_2^* = [-3, -1, \dots, -1]^T.$$

The initial point is taken as

$$x^0 = [0, -0.5, \dots, -0.5]^T.$$

Then the obtained numerical results with different size of  $n$  are shown in Table 2.

Size $n$		$\rho_{\min}$	20	100
100	iter	8	22	125
	CPU(s)	0.033798	0.075531	0.188725
	RSD	$7.4215e-007$	$9.9621e-007$	$9.6155e-007$
1500	iter	7	19	100
	CPU(s)	5.151696	13.954670	72.055416
	RSD	$5.5016e-007$	$8.7237e-007$	$9.6398e-007$
3000	iter	7	18	93
	CPU(s)	37.860998	95.470970	495.417176
	RSD	$3.8919e-007$	$9.2569e-007$	$9.9564e-007$
4000	iter	6	18	91
	CPU(s)	93.784429	258.326851	1381.492980
	RSD	$9.6312e-007$	$8.0178e-007$	$9.6084e-007$

**Table 2.**

For  $b = [-15, 0, \dots, 0, 0]^T$ , this example of the AVE admits at least two solutions, namely,

$$x_1^* = [1, 0.5, \dots, 0.5, 0.7857]^T \text{ and } x_2^* = [-3, 0, \dots, 0]^T.$$

Our starting point in the algorithm for this example is taken as

$$x^0 = [0, -0.5, \dots, -0.5, -0.5]^T.$$

The obtained numerical results with different size of  $n$  are shown in Table 3.

Size $n$		$\rho_{\min}$	20	100
100	iter	21	30	172
	CPU(s)	0.096385	0.075766	0.220155
	RSD	$7.6245e - 007$	$9.9112e - 007$	$9.5277e - 007$
1500	iter	21	30	172
	CPU(s)	18.841956	21.227324	123.081425
	RSD	$7.6245e - 007$	$9.9112e - 007$	$9.5277e - 007$
3000	iter	21	30	172
	CPU(s)	116.801005	154.224982	882.412729
	RSD	$7.6245e - 007$	$9.9112e - 007$	$9.5277e - 007$
4000	iter	21	30	172
	CPU(s)	294.215091	415.582267	2381.140220
	RSD	$7.6245e - 007$	$9.9112e - 007$	$9.5277e - 007$

**Table 3.**

Next, we deal with two examples of the AVEs which have a unique solution (see [2, 3, 5]).

**Problem 3.** Consider the AVE, where

$$A = \begin{bmatrix} -100 & 10 & 0 & \dots & 0 & 0 \\ 10 & -100 & 10 & \dots & 0 & 0 \\ 0 & 10 & -100 & \dots & 0 & \vdots \\ \vdots & \vdots & \ddots & \ddots & 10 & 0 \\ 0 & 0 & 0 & \dots & -100 & 10 \\ 0 & 0 & \dots & 0 & 10 & -100 \end{bmatrix},$$

and

$$B = \begin{bmatrix} -1 & 0.1 & 0 & \dots & 0 & 0 \\ 0.1 & -1 & 0.1 & \dots & 0 & 0 \\ 0 & 0.1 & -1 & \dots & 0 & \vdots \\ \vdots & \vdots & \ddots & \ddots & 0.1 & 0 \\ 0 & 0 & 0 & \dots & -1 & 0.1 \\ 0 & 0 & \dots & 0 & 0.1 & -1 \end{bmatrix}, \quad b = (A - I)e.$$

The numerical results with different size of  $n$  and with the initial point

$$x^0 = [0.1, \dots, 0.1]^T$$

are shown in Table 4.

Size $n$		$\rho_{\min}$	10	35
100	iter	3	6	37
	CPU(s)	0.013635	0.009922	0.044977
	RSD	$3.1876e - 009$	$4.9863e - 007$	$9.8002e - 007$
1500	iter	2	6	38
	CPU(s)	4.078783	5.753656	34.767854
	RSD	$4.2391e - 007$	$5.0486e - 007$	$7.7765e - 007$
3000	iter	2	6	38
	CPU(s)	30.693572	39.979472	259.846648
	RSD	$2.9980e - 007$	$5.0511e - 007$	$7.7887e - 007$
4000	iter	2	6	38
	CPU(s)	70.940271	95.628900	605.623886
	RSD	$2.5965e - 007$	$5.0518e - 007$	$7.7918e - 007$

**Table 4.**

Now, with and without spacing other initial point  $x^0 = [1, 2, \dots, n]^T$ , the numerical results are shown in Table 5.

Size $n$		$\rho_{\min}$	10	35
100	iter	3	8	53
	CPU(s)	0.022255	0.011792	0.055950
	RSD	$2.4503e - 007$	$6.1149e - 007$	$9.6970e - 007$
1500	iter	3	10	64
	CPU(s)	5.803212	8.905991	58.258065
	RSD	$9.5316e - 007$	$1.8358e - 007$	$9.9229e - 007$
3000	iter	4	10	67
	CPU(s)	44.731209	71.126180	458.376902
	RSD	$3.3368e - 009$	$3.7840e - 007$	$9.3035e - 007$
4000	iter	4	10	68
	CPU(s)	113.000257	156.209290	1065.611029
	RSD	$3.8532e - 009$	$5.0839e - 007$	$9.6915e - 007$

**Table 5.**

This example is uniquely solvable and for  $b = (A - I)e$ , the solution is

$$x^* = [1.0215, 1.0226, 1.0227, \dots, 1.0227, 1.0226, 1.0215]^T.$$

**Problem 4.** Consider the AVE, where

$$A = \begin{bmatrix} -25,5 & -2,5 & 0 & \dots & 0 & 0 \\ -2,5 & -25,5 & -2,5 & \dots & 0 & 0 \\ 0 & -2,5 & -25,5 & \dots & 0 & \vdots \\ \vdots & \vdots & \ddots & \ddots & -2,5 & 0 \\ 0 & 0 & 0 & \dots & -25,5 & -2,5 \\ 0 & 0 & \dots & 0 & -2,5 & -25,5 \end{bmatrix},$$

and

$$B = \begin{bmatrix} 0,6 & -0,01 & 0 & \cdots & 0 & 0 \\ -0,01 & 0,6 & -0,01 & \cdots & 0 & 0 \\ 0 & -0,01 & 0,6 & \cdots & 0 & \vdots \\ \vdots & \vdots & \ddots & \ddots & -0,01 & 0 \\ 0 & 0 & 0 & \cdots & 0,6 & -0,01 \\ 0 & 0 & \cdots & 0 & -0,01 & 0,6 \end{bmatrix}, \quad b = (A - I) e.$$

The numerical results with different size of  $n$  and with the starting point

$$x^0 = [1, 2, \dots, n]^T,$$

are summarized in Table 6.

Size $n$		$\rho_{\min}$	0.1	9
100	iter	6	5	50
	CPU(s)	0.025191	0.011119	0.056285
	RSD	$8.3305e - 008$	$2.2208e - 007$	$8.6286e - 007$
1500	iter	6	6	55
	CPU(s)	7.978099	5.531777	51.736639
	RSD	$1.7720e - 007$	$9.9349e - 008$	$9.0413e - 007$
3000	iter	6	6	56
	CPU(s)	57.503325	39.353990	370.091181
	RSD	$2.7508e - 007$	$2.0998e - 007$	$9.3224e - 007$
4000	iter	6	6	57
	CPU(s)	132.305173	93.222723	942.398052
	RSD	$3.4085e - 007$	$2.4286e - 007$	$8.3854e - 007$

**Table 6.**

This example has a unique solution if  $\sigma_{\min}(A) > \sigma_{\max}(B)$  in  $[2, 3, 5]$  given by

$$x^* = [1.0144, 1.0134, 1.0135, \dots, 1.0135, 1.0134, 1.0144]^T.$$

### 5 Concluding Remarks

In this paper, we have used the technique of DC programming for solving absolute value equations. For that, a quadratic optimization is considered, where its first-order optimality conditions are equivalent to the AVE (1) and where any local minimum of the quadratic problem is a solution of the AVE. Further, based on a suitable decomposition of the objective function  $q(x)$ , we have designed a simple DC algorithm for solving the AVE (1). Numerical results illustrate that the DC algorithm is efficient for solving some solvable AVE problems that can have either one unique solution or many solutions. A good topic of research in the future is suggesting other DC decompositions of the objective  $q(x)$  in order to design other DC algorithms for solving the AVE (1).

Our results have a great importance in application such as the solution of a linear complementarity problem including the linear and convex quadratic optimization, bimatrix games, interval matrix, hydrodynamic equation.

### Acknowledgment

This work has been supported by: La Direction Générale de la Recherche Scientifique et du Développement Technologique (DGRSDT-MESRS), under project PRFU number C00L03UN190120190004. Algérie.

### References

- [1] L. Abdellah, M. Haddou and T. Migot. Solving absolute value equations using complementarity and smoothing functions. *Journal of Computational and Applied Mathematics* **327** (2018) 196–207.
- [2] M. Achache. On the unique solvability and numerical study of absolute value equations. *J. Numer. Anal. Approx. Theory* **48** (2) (2019) 112–121.
- [3] M. Achache and N. Anane. On unique solvability and Picard’s iterative method for absolute value equations. *Bulletin of the Transilvani aUniversity of Brasov* **1(63)** (1) (2021) 13–26.
- [4] M. Achache. Complexity analysis and numerical implementation of a short-step primal-dual algorithm for linear complementarity problems. *Applied Mathematics and computation.* **216** (2010) 1889–1895.
- [5] M. Achache and N. Hazzam. Solving absolute value equations via complementarity and interior-point methods. *Journal of Nonlinear Functional Analysis.* **2018** (1) (2018) 1–10.
- [6] N. Anane and M. Achache. Preconditioned conjugate gradient methods for absolute value equations. *J. Numer. Anal. Approx. Theory* **48** (1) (2020) 3–14.
- [7] A. Yu. Aleksandrov. Delay-Independent Stability Conditions for a Class of Nonlinear Mechanical Systems. *Nonlinear Dynamics and Systems Theory* **21** (5) (2021) 447–456.
- [8] L. Caccetta, B. Qu and G. Zhou. A globally and quadratically convergent method for absolute value equations. *Computational Optimization and Applications* **48** (1) (2011) 45–58.
- [9] R.W. Cottle, J.S. Pang and R.E. Stone. *The linear Complementarity Problem.* Academic Press, New-York, 1992.
- [10] M. Hladik. Bounds for the solution of absolute value equations. *Computational Optimization and Applications* **69** (1) (2018) 243–266.
- [11] Z. Kebaili and M. Achache. Solving non monotone affine variational inequalities problem by DC programming and DCA. *Asian-European Journal of Mathematics* **13** (1) (2020) 2050067 (8 pages).
- [12] O.L. Mangasarian and R.R. Meyer. Absolute value equations. *Linear Algebra and Applications.* **419** (2-3) (2006) 359–367.
- [13] O.L. Mangasarian. A generalized Newton method for absolute value equation. *Optimization Letters* **3** (1) (2009) 101–108.
- [14] T. Pham Dinh and H.A. Le Thi. Convex analysis approach to dc programming. Theory, algorithms and applications. *Acta Math. Vietnam* **22** (1) (1997) 289–355.
- [15] T. Pham Dinh and H.A. Le Thi. A DC optimization algorithm for solving the trust-region subproblem. *SIAM Journal on Optimization* **8** (2) (1998) 476–505.
- [16] J. Rohn. On unique solvability of the absolute value equations. *Optimization Letters* (3) (2009) 603–606.
- [17] J. Rohn. An algorithm for computing all solutions of an absolute value equation. *Optimization Letters* (6) (2012) 851–856.



## Forecasting of Occupied Rooms in the Hotel Using Linear Support Vector Machine

M. Y. Anshori<sup>1</sup>, I. H. Santoso<sup>2\*</sup>, T. Herlambang<sup>3</sup>, D. Rahmalia<sup>4</sup>,  
K. Oktafianto<sup>5</sup>, and P. Katias<sup>1</sup>

<sup>1</sup> Department of Management, University Nahdlatul Ulama Surabaya, Indonesia.

<sup>2\*</sup> Department of Accounting Magister, University of Wijaya Kusuma, Surabaya, Indonesia.

<sup>3</sup> Department of Information System, University Nahdlatul Ulama Surabaya, Indonesia.

<sup>4</sup> Department of Mathematics, University of Islam Darul Ulum, Lamongan, Indonesia.

<sup>5</sup> Department of Mathematics, University of PGRI Ronggolawe, Tuban, Indonesia.

Received: October 6, 2022; Revised: April 2, 2023

**Abstract:** The hotel business is one of the important sectors in the tourism industry because it has a multiplier effect in social life and economics. Nowadays, the room reservation in hotels is more flexible so that the guests can extend or cancel their stay easily due to the development of technology. Based on the report on the number of room reservations, everyday, there are differences in the number of occupied rooms, so it is required that a forecasting in daily data be made. Forecasting is very important for the hotel management because it is affecting all hotel operations such as staff manning, amenities preparation, breakfast preparation, linen preparation to provide customer satisfaction. Customer satisfaction is a critical component of profitability [1]. The number of occupied rooms depends on in-house guests, same day reservation, extension of stay, early departure, today's cancellation, and walk-in. In this research, the classification method applied is the linear Support Vector Machine (SVM). The linear SVM uses the best hyperplane as a separator between two classes. In this method, we divide the dataset of guest reservation into training data and testing data in various proportions. Then the set of support vectors can be determined by the sequential programming method and we can test them in testing data. Based on simulation with various proportions of training data and testing data, the linear SVM can classify occupied rooms based on guest reservation with a good accuracy, error rate, recall, specificity, and precision.

**Keywords:** *classification; Support Vector Machine; pattern recognition; data mining*

**Mathematics Subject Classification (2010):** 68T45, 68T10.

---

\* Corresponding author: [mailto:ismanto\\_fe@uwks.ac.id](mailto:ismanto_fe@uwks.ac.id)

## 1 Introduction

Travelling is the activity which is often done by people when they also are looking for a hotel for a temporary stay. The hotel business is one of the important sectors in the tourism industry because it has a multiplier effect in social life and economics. Based on online hotel reservation sites, the purpose of booking a hotel is for a holiday, business, romance, or medical cure.

Nowadays, the room reservation in a hotel is more flexible so that the guests can extend or cancel their stay due to the development of technology. Based on the report on the number of room reservations, everyday, there are differences in the number of occupied rooms so that it is required that a forecasting in daily data be made. Forecasting is very important for the hotel management because it is affecting all hotel operations such as staff manning, amenities preparation, breakfast preparation, linen preparation to provide customer satisfaction. Moreover, customer satisfaction is also affecting the hotel performance, it is one of the measurements of the success of the hotel management in managing the hotel with all resources that they have [2]. The number of occupied rooms depends on in-house guests, same day reservation, extension of stay, early departure, today's cancellation, and walk-in. Using these variables, we can calculate the number of occupied rooms in a hotel. Based on the number of occupied rooms per day, they will be divided into two classes, i.e., the class where the number of occupied rooms is higher than its average and the other, where the number of occupied rooms is lower than its average.

In this research, there is a method for classifying the occupied rooms in a hotel, called the Support Vector Machine (SVM). The SVM uses the best hyperplane as a separator between two classes on input space [3]. This method has many applications in the classification of objects [4] or diagnosing the disease [5]. In this method, we divide the dataset of guest reservation into training data and testing data in various proportions. For training data, an optimization model of SVM is formed for determining the support vectors. After the set of support vectors can be determined by the sequential programming method [6], [7], we can test them in testing data.

In the previous researches, some clustering methods have been used, namely, clustering by the Kohonen Network in clustering airports [8] and clustering by the K-Means and Fuzzy Clustering Means in agriculture production [9]. Besides clustering, there are forecasting methods. The applications of a Neural Network have been used in forecasting by Backpropagation (BP) for forecasting of weather [10], estimation of AUV [11], [12], [13], estimation of the Vibrating Rod [14], estimation of disease spread [15], [16], forecasting of air temperature [17] and the Adaptive Neuro Fuzzy Inference System (ANFIS) in forecasting of humidity [18] or forecasting of sunlight intensity [19]. The forecasting methods are also applied by the Kalman Filter in stock price estimation [20], forefinger motion estimation [21], mobile robot estimation [22] and estimation of closed hotels and restaurants [23], [24], [25].

Based on simulation with various proportions of training data and testing data, the linear SVM can classify occupied rooms based on guest reservation with a good accuracy, error rate, recall, specificity, and precision.

## 2 Support Vector Machine (SVM)

Support Vector Machine (SVM) was introduced by Vapnik in 1992. SVM uses the best hyperplane as a separator between two classes on input space. The hyperplane can be determined by measuring the margin and optimizing the maximum point. The margin is the distance between the hyperplane and the closest pattern from each class. The closest pattern to the hyperplane is called the support vector. The illustration of SVM can be seen in Figure 1, with the red circle patterns being the class  $-1$ , blue square patterns being the class  $+1$  and the hyperplane between them [3].

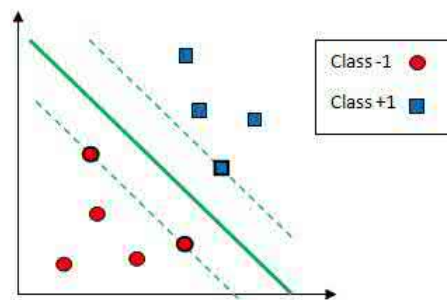


**Figure 1:** Support Vector Machine (SVM) Model.

Let  $x_1, x_2, \dots, x_n$  be the number of data and  $y_1, y_2, \dots, y_n \in -1, 1$  be the classes of  $x_1, x_2, \dots, x_n$ , respectively. The optimization model of SVM is the maximizing margin  $m$  with  $m = \frac{2}{\|w\|}$  subject to  $y_i (w^T x_i + b) \geq 1, i = 1, 2, \dots, n$ , so that the optimization model becomes

$$\min \frac{1}{2} \|w\|^2 \tag{1}$$

subject to

$$y_i (w^T x_i + b) \geq 1, \quad i = 1, 2, \dots, n. \tag{2}$$

In the constrained optimization above, we need to construct the Lagrange equation in equation (3) for optimizing the value of  $w, \alpha, b$ ,

$$L = \frac{1}{2} w^T w + \sum_{i=1}^n \alpha_i (1 - y_i (w^T x_i + b)). \tag{3}$$

For optimizing the value of  $w, \alpha, b$ , the first differential of the Lagrange equation will be used,

$$\begin{aligned} \frac{\partial L}{\partial w} &= w - \sum_{i=1}^n \alpha_i y_i x_i = 0, \\ w &= \sum_{i=1}^n \alpha_i y_i x_i, \end{aligned} \tag{4}$$

$$\frac{\partial L}{\partial b} = - \sum_{i=1}^n \alpha_i y_i = 0. \tag{5}$$

Substitute  $w = \alpha_i y_i x_i$  and  $-\sum_{i=1}^n \alpha_i y_i = 0$  into the Lagrange equation

$$\begin{aligned} L &= \frac{1}{2} (\alpha_i y_i x_i)^T (\alpha_i y_i x_i) + \sum_{i=1}^n \alpha_i (1 - y_i (w^T x_i + b)), \\ L &= -\frac{1}{2} \sum_{i=1}^n \sum_{j=1}^n \alpha_i \alpha_j y_i y_j x_i^T x_j + \sum_{i=1}^n \alpha_i \end{aligned} \quad (6)$$

so that the optimization model becomes

$$\begin{aligned} W(\alpha) &= \sum_{i=1}^n \alpha_i - \frac{1}{2} \sum_{i=1}^n \sum_{j=1}^n \alpha_i \alpha_j y_i y_j x_i^T x_j \\ \text{subject to } \sum_{i=1}^n \alpha_i y_i &= 0, \alpha_i \geq 0, i = 1, 2, \dots, n. \end{aligned} \quad (7)$$

In equation (7), an optimal  $\alpha_i \geq 0, i = 1, 2, \dots, n$ , can be found by the sequential programming method [6],[7].

Generally, two classes on input space cannot be separated perfectly as in Figure 2 and the constraint in equation (2) is not satisfied.

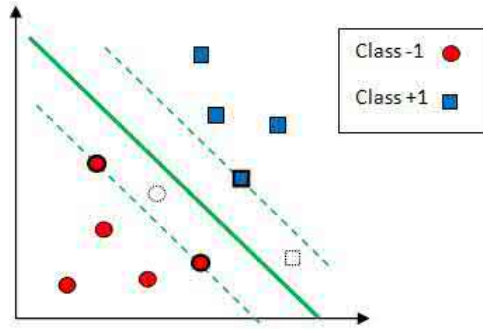


**Figure 2:** Soft Margin Method.

For solving this problem, the soft margin method will be applied using the slack variables  $\varepsilon_i \geq 0, i = 1, 2, \dots, n$ ,

$$\min \frac{1}{2} \|w\|^2 + C \sum_{i=1}^n \varepsilon_i \quad (8)$$

subject to

$$y_i (w^T x_i + b) \geq 1 - \varepsilon_i, \varepsilon_i \geq 0, i = 1, 2, \dots, n. \quad (9)$$

With a similar process in equation (3) - (6), the optimization model becomes

$$\begin{aligned} W(\alpha) &= \sum_{i=1}^n \alpha_i - \frac{1}{2} \sum_{i=1}^n \sum_{j=1}^n \alpha_i \alpha_j y_i y_j x_i^T x_j \\ \text{subject to } \sum_{i=1}^n \alpha_i y_i &= 0, C \geq \alpha_i \geq 0, i = 1, 2, \dots, n. \end{aligned} \quad (10)$$

For testing data with the new data  $z$ , we use a discriminant function in equation (11):

$$f(z) = \sum_{i \in V}^n \alpha_i y_i (x_i^T z) + b, \tag{11}$$

where  $V$  is the set of support vectors.

The constant  $b$  can be determined using the average of the sum of support vector discriminant,

$$b = \frac{1}{N_v} \sum_{i \in V} \left( y_v - \sum_{i \in V} \alpha_i y_i x_i^T x_v \right) \text{ with } y_v \in \{-1, 1\}. \tag{12}$$

If  $f(z) \geq 0$ , then the new data  $z$  is classified as the class +1 and if  $f(z) < 0$ , then the new data  $z$  is classified as the class -1.

### 3 Non Linear Support Vector Machine

When the SVM is applied to a nonlinear dataset, we need to define a feature mapping function  $x \rightarrow \phi(x)$  to the higher dimensional feature space as in Figure 3. The feature mapping function is called the kernel function. The kernel function uses the inner product in the feature space.

$$K(x_i, x_j) \rightarrow \phi(x_i)^T \phi(x_j). \tag{13}$$

Kernel functions which are often used are as in Table 1.

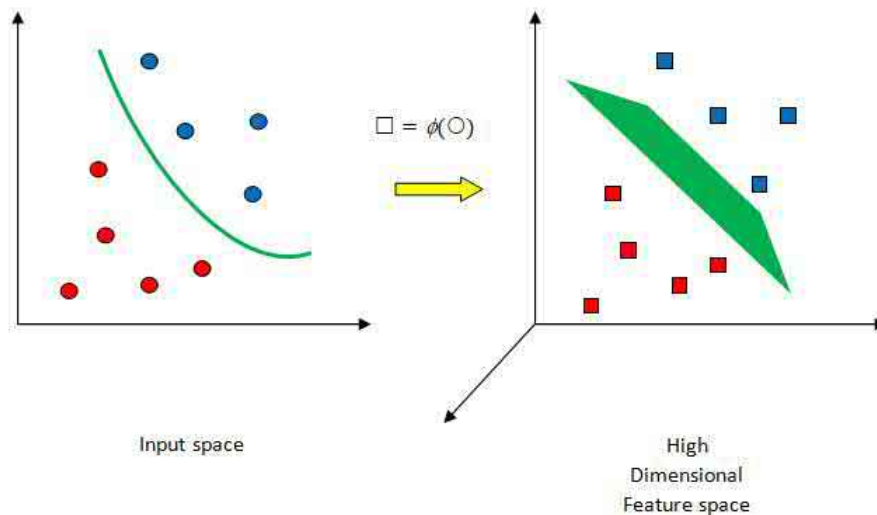


**Figure 3:** Transforming Data from the Input Space to the High Dimensional Feature Space.

Kernel Function	Type
$K(x_i, x_j) = (x_i^T x_j + 1)^d$	Polynomial Function
$K(x_i, x_j) = \exp\left(\frac{-\ x_i - x_j\ ^2}{2\sigma^2}\right)$	Radial Basis Function
$K(x_i, x_j) = \tanh(\kappa x_i^T x_j + \theta)$	Sigmoid Function

**Table 1:** Kernel Functions.

There are some modifications due to the kernel function so that equation (10) becomes

$$\begin{aligned}
 W(\alpha) &= \sum_{i=1}^n \alpha_i - \frac{1}{2} \sum_{i=1}^n \sum_{j=1}^n \alpha_i \alpha_j y_i y_j K(x_i, x_j) \\
 \text{subject to } \sum_{i=1}^n \alpha_i y_i &= 0, C \geq \alpha_i \geq 0, i = 1, 2, \dots, n.
 \end{aligned} \tag{14}$$

For testing data with the new data  $z$ , we use a discriminant function in equation (15),

$$f(z) = \sum_{i \in V} \alpha_i y_i K(x_i, z) + b \tag{15}$$

with  $V$  being the set of support vectors.

The constant  $b$  can be determined using the average of the sum of support vector discriminant,

$$b = \frac{1}{N_v} \sum_{i \in V} \left( y_v - \sum_{i \in V} \alpha_i y_i K(x_i, x_v) \right) \text{ with } y_v \in -1, 1. \tag{16}$$

If  $f(z) \geq 0$ , then the new data  $z$  is classified as the class +1, and if  $f(z) < 0$ , then the new data  $z$  is classified as the class -1.

#### 4 Methodology

In classifying occupied rooms in a hotel, there are reports on the number of room reservations by guests during 60 days, where the attributes which will be used as the inputs are: in-house guests, same day reservation, extension of stay, early departure, today's cancellation, and walk-in. The explanations of the attributes are:

1. In-house guest ( $x_1$ ):  
The guest who is staying for today.
2. Same day reservation ( $x_2$ ):  
The guest who makes a booking today for the check-in today as well.
3. Extension of stay ( $x_3$ ):  
The guest who extends the stay from the check-out time.
4. Early departure ( $x_4$ ):  
The guest who cuts the stay from the check-out time.

5. Today's cancellation ( $x_5$ ):

The guest who made a reservation on the previous days for today and makes a cancellation.

6. Walk-in ( $x_6$ ):

The guest who comes to the reception for today's check-in without a reservation.

These six attributes will be used to compute the number of occupied rooms by the formula:

Occupied rooms = In-house guests + Same day reservation + Extention of stays - Early departure - Today's cancellation + Walk-in

According to the number of occupied rooms on each day, they will be divided into two classes:

1. Class +1 : the number of occupied rooms is higher than the average during 60 days.
2. Class -1 : the number of occupied rooms is lower than the average during 60 days.

In the classification, the data used are the accuracy, error rate, recall, specificity, and precision specified by the following formulae [2]:

$$accuracy = \frac{TP + TN}{P + N} \times 100\%, \quad (17)$$

$$errorrate = \frac{FP + FN}{P + N} \times 100\%, \quad (18)$$

$$recall = \frac{TP}{P} \times 100\%, \quad (19)$$

$$specificity = \frac{TN}{N} \times 100\%, \quad (20)$$

$$precision = \frac{TP}{TP + FP} \times 100\% \quad (21)$$

with the explanations:

$TP$  : the number of positive tuples that are correctly labeled as positive by the classifier;

$TN$  : the number of negative tuples that are correctly labeled as negative by the classifier;

$FP$  : the number of negative tuples that are incorrectly labeled as positive by the classifier;

$FN$  : the number of positive tuples that are incorrectly labeled as negative by the classifier;

$P$  : the number of positive tuples in target data;

$N$  : the number of negative tuple in target data;

Before using SVM, data partition into training data and testing data is made in various proportions.

## 5 Simulation Results

In classifying occupied rooms in a hotel, there are reports on the number of room reservations by guests during 60 days, where the attributes which will be used as inputs are: in-house guests, same day reservation, extention of stay, early departure, today's cancellation, and walk-in. Then, they will be classified into the class +1 (the number of

occupied rooms is higher than the average during 60 days) and the class -1 (the number of occupied rooms is lower than the average during 60 days).

Before applying the classification process, five simulations of SVM will be applied with various proportions of training data and testing data.

- Classification model I : 50 % of training data and 50 % of testing data.
- Classification model II : 67 % of training data and 33 % of testing data.
- Classification model III : 75 % of training data and 25 % of testing data.
- Classification model IV : 80 % of training data and 20 % of testing data.
- Classification model V : 83 % of training data and 17 % of testing data.

After training data and testing data are determined, support vectors can be found by the sequential programming method aided by CPLEX software.

In the classification model I, the proportions of training data and testing data used are 50 % of training data and 50 % of testing data, with training data being the data which are not multiplied by 2 (1, 3, 5, ..., 59) and testing data being the data which are multiplied by 2 (2, 4, 6, ..., 60).

For training data, the best kernel function used is the polynomial kernel with degree  $d = 1$  (linear model) so that based on objective equation (14) with its constrains, the support vectors obtained are

$$\left[ \begin{array}{ccc} \alpha_5 = 0.013193 & \alpha_9 = 0.18556 & \alpha_{16} = 0.30668 \\ \alpha_{18} = 0.077692 & \alpha_{24} = 0.014615 & \alpha_{29} = 0.04201 \end{array} \right] \alpha_i \approx 0, \textit{ otherwise.}$$

The objective function in equation (14) is 0.32. Using the support vectors obtained, we can find the best hyperplane for the training data. Then we use the best hyperplane for the new testing data, with the performance as follows.

	Training data	Testing data
Accuracy	100%	96.67%
Error rate	0%	3.33%
Recall	100%	94.7368%
Specificity	100%	100%
Precision	100%	100%

**Table 2:** Results of SVM Performance with 50 % of training data and 50 % of testing data.

In the classification model II, the proportions of training data and testing data used 67 % of training data and 33 % of testing data, with training data being the data which are not multiplied by 3 (1, 2, 4, 5, ..., 59) and testing data being the data which are multiplied by 3 (3, 6, 9, ..., 60).

For training data, the best kernel function used is the polynomial kernel with degree  $d = 1$  (linear model) so that based on objective equation (14) with its constrains, the support vectors obtained are

$$\left[ \begin{array}{ccc} \alpha_5 = 0.065524 & \alpha_6 = 0.0054547 & \alpha_{12} = 0.3411 \\ \alpha_{21} = 0.4495 & \alpha_{22} = 0.015323 & \alpha_{27} = 0.02614 \end{array} \right] \alpha_i \approx 0, \textit{ otherwise.}$$

The objective function in equation (14) is 0.52. Using the support vectors obtained, we can find the best hyperplane for the training data. Then we use the best hyperplane for the new testing data, with the performance as follows.

	Training data	Testing data
Accuracy	100%	100%
Error rate	0%	0%
Recall	100%	100%
Specificity	100%	100%
Precision	100%	100%

**Table 3:** Results of SVM Performance with 67 % of training data and 33 % of testing data.

In the classification model III, the proportions of training data and testing data used are 75 % of training data and 25 % of testing data, with training data being the data which are not multiplied by 4 (1, 2, 3, 5, . . . , 59) and testing data being the data which are multiplied by 4 (4, 8, . . . , 60).

For training data, the best kernel function used is the polynomial kernel with degree  $d = 1$  (linear model) so that based on objective equation (14) with its constrains, the support vectors obtained are

$$\left[ \begin{array}{ccc} \alpha_7 = 0.013193 & \alpha_{13} = 0.18556 & \alpha_{24} = 0.30668 \\ \alpha_{27} = 0.077692 & \alpha_{36} = 0.014615 & \alpha_{43} = 0.04201 \end{array} \right] \alpha_i \approx 0, \textit{ otherwise}.$$

The objective function in equation (14) is 0.32. From the support vectors obtained, we can find the best hyperplane for the training data. Then we use the best hyperplane for the new testing data, with the performance as follows.

	Training data	Testing data
Accuracy	100%	93.33%
Error rate	0%	6.67%
Recall	100%	90%
Specificity	100%	100%
Precision	100%	100%

**Table 4:** Results of SVM Performance with 75 % of training data and 25 % of testing data.

In the classification model IV, the proportions of training data and testing data used are 80 % of training data and 20 % of testing data, with training data being the data which are not multiplied by 5 (1, 2, 3, 4, 6, . . . , 59) and testing data being the data which are multiplied by 5 (5, 10, 15, . . . , 60).

For training data, the best kernel function used is the polynomial kernel with degree  $d = 1$  (linear model) so that based on objective equation (14) with its constrains, the support vectors obtained are

$$\left[ \begin{array}{ccc} \alpha_6 = 0.070096 & \alpha_7 = 0.0091087 & \alpha_{14} = 0.34108 \\ \alpha_{25} = 0.4266 & \alpha_{26} = 0.1492 & \alpha_{46} = 0.015526 \end{array} \right] \alpha_i \approx 0, \textit{ otherwise}.$$

with the objective function in equation (14) being 0.506. From the support vectors obtained, we can find the best hyperplane for the training data. Then we use the best hyperplane for the new testing data, with the performance as follows.

	Training data	Testing data
Accuracy	100%	91.67%
Error rate	0%	8.33%
Recall	100%	87.5%
Specificity	100%	100%
Precision	100%	100%

**Table 5:** Results of SVM Performance with 80 % of training data and 20 % of testing data.

In the classification model V, the proportions of training data and testing data used are 83 % of training data and 17 % of testing data, with training data being the data which are not multiplied by 6 (1, 2, 3, 4, 5, 7, . . . , 59) and testing data being the data which are multiplied by 6 (6, 12, 18, . . . , 60).

For training data, the best kernel function used is polynomial kernel with degree  $d = 1$  (linear model) so that based on objective equation (14) with its constrains, the support vectors obtained are

$$\left[ \begin{array}{ccc} \alpha_6 = 0.065524 & \alpha_7 = 0.0054547 & \alpha_{15} = 0.3411 \\ \alpha_{26} = 0.4495 & \alpha_{27} = 0.15323 & \alpha_{34} = 0.02614 \end{array} \right] \alpha_i \approx 0, \textit{ otherwise}.$$

with objective function in equation (14) is 0.52. From the support vectors obtained, we can find the best hyperplane for the training data. Then we use the best hyperplane for the new testing data, with the performance as follows.

	Training data	Testing data
Accuracy	100%	100%
Error rate	0%	0%
Recall	100%	100%
Specificity	100%	100%
Precision	100%	100%

**Table 6:** Results of SVM Performance with 83 % of training data and 17 % of testing data.

## 6 Conclusion

Forecasting is significantly important for the hotel operation. It can help the hotel management to prepare guest amenities and supplies, scheduling of the staff, and controlling energy. Shortly, accurate forecasting will help the hotel management to manage the hotel efficiently without sacrificing service quality. The linear SVM uses the best hyperplane as a separator between two classes. In this method, we divide the dataset of guest reservation into training data and testing data in various proportions. For training data, the optimization model of SVM is formed for determining the support vectors. After the

set of support vectors can be determined by the sequential programming method, we can test them in testing data. Based on simulation with various proportions of training data and testing data, the linear SVM can classify the occupied rooms based on guest reservation with accuracy, error rate, recall, specificity, and precision. The developments of this research are classification techniques with big data using the machine learning process.

### Acknowledgment

This research was supported by LPPM - Universitas Nahdlatul Ulama Surabaya.

### References

- [1] M. Y. Anshori and V. Langner. The Importance of Customer Satisfaction and Supreme Service Provision in the Hotel Industry: A Case Study of Surabaya Plaza Hotel. *Jurnal Manajemen Perhotelan* **3** (1) (2007) 18–25.
- [2] M. Y. Anshori. *Manajemen Strategi Hotel: Strategi Meningkatkan Inovasi Dan Kinerja*. ITS Press, Second Edition, August 2010.
- [3] J. Han, M. Kamber and J. Pei. *Data Mining Concepts and Techniques*. Elsevier, USA, 2012.
- [4] G. Garsva, and P. Danenas. Particle Swarm Optimization for Linear Support Vector Machines Based Classifier Selection. *Nonlinear Analysis: Modelling and Control* **19** (1) (2014) 26–42.
- [5] X. Liu and H. Fu. PSO-Based Support Vector Machine with Cuckoo Search Technique for Clinical Disease Diagnoses. *The Scientific World Journal* (2014) 1–7.
- [6] I. Griva, S. G. Nash and A. Sofer. *Linear and Nonlinear Optimization*. SIAM, 2009.
- [7] S. Vijayakumar and S. Wu. Sequential Support Vector Classifiers and Regression (1999) 1–10.
- [8] D. Rahmalia and T. Herlambang. Application Kohonen Network and Fuzzy C Means for Clustering Airports Based on Frequency of Flight. *Kinetik : Game Technology, Information System, Computer Network, Computing* **3** (3) (2018) 229–236.
- [9] A. Rahmatullah, D. Rahmalia and M. S. Pradana. Klasterisasi Data Pertanian di Kabupaten Lamongan Menggunakan Algoritma K-Means dan Fuzzy C Means. *Jurnal Ilmiah Teknosains* **5** (2) (2020) 86–93.
- [10] D. Rahmalia and T. Herlambang. Prediksi Cuaca Menggunakan Algoritma Particle Swarm Optimization-Neural Network (PSO-NN). *Prosiding Seminar Nasional Matematika dan Aplikasinya*. Surabaya, Indonesia, 2017.
- [11] T. Herlambang, D. Rahmalia, H. Nurhadi, D. Adzkiya and S. Subchan. Optimization of Linear Quadratic Regulator with Tracking Applied to Autonomous Underwater Vehicle (AUV) Using Cuckoo Search. *Nonlinear Dynamics and Systems Theory* **20** (3) (2021) 282–298.
- [12] T. Herlambang, S. Subchan, H. Nurhadi and D. Adzkiya. Motion Control Design of UN-USAITS AUV Using Sliding PID. *Nonlinear Dynamics and Systems Theory* **20** (1) (2020) 51–60.
- [13] K. Oktafianto, T. Herlambang, Mardlijah and H. Nurhadi. Design of autonomous underwater vehicle motion control using sliding mode control method. In: *Proc. International Conference on Advanced Mechatronics, Intelligent Manufacture, and Industrial Automation (ICAMIMIA)* Surabaya, Indonesia, 2015, 162–166.

- [14] A. Khernane. Numerical Approximation of the Exact Control for the Vibrating Rod with Improvement of the Final Error by Particle Swarm Optimization. *Nonlinear Dynamics and Systems Theory* **20** (2) (2021) 179–190.
- [15] D. Rahmalia and M. S. Pradana. Backpropagation Neural Network pada Data yang tak Stasioner (Studi Kasus: Jumlah Penderita Penyakit Ebola). *Jurnal Riset dan Aplikasi Matematika (JRAM)* **3** (1) (2019) 32–42.
- [16] F. S. Rini, T. D. Wulan and T. Herlambang. Forecasting the number of demam berdarah dengue (DBD) patients using the fuzzy method at the Siwalankerto public health center. *The First International Conference on Neuroscience and Learning Technology (ICON-SATIN 2021)*.
- [17] D. Rahmalia, and N. Aini. Pengaruh Korelasi Data pada Peramalan Suhu Udara Menggunakan Backpropagation Neural Network. *Zeta-Math Journal* **4** (1) (2018) 1–6.
- [18] D. Rahmalia and A. Rohmatullah. Pengaruh Korelasi Data pada Peramalan Kelembaban Udara Menggunakan Adaptive Neuro Fuzzy Inference System (ANFIS). *Applied Technology and Computing Science* **2** (1) (2019) 10–24.
- [19] D. Rahmalia. Comparison between Neural Network (NN) and Adaptive Neuro Fuzzy Inference System (ANFIS) on Sunlight Intensity Prediction Based on Air Temperature and Humidity. *Journal of Physics: Conference Series* **1538** (2020) 012044.
- [20] D. F. Karya, P. Katias, T. Herlambang, and D. Rahmalia. Development of Unscented Kalman Filter Algorithm for Stock Price Estimation. *Journal of Physics: Conference Series* **1211** (2019) 012031.
- [21] T. Herlambang, H. Nurhadi, A. Muhith, A. Suryowinoto and K. Oktafianto. Estimation of Forefinger Motion with Multi-DOF Using Advanced Kalman Filter. *Nonlinear Dynamics and Systems Theory* **23** (1) (2023) 24–33.
- [22] T. Herlambang, F. A. Susanto, D. Adzkiya, A. Suryowinoto and K. Oktafianto. Design of Navigation and Guidance Control System of Mobile Robot with Position Estimation Using Ensemble Kalman Filter (EnKF) and Square Root Ensemble Kalman Filter (SR-EnKF). *Nonlinear Dynamics and Systems Theory* **22** (4) (2022) 390–399.
- [23] F. A. Susanto, M. Y. Anshori, D. Rahmalia, K. Oktafianto, D. Adzkiya, P. Katias and T. Herlambang. Estimation of Closed Hotels and Restaurants in Jakarta as Impact of Corona Virus Disease (Covid-19) Spread Using Backpropagation Neural Network. *Nonlinear Dynamics and Systems Theory* **22** (4) (2022) 457–467.
- [24] A. Muhith, I. H. Susanto, D. Rahmalia, D. Adzkiya and T. Herlambang. The Analysis of Demand and Supply of Blood in Hospital in Surabaya City Using Panel Data Regression. *Nonlinear Dynamics and Systems Theory* **22** (5) (2022) 550–560.
- [25] M. Y. Anshori, T. Shawyun, D. V. Madrigal, D. Rahmalia, F. A. Susanto, T. Herlambang and D. Adzkiya. Estimation of closed hotels and restaurants in Jakarta as impact of corona virus disease spread using adaptive neuro fuzzy inference system. *IAES International Journal of Artificial Intelligence (IJ-AI)* **11** (2) (2022) 462–472.



# Contact Problem for Thermo-Elasto-Viscoplastic Material with Friction

N. Bensebaa\* and N. Lebri

*Department of Mathematics, Faculty of Sciences, University of Setif 1, 19000, Algeria*

Received: January 20, 2023; Revised: April 6, 2023

**Abstract:** We consider a quasistatic contact problem for thermo-elasto-viscoplastic material with thermal effects. The contact is modeled with the normal damped response condition, associated to Coulomb's law of dry friction. A variational formulation of the model is derived, and the existence of a unique weak solution is proved. The proofs are based on the arguments of evolutionary quasivariational inequality, the classical result of nonlinear first order evolution inequalities, and the fixed point arguments. We also study the dependence of the solution and prove a convergence result.

**Keywords:** *thermo-elasto-viscoplastic material; friction contact; normal damped response condition; Coulomb's friction; evolution equation; weak solution; fixed point.*

**Mathematics Subject Classification (2010):** 74F05, 74H25, 74M10, 74M25, 70K70, 70K75.

## 1 Introduction

Scientific research and recent papers in mechanics are articulated around two main components, one devoted to the laws of behavior and other devoted to the boundary conditions imposed on the body. The boundary conditions reflect the binding of the body with the outside world. The frictional contact between deformable bodies can be frequently found in industry and everyday life. Because of the importance in metal forming and automotive industry, a considerable effort has been made towards the modeling and numerical simulations of contact problems and the engineering literature concerning this topic is rather extensive. An excellent reference in the field of contact problems with or without friction is [8]. The constitutive law with internal variables has been used in various publications in order to model the effect of internal variables on the behavior

---

\* Corresponding author: <mailto:nadjet.bensebaa@univ-setif.dz>

of real bodies such as metal and rocks polymers. Some of the internal state variables considered by many authors are the spatial display of dislocation, the work-hardening of materials, the absolute temperature and the damage fields. The cases of hardening, temperature and other internal state variables were considered in [2, 5, 17, 18], general models for contact processes with thermal effects can be found in [4, 10, 19]. Elastic or viscoelastic frictional contact problems, with thermal considerations, can be found in [1, 3, 14] and the references therein. The purpose of this paper is to make the coupling of an elasto-viscoplastic material with thermal effects and friction. We study a quasistatic problem of frictional contact with the normal damped response condition and the associated version of Coulomb's law of dry friction. We derive a variational formulation of the problem and prove that the proposed model has a unique weak solution by using the evolutionary quasivariational inequality. Also, we study the continuous dependence of the weak solution of the problem and prove a convergence result.

The paper is structured as follows. In Section 2, we present notation and some preliminaries. The model is described in Section 3, where the variational formulation is given. In Section 4, we present our existence and uniqueness result and the proof is based on the arguments for functional analysis concerning the evolutionary quasivariational inequality, the classical result for nonlinear first order evolution inequalities and the fixed point arguments. In Section 5, we study the dependence of the solution and prove a convergence result.

## 2 Notation and Preliminaries

In this section, we list the assumptions on the data, derive a variational formulation for the contact problem (9)–(18) and state our main existence and uniqueness result, Theorem 4.2. To this end, we need to introduce some notation and preliminary material.

We recall that the inner products and the corresponding norms on  $\mathbb{R}^d$  and  $\mathbb{S}^d$  are given by

$$\begin{aligned} u.v &= u_i v_i, & \|v\| &= (v.v)^{\frac{1}{2}} & \forall u, v \in \mathbb{R}^d, \\ \sigma.\tau &= \sigma_{ij} \tau_{ij}, & \|\tau\| &= (\tau.\tau)^{\frac{1}{2}} & \forall \sigma, \tau \in \mathbb{S}^d. \end{aligned}$$

Here and everywhere in this paper,  $i, j$  run from 1 to  $d$ , the summation over repeated indices is used and the index which follows the comma represents the partial derivative. We use the classical notation for  $L^p$  and Sobolev spaces associated to  $\Omega$  and  $\Gamma$ . Moreover, we use the notation  $H$ ,  $\mathcal{H}$ ,  $H_1$  and  $\mathcal{H}_1$  for the following spaces:

$$\begin{aligned} H &= L^2(\Omega)^d = \{v = (v_i) / v_i \in L^2(\Omega)\}, \\ \mathcal{H} &= \{\sigma = (\sigma_{ij}) / \sigma_{ij} = \sigma_{ji} \in L^2(\Omega)\}, \\ H_1 &= \{u = (u_i) / \varepsilon(u) \in \mathcal{H}\}, \\ \mathcal{H}_1 &= \{\sigma \in \mathcal{H} / \text{Div } \sigma \in H\}. \end{aligned}$$

The spaces  $H$ ,  $\mathcal{H}$ ,  $H_1$  and  $\mathcal{H}_1$  are the real Hilbert spaces endowed with the canonical inner products given by

$$\begin{aligned} (u, v)_H &= \int_{\Omega} u.v dx, & (\sigma, \tau)_{\mathcal{H}} &= \int_{\Omega} \sigma.\tau dx, \\ (u, v)_{H_1} &= (u, v)_H + (\varepsilon(u), \varepsilon(v))_{\mathcal{H}}, & (\sigma, \tau)_{\mathcal{H}_1} &= (\sigma, \tau)_{\mathcal{H}} + (\text{Div } \sigma, \text{Div } \tau)_H, \end{aligned}$$

and the associated norms  $\|\cdot\|_H, \|\cdot\|_{\mathcal{H}}, \|\cdot\|_{H_1}$  and  $\|\cdot\|_{\mathcal{H}_1}$ , respectively. Here and below, we use the notation

$$\begin{aligned} \varepsilon(v) &= (\varepsilon_{ij}(v)), \quad \varepsilon_{ij}(v) = \frac{1}{2}(v_{i,j} + v_{j,i}) \quad \forall v \in H^1(\Omega)^d, \\ \text{Div } \tau &= (\tau_{ij,j}) \quad \forall \tau \in \mathcal{H}_1. \end{aligned}$$

For every element  $v \in H_1$ , we also write  $v$  for the trace of  $v$  on  $\Gamma$  and we denote by  $v_\nu$  and  $v_\tau$  the normal and tangential components of  $v$  on  $\Gamma$  given by  $v_\nu = v \cdot \nu, v_\tau = v - v_\nu \nu$ . We also denote by  $\sigma_\nu$  and  $\sigma_\tau$  the normal and the tangential traces of a function  $\sigma \in \mathcal{H}_1$ , and we recall that when  $\sigma$  is a regular function, then  $\sigma_\nu = (\sigma \nu) \cdot \nu, \sigma_\tau = \sigma \nu - \sigma_\nu \nu$ , and the following Green’s formula holds:

$$(\sigma, \varepsilon(v))_{\mathcal{H}} + (\text{Div } \sigma, v)_H = \int_{\Gamma} \sigma \nu \cdot v \, da \quad \forall v \in H_1.$$

Let  $T > 0$ . For every real Banach space  $X$ , we use the notation  $C(0, T; X)$  and  $C^1(0, T; X)$  for the space of continuous and continuously differentiable functions from  $[0, T]$  to  $X$ , respectively;  $C(0, T; X)$  is a real Banach space with the norm  $\|f\|_{C(0,T;X)} = \max_{t \in [0,T]} \|f(t)\|_X$ ,

while  $C^1(0, T; X)$  is a real Banach space with the norm  $\|f\|_{C^1(0,T;X)} = \max_{t \in [0,T]} \|f(t)\|_X +$

$\max_{t \in [0,T]} \|\dot{f}(t)\|_X$ . Finally, for  $k \in \mathbb{N}$  and  $p \in [1, \infty]$ , we use the standard notation for the

Lebesgue spaces  $L^p(0, T; X)$  and for the Sobolev spaces  $W^{k,p}(0, T; X)$ . Moreover, for a real number  $r$ , we use  $r_+$  to represent its positive part, that is,  $r_+ = \max\{0, r\}$ . Moreover, if  $X_1$  and  $X_2$  are real Hilbert spaces, then  $X_1 \times X_2$  denotes the product Hilbert space endowed with the canonical inner product  $(\cdot, \cdot)_{X_1 \times X_2}$ .

Let  $X$  be a real Hilbert space with the inner product  $(\cdot, \cdot)_X$  and the associated norm  $\|\cdot\|$ , and consider the problem of finding  $u : [0, T] \rightarrow X$  such that

$$\begin{cases} (A\dot{u}(t), v - \dot{u}(t))_V + (Bu(t), v - \dot{u}(t))_V + j(\dot{u}(t), v) \\ -j(\dot{u}(t), \dot{u}(t)) \geq (f(t), v - \dot{u}(t))_V \quad \forall v \in X, t \in [0, T]. \\ u(0) = u_0. \end{cases} \tag{1}$$

To study problem (1), we need the following assumptions.

The operator  $A : X \rightarrow X$  is Lipschitz continuous and strongly monotone, i.e.,

$$\begin{cases} a) \text{ There exists } L_A > 0 \text{ such that} \\ \|Au_1 - Au_2\|_X \leq L_A \|u_1 - u_2\|_X \quad \forall u_1, u_2 \in X, \\ c) \text{ There exists } m_A > 0 \text{ such that} \\ (Au_1 - Au_2, u_1 - u_2)_X \geq m_A \|u_1 - u_2\|_X^2 \quad \forall u_1, u_2 \in X. \end{cases} \tag{2}$$

The nonlinear operator  $B : X \rightarrow X$  is Lipschitz continuous, i.e.,

$$\begin{cases} \text{There exists } L_B > 0 \text{ such that} \\ \|Bu_1 - Bu_2\|_X \leq L_B \|u_1 - u_2\|_X \quad \forall u_1, u_2 \in X. \end{cases} \tag{3}$$

The functional  $j : X \times X \rightarrow \mathbb{R}$  satisfies the following conditions:

$$\begin{cases} a) j(u, \cdot) \text{ is convex and i.s.c on } X \text{ for all } u \in X. \\ b) \text{ There exists } \alpha > 0 \text{ such that} \\ j(u_1, v_2) + j(u_1, v_1) + j(u_2, v_1) + j(u_2, v_2) \\ \leq \alpha \|u_1 - u_2\|_X \|v_1 - v_2\|_X, \quad \forall u_1, u_2, v_1, v_2 \in X. \end{cases} \tag{4}$$

$$f \in C(0, T; X), \quad (5)$$

$$u_0 \in X, \quad (6)$$

$$m_{\mathcal{A}} > \alpha. \quad (7)$$

We have the following existence and uniqueness result which can be found in [16].

**Theorem 2.1** *Assume that (2)-(7) hold. Then there exists a unique solution  $u$  to problem (1). Moreover, the solution satisfies  $u \in C^1([0, T]; X)$ .*

### 3 Mechanical and Variational Formulations

We consider a thermo-elasto-viscoplastic body which occupies a bounded domain  $\Omega \subset \mathbb{R}^d$  ( $d = 2, 3$ ) with a Lipschitz continuous boundary  $\Gamma$  that is divided into three disjoint measurable parts  $\Gamma_1, \Gamma_2$  and  $\Gamma_3$  such that  $\text{meas } \Gamma_1 > 0$ . Let  $T > 0$  and let  $[0, T]$  be the time interval of interest. The body is clamped on  $\Gamma_1 \times (0, T)$ , so the displacement field vanishes there. The surface tractions of density  $f_2$  act on  $\Gamma_2 \times (0, T)$ , and the body force of density  $f_0$  acts in  $\Omega \times (0, T)$ . The contact between the body and the foundation, over the contact surface  $\Gamma_3$ , is modeled with the normal damped response and the associated general version of Coulomb's law of dry friction. Moreover, the process is quasistatic, i.e., the inertial terms are neglected in the equation of motion. The material is assumed to behave according to the general elasto-viscoplastic constitutive law with thermal effects given by

$$\sigma = \mathcal{A}\varepsilon(\dot{u}) + \mathcal{F}\varepsilon(u) + \int_0^t \mathcal{G}(\sigma(s) - \mathcal{A}\varepsilon(\dot{u}(s)), \varepsilon(u(s))) ds - \mathcal{M}\theta(t), \quad (8)$$

where  $\sigma$  denotes the stress tensor,  $u$  represents the displacement field,  $\dot{u}$  is the velocity,  $\varepsilon(u)$  is the small strain tensor, and  $\theta$  is the temperature field. Here,  $\mathcal{A}$  and  $\mathcal{F}$  are nonlinear operators describing the purely viscous and the elastic properties of the material, respectively.  $\mathcal{G}$  is a general nonlinear constitutive function describing the viscoplastic behavior of the material.  $\mathcal{M} = (m_{ij})$  represents the thermal expansion tensor. We use dots for derivatives with respect to the time variable  $t$ . It follows from (8) that at each time moment, the stress tensor  $\sigma(t)$  is split into two parts:  $\sigma(t) = \sigma^V(t) + \sigma^R(t)$ , where  $\sigma^V(t) = \mathcal{A}\varepsilon(\dot{u})$  represents the purely viscous part of the stress, whereas  $\sigma^R(t)$  satisfies a rate-type thermo-elasto-viscoplastic relation

$$\sigma^R(t) = \mathcal{F}\varepsilon(u) + \int_0^t \mathcal{G}(\sigma^R(s), \varepsilon(u(s))) ds - \mathcal{M}\theta(t).$$

The evolution of the temperature field  $\theta$  is governed by the heat equation (see [1]), obtained from the conservation of energy, and defined by the following differential equation for the temperature:

$$\dot{\theta} - \text{div}(k\nabla\theta) = q - \mathcal{M}\nabla\dot{u},$$

where  $K = (k_{ij})$  represents the thermal conductivity tensor,  $\text{div}(k\nabla\theta) = (k_{ij}\theta_{,i})_{,i}$  and  $q$  represents the density of volume heat sources.

The associated temperature boundary condition on  $\Gamma_3$  is described by

$$k_{ij}\theta_{,i}n_j = -k_e(\theta - \theta_R) + h_\tau(|\dot{u}_\tau|) \quad \text{on } \Gamma_3 \times (0, T),$$

where  $\theta_R$  is the temperature of the foundation,  $k_e$  is the heat exchange coefficient between the body and the obstacle and  $h_\tau : \Gamma_3 \times R_+ \rightarrow R_+$  is a given tangential function.

Then, the classical formulation of the mechanical problem is as follows.

**Problem P:** Find a displacement field  $u : \Omega \times [0, T] \rightarrow \mathbb{R}^d$ , a stress field  $\sigma : \Omega \times [0, T] \rightarrow S^d$  and a temperature  $\theta : \Omega \times [0, T] \rightarrow \mathbb{R}$  such that

$$\sigma = \mathcal{A}\varepsilon(\dot{u}) + \mathcal{F}\varepsilon(u) + \int_0^t \mathcal{G}(\sigma(s) - \mathcal{A}\varepsilon(\dot{u}(s)), \varepsilon(u(s))) ds \tag{9}$$

$$-\mathcal{M}\theta(t) \text{ in } \Omega \times (0, T),$$

$$\dot{\theta} - \operatorname{div}(k\nabla\theta) = q - \mathcal{M}\nabla\dot{u} \text{ in } \Omega \times (0, T), \tag{10}$$

$$\operatorname{Div} \sigma + f_0 = 0 \text{ in } \Omega \times (0, T), \tag{11}$$

$$u = 0 \text{ on } \Gamma_1 \times (0, T), \tag{12}$$

$$\sigma\nu = f_2 \text{ on } \Gamma_2 \times (0, T), \tag{13}$$

$$-\sigma_\nu = p_\nu(\dot{u}_\nu) \text{ on } \Gamma_3 \times (0, T), \tag{14}$$

$$\begin{cases} \|\sigma_\tau\| \leq \mu p_\nu(\dot{u}_\nu) \\ \|\sigma_\tau\| < \mu p_\nu(\dot{u}_\nu) \Rightarrow \dot{u}_\tau = 0 \\ \|\sigma_\tau\| = \mu p_\nu(\dot{u}_\nu) \Rightarrow \exists \lambda \geq 0 \quad \sigma_\tau = -\lambda \dot{u}_\tau \end{cases} \text{ on } \Gamma_3 \times (0, T), \tag{15}$$

$$-k_{ij} \frac{\partial \theta}{\partial \nu} = k_e(\theta - \theta_R) - h_\tau(|\dot{u}_\tau|) \text{ on } \Gamma_3 \times (0, T), \tag{16}$$

$$\theta = 0 \text{ on } (\Gamma_1 \cup \Gamma_2) \times (0, T), \tag{17}$$

$$u(0) = u_0, \theta(0) = \theta_0 \text{ in } \Omega. \tag{18}$$

We now provide some comments on the equations and conditions of problem (9)–(18).

First, (9)–(10) represent the thermo-elasto-viscoplastic constitutive law and the evolution equation of the heat field, respectively. (11) is the equilibrium equation. (12) and (13) represent the displacement and traction boundary conditions, respectively. Conditions (16) and (17) represent the temperature boundary conditions, where (17) means that the temperature vanishes on  $(\Gamma_1 \cup \Gamma_2) \times (0, T)$ . Conditions (14) and (15) are Coulomb’s friction law, where  $\mu \geq 0, \lambda \geq 0$ , and they state a general normal damped response condition, where  $\dot{u}_\nu$  represents the normal velocity,  $p_\nu$  is a prescribed function,  $\sigma_\nu$  is the normal stress,  $\dot{u}_\tau$  denotes the tangential velocity and  $\sigma_\tau$  represents the tangential force on the contact boundary. Denote by  $u_0$  and  $\theta_0$  the initial displacement and the initial temperature, respectively. To simplify the notation, we do not indicate explicitly the dependence of various functions on the variables  $x \in \Omega \cup \Gamma$  and  $t \in [0, T]$ . To obtain a variational formulation of the problem (9)–(18), we need additional notations. Let  $E$  denote the closed subspace of  $H^1(\Omega)$  given by

$$E = \{\gamma \in H^1(\Omega) / \gamma = 0 \text{ on } \Gamma_1 \cup \Gamma_2\}.$$

Let us now consider the closed subspace of  $H_1$  defined by

$$V = \{v \in H_1 / v = 0 \text{ on } \Gamma_1\}.$$

Since  $\text{meas}(\Gamma_1) > 0$ , the following Korn's inequality holds:

$$\|\varepsilon(v)\|_{\mathcal{H}} \geq c_k \|v\|_{H_1} \quad \forall v \in V, \quad (19)$$

where  $c_k > 0$  is a constant which depends only on  $\Omega$  and  $\Gamma_1$ . On the space  $V$ , we consider the inner product and the associated norm given by

$$(u, v)_V = (\varepsilon(u), \varepsilon(v))_{\mathcal{H}}, \quad \|v\|_V = \|\varepsilon(v)\|_{\mathcal{H}} \quad \forall u, v \in V. \quad (20)$$

It follows from Korn's inequality that  $\|\cdot\|_{H_1}$  and  $\|\cdot\|_V$  are equivalent norms on  $V$ . Therefore  $(V, \|\cdot\|_V)$  is a real Hilbert space. Moreover, by the Sobolev trace theorem and (20), there exists a constant  $c_0 > 0$  depending only on the domain  $\Omega$ ,  $\Gamma_1$  and  $\Gamma_3$  such that

$$\|v\|_{L^2(\Gamma_3)^d} \leq c_0 \|v\|_V \quad \forall v \in V. \quad (21)$$

In the study of the mechanical problem (9)–(18), we assume that the viscosity operator  $\mathcal{A} : \Omega \times \mathbb{S}^d \rightarrow \mathbb{S}^d$  satisfies the conditions:

$$\left\{ \begin{array}{l} (a) \text{ There exists a constant } L_{\mathcal{A}} > 0 \text{ such that} \\ \|\mathcal{A}(x, \varepsilon_1) - \mathcal{A}(x, \varepsilon_2)\| \leq L_{\mathcal{A}} \|\varepsilon_1 - \varepsilon_2\| \quad \forall \varepsilon_1, \varepsilon_2 \in \mathbb{S}^d, \text{ a.e. } x \in \Omega. \\ (b) \text{ There exists a constant } m_{\mathcal{A}} > 0 \text{ such that} \\ (\mathcal{A}(x, \varepsilon_1) - \mathcal{A}(x, \varepsilon_2)) \cdot (\varepsilon_1 - \varepsilon_2) \geq m_{\mathcal{A}} \|\varepsilon_1 - \varepsilon_2\|^2, \quad \forall \varepsilon_1, \varepsilon_2 \in \mathbb{S}^d, \text{ a.e. } x \in \Omega. \\ (c) \text{ The mapping } x \mapsto \mathcal{A}(x, \varepsilon) \text{ is Lebesgue measurable on } \Omega, \text{ for any } \varepsilon \in \mathbb{S}^d. \\ (d) \text{ The mapping } x \mapsto \mathcal{A}(x, 0) \in \mathcal{H}. \end{array} \right. \quad (22)$$

The elasticity operator  $\mathcal{F} : \Omega \times S^d \times \mathbb{R} \rightarrow S^d$  satisfies the conditions:

$$\left\{ \begin{array}{l} (a) \text{ There exists a constant } L_{\mathcal{F}} > 0 \text{ such that} \\ \|\mathcal{F}(x, \varepsilon_1) - \mathcal{F}(x, \varepsilon_2)\| \leq L_{\mathcal{F}} \|\varepsilon_1 - \varepsilon_2\| \quad \forall \varepsilon_1, \varepsilon_2 \in S^d, \text{ a.e. } x \in \Omega. \\ \forall \varepsilon_1, \varepsilon_2 \in S^d, \text{ a.e. } x \in \Omega. \\ (b) \text{ The mapping } x \rightarrow \mathcal{F}(x, \varepsilon) \text{ is Lebesgue measurable on } \Omega, \text{ for any } \varepsilon \in S^d. \\ (c) \text{ The mapping } x \rightarrow \mathcal{F}(x, 0) \in \mathcal{H}. \end{array} \right. \quad (23)$$

The visco-plasticity operator  $\mathcal{G} : \Omega \times S^d \times S^d \rightarrow S^d$  satisfies the conditions:

$$\left\{ \begin{array}{l} (a) \text{ There exists a constant } L_{\mathcal{G}} > 0 \text{ such that} \\ \|\mathcal{G}(x, \sigma_1, \varepsilon_1) - \mathcal{G}(x, \sigma_2, \varepsilon_2)\| \leq L_{\mathcal{G}} (\|\varepsilon_1 - \varepsilon_2\| + \|\sigma_1 - \sigma_2\|) \\ \forall \varepsilon_1, \varepsilon_2, \sigma_1, \sigma_2 \in S^d, \text{ a.e. } x \in \Omega. \\ (b) \text{ The mapping } x \rightarrow \mathcal{G}(x, \sigma, \varepsilon) \text{ is Lebesgue measurable on } \Omega, \text{ for any } \varepsilon, \sigma \in S^d. \\ (c) \text{ The mapping } x \rightarrow \mathcal{G}(x, 0, 0) \in \mathcal{H}. \end{array} \right. \quad (24)$$

The contact function  $p_{\nu} : \Gamma_3 \times \mathbb{R} \rightarrow \mathbb{R}^+$  satisfies the conditions:

$$\left\{ \begin{array}{l} (a) \text{ There exists a constant } L_{\nu} > 0 \text{ such that} \\ \|p_{\nu}(x, r_1) - p_{\nu}(x, r_2)\| \leq L_{\nu} \|r_1 - r_2\| \quad \forall r_1, r_2 \in \mathbb{R}, \text{ a.e. } x \in \Gamma_3. \\ (d) \text{ The mapping } x \mapsto p_{\nu}(x, r) \text{ is Lebesgue measurable on } \Gamma_3, \text{ for any } r \in \mathbb{R}. \\ (f) \text{ The mapping } x \mapsto p_{\nu}(x, r) \text{ belongs to } L^2(\Gamma_3). \end{array} \right. \quad (25)$$

The tangential function  $h_{\tau} : \Gamma_3 \times \mathbb{R}^+ \rightarrow \mathbb{R}^+$  satisfies the conditions:

$$\left\{ \begin{array}{l} (a) \text{ There exists a constant } L_h > 0 \text{ such that} \\ \|h_{\tau}(x, r_1) - h_{\tau}(x, r_2)\| \leq L_h \|r_1 - r_2\| \quad \forall r_1, r_2 \in \mathbb{R}^+, \text{ a.e. } x \in \Gamma_3. \\ (b) \text{ The mapping } x \rightarrow h_{\tau}(x, r) \in L^2(\Gamma_3) \text{ is Lebesgue measurable on } \Gamma_3, \forall r \in \mathbb{R}^+. \end{array} \right. \quad (26)$$

The body forces and surface tractions have the regularity

$$f_0 \in C(0, T; H), \quad f_2 \in C(0, T; L^2(\Gamma_2)^d). \tag{27}$$

The coefficient  $\mu$  satisfies the following conditions:

$$\mu \in L^\infty(\Gamma_3) \quad \mu(x) \geq 0 \text{ a.e. on } \Gamma_3. \tag{28}$$

The thermal tensors and the heat source density satisfy the conditions:

$$\begin{cases} \mathcal{M} = (m_{ij}), & m_{ij} = m_{ji} \in L^\infty(\Omega). \\ K = (k_{ij}), & k_{ij} = k_{ji} \in L^\infty(\Omega), k_{ij}\zeta_i\zeta_j \geq c_k\zeta_i\zeta_j, \\ & \text{for some } c_k > 0, \text{ for all } (\zeta_i) \in \mathbb{R}^d. \\ q \in L^2(0, T; L^2(\Omega)). \end{cases} \tag{29}$$

Finally, the boundary and initial data verify that

$$u_0 \in V, \quad \theta_0 \in E, \quad \theta_R \in L^2(0, T; L^2(\Gamma_3)), \quad k_e \in L^\infty(\Omega, \mathbb{R}^+). \tag{30}$$

We define the function  $f : [0, T] \rightarrow V$  by

$$(f(t), v) = \int_\Omega f_0(t) \cdot v dx + \int_{\Gamma_2} f_2(t) \cdot v da. \quad \forall v \in V, \forall t \in [0, T]. \tag{31}$$

Next, we denote by  $j : V \times V \rightarrow \mathbb{R}$  the functional defined by

$$j(u, v) = \int_{\Gamma_3} p_\nu(u) \cdot v_\nu da + \int_{\Gamma_3} \mu p_\nu(u) \cdot \|v_\tau\| da \quad \forall u, v \in V. \tag{32}$$

We note that condition (27) implies

$$f \in C([0, T], V). \tag{33}$$

Using standard arguments, we obtain the variational formulation of the mechanical problem (9)-(18).

**Problem PV.** Find a displacement field  $u : [0, T] \rightarrow V$ , a stress field  $\sigma : [0, T] \rightarrow \mathcal{H}$  and a temperature field  $\theta : [0, T] \rightarrow E$  such that for all  $t \in [0, T]$ ,

$$\sigma = \mathcal{A}\varepsilon(\dot{u}) + \mathcal{F}\varepsilon(u) + \int_0^t \mathcal{G}(\sigma(s) - \mathcal{A}\varepsilon(\dot{u}(s)), \varepsilon(u(s))) ds - \mathcal{M}\theta(t), \tag{34}$$

$$(\sigma(t), \varepsilon(v) - \varepsilon(\dot{u}))_{\mathcal{H}} + j(\dot{u}(t), v) - j(\dot{u}(t), \dot{u}(t)) \geq (f(t), v - \dot{u})_V. \tag{35}$$

$$\dot{\theta}(t) + K\theta(t) = R\dot{u}(t) + Q(t) \quad \text{in } E', \tag{36}$$

$$u(0) = u_0, \quad \theta(0) = \theta_0, \tag{37}$$

where  $K : E \rightarrow E'$ ,  $R : V \rightarrow E'$  and  $Q : [0, T] \rightarrow E'$  are given by

$$(K\tau, \omega)_{E' \times E} = \sum_{i,j=1}^d \int_\Omega k_{ij} \frac{\partial \tau}{\partial x_j} \frac{\partial \omega}{\partial x_i} dx + \int_{\Gamma_3} k_e \tau \omega da,$$

$$(Rv, \omega)_{E' \times E} = \int_{\Gamma_3} h_\tau(|v_\tau|) \omega da - \int_\Omega m_{ij} \frac{\partial v_i}{\partial x_j} \omega dx,$$

$$(Q(t), \omega)_{E' \times E} = \int_{\Gamma_3} k_e \theta_R(t) \omega da + \int_\Omega q(t) \omega dx$$

for all  $v \in V, \tau, \omega \in E$ .

#### 4 Existence and Uniqueness Result

Now, we propose our existence and uniqueness result.

**Theorem 4.1** *Assume that (22)-(30) hold. Then there exists  $L_0 > 0$  depending only on  $\Omega, \Gamma_1, \Gamma_3$  and  $\mathcal{A}$  such that if  $L_\nu(\|\mu\|_{L^\infty(\Gamma_3)} + 1) < L_0$ , problem PV has a unique solution which satisfies the conditions:*

$$u \in C^1([0, T], V), \quad \sigma \in C([0, T], \mathcal{H}_1), \quad (38)$$

$$\theta \in W^{1,2}(0, T; E') \cap L^2(0, T; E) \cap C(0, T; L^2(\Omega)). \quad (39)$$

The functions  $u, \sigma$  and  $\theta$  which satisfy (34)-(37) are called a weak solution of the contact problem  $P$ . We conclude that, under the assumptions (22)–(30), the mechanical problem (9)-(18) has a unique weak solution satisfying (38)-(39).

The proof of Theorem 4.2 is carried out in several steps that we prove in what follows, everywhere in this section we suppose that the assumptions of Theorem 4.2 hold, and we consider that  $C$  is a generic positive constant which is independent of time and whose value may change from one occurrence to another.

Let  $\eta \in C(0, T; \mathcal{H})$  be given; in the first step, we consider the following variational problem.

**Problem  $PV_\eta$**  : Find a displacement field  $u_\eta : [0, T] \rightarrow V$  such that

$$\begin{aligned} (\mathcal{A}\varepsilon(\dot{u}_\eta), \varepsilon(v) - \varepsilon(\dot{u}_\eta))_{\mathcal{H}} + (\mathcal{F}\varepsilon(u_\eta), \varepsilon(v) - \varepsilon(\dot{u}_\eta))_{\mathcal{H}} + (\eta(t), \varepsilon(v) - \varepsilon(\dot{u}_\eta))_{\mathcal{H}} \\ + j(\dot{u}_\eta(t), v) - j(\dot{u}_\eta(t), \dot{u}_\eta(t)) \geq (f(t), v - \dot{u}_\eta)_V. \end{aligned} \quad (40)$$

$$u_\eta(0) = u_0. \quad (41)$$

We have the following result for the problem.

**Lemma 4.1** *There exists  $L_0$  depending only on  $\Omega, \Gamma_1, \Gamma_3$  and  $\mathcal{A}$  such that if  $L_\nu(\|\mu\|_{L^\infty(\Gamma_3)} + 1) < L_0$ , the problem PV has a unique solution  $u_\eta \in C^1([0, T], V)$ .*

**Proof.** We define the operators  $A : V \rightarrow V$ ,  $F : V \rightarrow V$  and the function  $f_\eta : [0, T] \rightarrow V$  by

$$(Au, v)_V = (\mathcal{A}\varepsilon(u), \varepsilon(v))_{\mathcal{H}}, \quad (42)$$

$$(Fu, v)_V = (\mathcal{F}\varepsilon(u), \varepsilon(v))_{\mathcal{H}}, \quad (43)$$

$$(f_\eta, v)_V = (f(t), v)_V - (\eta(t), \varepsilon(v))_{\mathcal{H}} \quad (44)$$

for all  $u, v \in V$  and  $t \in [0, T]$ .

We use (42), (22)(b) and (22)(c) to find that

$$\|Au_1 - Au_2\| \leq L_{\mathcal{A}} \|u_1 - u_2\|_V. \quad (45)$$

$$(Au_1 - Au_2, u_1 - u_2)_V \geq m_{\mathcal{A}} \|u_1 - u_2\|_V^2. \quad (46)$$

From (23)(a) and (43), we have

$$\|Fu_1 - Fu_2\| \leq L_{\mathcal{F}} \|u_1 - u_2\|_V. \quad (47)$$

From (46) and (45),  $A$  is a strongly monotone Lipschitz continuous operator, then from (47),  $F$  is a Lipschitz continuous operator. We use (27), we find that the function  $f$

defined by (31) satisfies  $f \in C([0, T], V)$ , and keeping in mind that  $\eta \in C([0, T], \mathcal{H})$ , we deduce by (44) that  $f_\eta \in C([0, T], V)$  and  $u_0 \in V$ . We use (25), (28) and (21), we find that the function  $j$  given by (32) satisfies the condition (4)(a). Moreover,

$$\begin{aligned} & j(u_1, v_2) - j(u_1, v_1) + j(u_2, v_1) - j(u_2, v_2) \\ & \leq c_0^2 L_\nu (\|\mu\|_{L^\infty(\Gamma_3)} + 1) \|u_1 - u_2\|_V \|v_1 - v_2\|_V \end{aligned} \tag{48}$$

for all  $u_1, u_2, v_1, v_2 \in V$ , which implies that the function  $j$  satisfies the condition (4)(b) on  $X = V$  with  $\alpha = c_0^2 L_\nu (\|\mu\|_{L^\infty(\Gamma_3)} + 1)$ . Let  $L_0 = \frac{m_{\mathcal{A}}}{c_0^2}$  and note that  $L_0$  depends only on  $\Omega, \Gamma_1, \Gamma_3$  and  $\mathcal{A}$ . Then, if  $L_\nu (\|\mu\|_{L^\infty(\Gamma_3)} + 1) < L_0$ , we have

$$m_{\mathcal{A}} > \alpha, \tag{49}$$

and it follows from Theorem 4.1 that there exists a unique function  $u_\eta \in C^1([0, T], V)$  such that

$$\begin{aligned} & (A\dot{u}_\eta(t), v - \dot{u}_\eta(t))_V + (Fu_\eta(t), v - \dot{u}_\eta(t))_V + j(\dot{u}_\eta(t), v) \\ & - j(\dot{u}_\eta(t), \dot{u}_\eta(t)) \geq (f_\eta(t), v - \dot{u}_\eta(t))_V. \quad \forall v \in V, t \in [0, T]. \end{aligned} \tag{50}$$

$$u_\eta(0) = u_0. \tag{51}$$

We use (42), (43), (50) and (51) to see that  $u_\eta$  is the unique solution to  $PV_\eta$ .

Let  $u_\eta : [0, T] \rightarrow V$  be the function defined by

$$u = \int_0^t v_\eta(s) ds + u_0, \quad \forall t \in [0, T]. \tag{52}$$

In the second step, let  $\eta \in C([0, T], \mathcal{H})$ , we use the displacement field  $u_\eta$  obtained in Lemma 4.1 and we consider the following variational problem.

**Problem  $QV_\eta$ .** Find the temperature field  $\theta_\eta : [0, T] \rightarrow E$  such that

$$\dot{\theta}_\eta(t) + K\theta_\eta(t) = R\dot{u}_\eta(t) + Q(t), \tag{53}$$

$$\theta_\eta(0) = \theta_0. \tag{54}$$

We have the following result.

**Lemma 4.2** *Problem  $QV_\eta$  has a unique solution  $\theta_\eta$  which satisfies the regularity (39), then we have for all  $t \in [0, T]$ ,*

$$\|\theta_{\eta_1}(t) - \theta_{\eta_2}(t)\|_{L^2(\Omega)}^2 \leq C \int_0^t \|\dot{u}_{\eta_1}(s) - \dot{u}_{\eta_2}(s)\|_V^2 ds. \tag{55}$$

**Proof.** We use a classical result for the first order evolution equation given in [15]. We have the Gelfand triple

$$E \subset L^2(\Omega) \equiv (L^2(\Omega))' \subset E'.$$

The operator  $K$  is linear and coercive. By Korn's inequality

$$(K\tau, \tau)_{E' \times E} \geq C |\tau|_E^2, \quad C > 0.$$

Now, for  $\theta_{\eta_i} \in E, i = 1, 2$ , let  $t \in [0, T]$ .

We have

$$\begin{aligned} & \left( \dot{\theta}_{\eta_1}(t) - \dot{\theta}_{\eta_2}(t), \theta_{\eta_1}(t) - \theta_{\eta_2}(t) \right)_{E' \times E} + (K\theta_{\eta_1}(t) - K\theta_{\eta_2}(t), \theta_{\eta_1}(t) - \theta_{\eta_2}(t))_{E' \times E} \\ & = (R\dot{u}_{\eta_1}(t) - R\dot{u}_{\eta_2}(t), \theta_{\eta_1}(t) - \theta_{\eta_2}(t))_{E' \times E}, \end{aligned} \quad (56)$$

we integrate (56) over  $(0, t)$  and we use the coercivity of  $K$  and the Lipschitz continuity of  $R : V \rightarrow E'$  to deduce that (55) is satisfied for all  $t \in [0, T]$ .

In the third step, we use the displacement field  $u_\eta$  obtained in Lemma 4.1 and the temperature field  $\theta_\eta$  obtained in Lemma 4.2 to construct the following Cauchy problem for the stress field.

**Problem  $PV\sigma_\eta$ .** Find the stress field  $\sigma_\eta : [0, T] \rightarrow \mathcal{H}$  such that

$$\sigma_\eta(t) = \mathcal{F}\varepsilon(u_\eta(t)) + \int_0^t \mathcal{G}(\sigma_\eta(s), \varepsilon(u_\eta(s))) ds - \mathcal{M}\theta_\eta(t) \quad \forall t \in [0, T]. \quad (57)$$

In the study of problem  $PV\sigma_\eta$ , we have the following result.

**Lemma 4.3** *There exists a unique solution of problem  $PV\sigma_\eta$  and it satisfies  $\sigma_\eta \in C^1([0, T], \mathcal{H})$ . Moreover, if  $u_i, \sigma_i$  and  $\theta_i$  represent the solutions of the problems  $PV\eta_i, PV\sigma_{\eta_i}$  and  $QV\eta_i$ , respectively, for  $\eta_i \in C(0, T; \mathcal{H})$ ,  $i = 1, 2$ , then there exists  $C > 0$  such that*

$$\begin{aligned} \|\sigma_1(t) - \sigma_2(t)\|_{\mathcal{H}}^2 & \leq C(\|u_1(t) - u_2(t)\|_V^2 + \|\theta_1(t) - \theta_2(t)\|_{L^2(\Omega)}^2 \\ & + \int_0^t \|u_1(s) - u_2(s)\|_V^2 ds), \quad \forall t \in [0, T]. \end{aligned} \quad (58)$$

**Proof.** Let  $\Lambda_\eta : C(0, T; \mathcal{H}) \rightarrow C(0, T; \mathcal{H})$  be the operator given by

$$\Lambda_\eta\sigma(t) = \mathcal{F}\varepsilon(u_\eta(t)) + \int_0^t \mathcal{G}(\sigma(s), \varepsilon(u_\eta(s))) ds - \mathcal{M}\theta_\eta(t) \quad (59)$$

for  $\sigma \in C(0, T; \mathcal{H})$  and  $t \in [0, T]$ . For  $\sigma_1, \sigma_2 \in C(0, T; \mathcal{H})$ , we obtain for all  $t \in [0, T]$ ,

$$\|\Lambda_\eta\sigma_1 - \Lambda_\eta\sigma_2\|_{\mathcal{H}} \leq L_{\mathcal{G}} \int_0^t \|\sigma_1(s) - \sigma_2(s)\| ds.$$

It follows from this inequality that for  $p$  large enough, the operator  $\Lambda_\eta^p$  is a contraction on the Banach space  $C(0, T; \mathcal{H})$  and, therefore, there exists a unique element  $\sigma_\eta \in C(0, T; \mathcal{H})$  such that  $\Lambda_\eta\sigma = \sigma_\eta$ . Moreover,  $\sigma_\eta$  is the unique solution of problem  $PV\sigma_\eta$  and, when using (57), the regularity of  $u_\eta$ , the regularity of  $\theta_\eta$  and the properties of the operators  $\mathcal{F}$  and  $\mathcal{G}$ , it follows that  $\sigma_\eta \in C^1(0, T; \mathcal{H})$ .

Consider now  $\eta_1, \eta_2 \in C(0, T; \mathcal{H})$  and for  $i = 1, 2$ , denote  $u_{\eta_i} = u_i, \sigma_{\eta_i} = \sigma_i$  and  $\theta_{\eta_i} = \theta_i$ . We have

$$\sigma_i(t) = \mathcal{F}\varepsilon(u_i(t)) + \int_0^t \mathcal{G}(\sigma_i(s), \varepsilon(u_i(s))) ds - \mathcal{M}\theta_i(t), \quad \forall t \in [0, T],$$

and, using the properties (23) and (24) of  $\mathcal{F}$  and  $\mathcal{G}$ , we find

$$\begin{aligned} \|\sigma_1(t) - \sigma_2(t)\|_{\mathcal{H}}^2 & \leq C(\|u_1(t) - u_2(t)\|_V^2 + \int_0^t \|\sigma_1(s) - \sigma_2(s)\|_{\mathcal{H}}^2 ds \\ & + \int_0^t \|u_1(s) - u_2(s)\|_V^2 ds + \|\theta_1(t) - \theta_2(t)\|_{L^2(\Omega)}^2) \quad \forall t \in [0, T]. \end{aligned}$$

We use the Gronwall argument in the obtained inequality to deduce the estimate (58).

Finally, we consider the operator  $\Lambda : C(0, T; \mathcal{H}) \rightarrow C(0, T; \mathcal{H})$  defined by

$$\Lambda \eta = \int_0^t \mathcal{G}(\sigma_\eta(s), \varepsilon(u_\eta(s))) ds - \mathcal{M}\theta_\eta. \tag{60}$$

Here, for every  $\eta \in C(0, T; \mathcal{H})$ ,  $u_\eta, \theta_\eta$  and  $\sigma_\eta$  represent the displacement field, the temperature field and the stress field which are obtained in Lemma 4.1, Lemma 4.2 and Lemma 4.3, respectively. We have the following result.

**Lemma 4.4** *The operator  $\Lambda$  has a unique fixed point  $\eta^* \in C(0, T; \mathcal{H})$  such that  $\Lambda \eta^* = \eta^*$ .*

**Proof.** Let now  $\eta_1, \eta_2 \in C(0, T; \mathcal{H})$ . We use the notation  $u_{\eta_i} = u_i$ ,  $\dot{u}_{\eta_i} = v_{\eta_i} \doteq v_i$ ,  $\theta_{\eta_1} = \dot{\theta}_{\eta_1}$  and  $\sigma_{\eta_i} = \sigma_i$  for  $i = 1, 2$ . Using (24), (20), (29) and (60), we deduce that

$$\begin{aligned} \|\Lambda \eta_1(t) - \Lambda \eta_2(t)\|_{\mathcal{H}}^2 &\leq C \left( \int_0^t \|\sigma_1(s) - \sigma_2(s)\|_{\mathcal{H}}^2 ds + \int_0^t \|u_1(s) - u_2(s)\|_V^2 ds \right. \\ &\quad \left. + \|\theta_1(t) - \theta_2(t)\|_{L^2(\Omega)}^2 \right). \end{aligned} \tag{61}$$

We use the estimate (58) to obtain

$$\begin{aligned} \|\Lambda \eta_1(t) - \Lambda \eta_2(t)\|_{\mathcal{H}}^2 &\leq C \left( \int_0^t \|u_1(s) - u_2(s)\|_V^2 ds + \|\theta_1(t) - \theta_2(t)\|_{L^2(\Omega)}^2 \right. \\ &\quad \left. + \int_0^t \|\theta_1(s) - \theta_2(s)\|_{L^2(\Omega)}^2 ds \right). \end{aligned}$$

Moreover, from (40), we obtain

$$\begin{aligned} (\mathcal{A}\varepsilon(v_1) - \mathcal{A}\varepsilon(v_2), \varepsilon(v_1) - \varepsilon(v_2))_{\mathcal{H}} - (\mathcal{F}\varepsilon(u_1) - \mathcal{F}\varepsilon(u_2), \varepsilon(v_2) - \varepsilon(v_1))_{\mathcal{H}} \\ - (\eta_1(t) - \eta_2, \varepsilon(v_2) - \varepsilon(v_1))_{\mathcal{H}} \leq j(v_1, v_2) - j(v_1, v_1) + j(v_2, v_1) - j(v_2, v_2). \end{aligned}$$

We use the assumptions (22), (23) and the estimation (48) to find that

$$\begin{aligned} m_{\mathcal{A}} \|v_1 - v_2\|_V^2 &\leq L_{\mathcal{F}} \|u_1 - u_2\|_V \|v_1 - v_2\|_V + \|\eta_1 - \eta_2\|_{\mathcal{H}} \|v_1 - v_2\|_V \\ &\quad + c_0^2 L_{\nu} (\|\mu\|_{L^\infty(\Gamma_3)} + 1) \|v_1 - v_2\|_V^2. \end{aligned}$$

Then, by (49), we have

$$\|v_1 - v_2\|_V \leq C (\|u_1 - u_2\|_V + \|\eta_1 - \eta_2\|_{\mathcal{H}}). \tag{62}$$

Since

$$u_i(t) = \int_0^t v_i(s) ds + u_0 \quad \forall t \in [0, T],$$

we have

$$\|u_1(t) - u_2(t)\|_V \leq C \int_0^t \|v_1(s) - v_2(s)\|_V ds. \tag{63}$$

Next, we use (62), (63) and we apply Gronwall's inequality to deduce

$$\|v_1(t) - v_2(t)\|_V^2 \leq C \|\eta_1(t) - \eta_2(t)\|_{\mathcal{H}}^2, \tag{64}$$

and from (56) and (64), we obtain

$$\|\theta_1(t) - \theta_2(t)\|_{L^2(\Omega)}^2 \leq C \int_0^t \|\eta_1(s) - \eta_2(s)\|_{\mathcal{H}}^2 ds. \tag{65}$$

We substitute (63),(64) and (65) to obtain

$$\|\Lambda\eta_1 - \Lambda\eta_2\|_{\mathcal{H}}^2 \leq C \int_0^t \|\eta_1(s) - \eta_2(s)\|_{\mathcal{H}}^2 ds.$$

Reiterating this inequality  $m$  times leads to

$$\|\Lambda^m\eta_1 - \Lambda^m\eta_2\|_{C(0,T;\mathcal{H})}^2 \leq \frac{C^m T^m}{m!} \|\eta_1 - \eta_2\|_{C(0,T;\mathcal{H})}^2.$$

For  $m$  sufficiently large,  $\Lambda^m$  is a contraction on the Banach space  $C(0,T;\mathcal{H})$ , and so  $\Lambda$  has a unique fixed point.

Now, we have all the ingredients needed to prove Theorem 4.1.

**Proof. Existence.** Let  $\eta^* \in C(0,T;\mathcal{H})$  be the fixed point of  $\Lambda$  defined by (60), and let  $u_{\eta^*}$ ,  $\sigma_{\eta^*}$  and  $\theta_{\eta^*}$  be the solutions of the problems  $PV_{\eta^*}$ ,  $PV\sigma_{\eta^*}$  and  $QV_{\eta^*}$ , respectively, for  $\eta = \eta^*$ , and denote

$$u = u_{\eta^*}, \quad \dot{u} = \dot{u}_{\eta^*}, \quad \theta = \theta_{\eta^*}, \quad (66)$$

$$\sigma = \mathcal{A}\varepsilon(\dot{u}) + \mathcal{F}\varepsilon(u) + \sigma_{\eta^*}. \quad (67)$$

We prove that  $(u, \sigma, \theta)$  satisfies (34)-(37) and (38)-(39). Indeed, we write (57) for  $\eta = \eta^*$  and use (66)-(67) to obtain (34). We consider (40) for  $\eta = \eta^*$  and use the equality  $\Lambda\eta^* = \eta^*$  combined with (60) and (66)-(67) to conclude that (35) is satisfied. We write (53) for  $\eta = \eta^*$  and use (66) to find that (36) is also satisfied. Next, (37) and the regularities (38)-(39) follow from Lemmas 4.1 and 4.2. The regularity of  $\sigma$  is a consequence of Lemmas 4.1, 4.2, 4.3, the relations (66)-(67) and the assumptions on  $\mathcal{A}$  and  $\mathcal{F}$ .

**Uniqueness.** The uniqueness of the solution is a consequence of the uniqueness of the fixed point of the operator  $\Lambda$  defined by (60) and the unique solvability of the problems  $PV_{\eta}$ ,  $QV_{\eta}$  and  $PV\sigma_{\eta}$ .

## 5 Convergence Results

In this section, we study the dependence of the solution to problem  $PV$  when we introduce the perturbation of certain data. We suppose that the assumptions (22)-(30) are satisfied. Moreover, we assume that  $L_{\nu}(\|\mu\|_{L^{\infty}(\Gamma_3)} + 1) < L_0$ , where  $L_0 = \frac{m_A}{c_0^2}$ . Let  $(u, \sigma, \theta)$  be the solution of  $PV$  which is obtained by Theorem 4.1 for every  $\rho > 0$ , let  $\mathcal{F}_{\rho}$ ,  $p_{\nu}^{\rho}$  and  $L_{\nu}^{\rho}$  be the perturbations of  $\mathcal{F}$ ,  $p_{\nu}$  and  $L_{\nu}$ , respectively, which satisfy the conditions (23) and (25).

We define the function  $j_{\rho} : V \times V \rightarrow \mathbb{R}$  by

$$j_{\rho}(u, v) = \int_0^t p_{\nu}^{\rho}(u_{\nu}) \cdot v_{\nu} da + \int_0^t \mu p_{\nu}^{\rho}(u_{\nu}) \cdot \|v_{\tau}\| da \quad \forall u, v \in V. \quad (68)$$

Under these assumptions, we consider the following variational problem.

**Problem  $PV_{\rho}$ .** Find a displacement field  $u_{\rho} : [0, T] \rightarrow V$ , a stress field  $\sigma_{\rho} : [0, T] \rightarrow \mathcal{H}$  and a temperature field  $\theta_{\rho} : [0, T] \rightarrow E$  such that for all  $t \in [0, T]$ ,

$$\sigma_{\rho}(t) = \mathcal{A}\varepsilon(\dot{u}_{\rho}(t)) + \mathcal{F}\varepsilon(u_{\rho}(t)) + \int_0^t \mathcal{G}(\sigma_{\rho}(s) - \mathcal{A}\varepsilon(\dot{u}_{\rho}(s)), \varepsilon(u_{\rho}(s))) ds - \mathcal{M}\theta_{\rho}(t). \quad (69)$$

$$(\sigma_\rho(t), \varepsilon(v) - \varepsilon(\dot{u}_\rho))_{\mathcal{H}} + j_\rho(\dot{u}_\rho(t), v) - j_\rho(\dot{u}_\rho(t), \dot{u}_\rho(t)) \geq (f(t), v - \dot{u}_\rho(t))_V. \tag{70}$$

$$\dot{\theta}_\rho(t) + K\theta_\rho(t) = R\dot{u}_\rho(t) + Q(t) \text{ in } E', \tag{71}$$

$$u_\rho(0) = u_0, \quad \theta_\rho(0) = \theta_0. \tag{72}$$

Assume that

$$L_\nu^\rho(\|\mu\|_{L^\infty(\Gamma_3)} + 1) < L_0 \quad \forall \rho > 0.$$

We deduce from Theorem 4.1 that for each  $\rho > 0$ , the problem  $PV_\rho$  has a unique solution  $(u_\rho, \sigma_\rho, \theta_\rho)$  satisfying  $u_\rho \in C^1([0, T], V)$ ,  $\sigma_\rho \in C([0, T], \mathcal{H}_1)$  and  $\theta_\rho \in W^{1,2}(0, T; E') \cap L^2(0, T; E) \cap C(0, T; L^2(\Omega))$ .

Let us suppose  $\mathcal{F}_\rho, \mathcal{F}, p_\nu^\rho$  and  $p_\nu$  satisfy the following assumptions:

$$\left\{ \begin{array}{l} \text{There exists } B : \mathbb{R}_+ \rightarrow \mathbb{R}_+ \text{ such that} \\ a) \|\mathcal{F}_\rho(x, \varepsilon) - \mathcal{F}(x, \varepsilon)\| \leq B(\rho) \\ \forall \varepsilon \in S^d, \text{ a.e. } x \in \Omega, \text{ for each } \rho > 0. \\ b) \lim_{\rho \rightarrow 0} B(\rho) = 0. \end{array} \right. \tag{73}$$

$$\left\{ \begin{array}{l} \text{There exists } G_\nu : \mathbb{R}_+ \rightarrow \mathbb{R}_+ \text{ such that} \\ a) |p_\nu^\rho(x, r) - p_\nu(x, r)| \leq G_\nu(\rho) \\ \forall r \in \mathbb{R}, \text{ a.e. } x \in \Gamma_3, \text{ for each } \rho > 0. \\ b) \lim_{\rho \rightarrow 0} G_\nu(\rho) = 0. \end{array} \right. \tag{74}$$

We have the following convergence result.

**Theorem 5.1** *Assume that (73)-(74) hold, the solution  $(u_\rho, \sigma_\rho, \theta_\rho)$  of the problem  $PV_\rho$  converges to the solution  $(u, \sigma, \theta)$  of problem  $PV_\eta$ ,*

$$u_\rho \rightarrow u \text{ in } C^1(0, T; V) \text{ as } \rho \rightarrow 0; \tag{75}$$

$$\sigma_\rho \rightarrow \sigma \text{ in } C(0, T; \mathcal{H}_1) \text{ as } \rho \rightarrow 0; \tag{76}$$

$$\theta_\rho \rightarrow \theta \text{ in } C(0, T; L^2(\Omega)) \text{ as } \rho \rightarrow 0. \tag{77}$$

In addition to the mathematical interest of convergence result (75)-(77), it is important in mechanical applications because it indicates that small perturbations of the contact conditions and of the elasticity operator lead to small perturbations of the weak solution of the problem  $P$ .

**Proof.** Let  $\rho > 0$  and  $t \in [0, T]$ , we use  $v = \dot{u}(t)$  in (70) and  $v = \dot{u}_\rho(t)$  in (35), then in addition to the two inequalities, we get

$$(\sigma_\rho(t) - \sigma(t), \varepsilon(\dot{u}_\rho(t)) - \varepsilon(\dot{u}(t)))_{\mathcal{H}} \leq j_\rho(\dot{u}_\rho(t), \dot{u}(t)) - j_\rho(\dot{u}_\rho(t), \dot{u}_\rho(t)) + j(\dot{u}(t), \dot{u}_\rho(t)) - j(\dot{u}(t), \dot{u}(t)). \tag{78}$$

We have

$$\sigma_\rho^R(t) = \sigma_\rho(t) - \mathcal{A}\varepsilon(\dot{u}_\rho(t)), \quad \sigma^R(t) = \sigma(t) - \mathcal{A}\varepsilon(\dot{u}(t)), \tag{79}$$

where

$$\sigma_\rho^R(t) = \mathcal{F}_\rho \varepsilon(u_\rho(t)) + \int_0^t \mathcal{G}(\sigma_\rho^R(s), \varepsilon(u_\rho(s))) ds - \mathcal{M}\theta_\rho(t), \tag{80}$$

$$\sigma^R(t) = \mathcal{F}\varepsilon(u(t)) + \int_0^t \mathcal{G}(\sigma^R(s), \varepsilon(u(s))) ds - \mathcal{M}\theta(t). \quad (81)$$

We combine (78) and (79) to obtain

$$\begin{aligned} & (\mathcal{A}\varepsilon(\dot{u}_\rho(t)) - \mathcal{A}\varepsilon(\dot{u}(t)), \varepsilon(\dot{u}_\rho(t)) - \varepsilon(\dot{u}(t)))_{\mathcal{H}} + (\sigma_\rho^R(t) - \sigma^R(t), \varepsilon(\dot{u}_\rho(t)) - \varepsilon(\dot{u}(t)))_{\mathcal{H}} \\ & \leq j_\rho(\dot{u}_\rho(t), \dot{u}(t)) - j_\rho(\dot{u}_\rho(t), \dot{u}_\rho(t)) + j(\dot{u}(t), \dot{u}_\rho(t)) - j(\dot{u}(t), \dot{u}(t)). \end{aligned} \quad (82)$$

Moreover, from (22), it follows that for a.e.  $t \in [0, T]$ ,

$$(\mathcal{A}\varepsilon(\dot{u}_\rho(t)) - \mathcal{A}\varepsilon(\dot{u}(t)), \varepsilon(\dot{u}_\rho(t)) - \varepsilon(\dot{u}(t)))_{\mathcal{H}} \geq m_{\mathcal{A}} \|\dot{u}_\rho(t) - \dot{u}(t)\|_V^2. \quad (83)$$

Using (80) and (81), we get

$$\begin{aligned} \sigma_\rho^R(t) - \sigma^R(t) &= \mathcal{F}_\rho \varepsilon(u_\rho(t)) - \mathcal{F}\varepsilon(u(t)) + \int_0^t \mathcal{G}(\sigma_\rho^R(s), \varepsilon(u_\rho(s))) ds \\ &\quad - \int_0^t \mathcal{G}(\sigma^R(s), \varepsilon(u(s))) ds + \mathcal{M}\theta(t) - \mathcal{M}\theta_\rho(t). \end{aligned}$$

We now use (20), (23), (24), (29) and (73) to obtain

$$\begin{aligned} \|\sigma_\rho^R(t) - \sigma^R(t)\|_{\mathcal{H}} &\leq B(\rho) + L_{\mathcal{F}} \|u_\rho(t) - u(t)\|_V + L_{\mathcal{G}} \int_0^t \|\sigma_\rho^R(s) - \sigma^R(s)\|_{\mathcal{H}} ds \\ &\quad + L_{\mathcal{G}} \int_0^t \|u_\rho(s) - u(s)\|_V ds + \|\mathcal{M}\| \|\theta_\rho(t) - \theta(t)\|_{L^2(\Omega)}. \end{aligned}$$

By the Gronwall inequality, we find

$$\begin{aligned} \|\sigma_\rho^R(t) - \sigma^R(t)\|_{\mathcal{H}} &\leq B(\rho) + L_{\mathcal{F}} \|u_\rho(t) - u(t)\|_V \\ &\quad + L_{\mathcal{G}} \int_0^t \|u_\rho(s) - u(s)\|_V ds + \|\mathcal{M}\| \|\theta_\rho(t) - \theta(t)\|_{L^2(\Omega)}. \end{aligned} \quad (84)$$

From (71) and (36), we obtain

$$\|\theta_\rho(t) - \theta(t)\|_{L^2(\Omega)}^2 \leq C \int_0^t \|\dot{u}_\rho(s) - \dot{u}(s)\|_V^2 ds. \quad (85)$$

The estimation (84) becomes

$$\|\sigma_\rho^R(t) - \sigma^R(t)\|_{\mathcal{H}} \leq B(\rho) + C \left( \int_0^t \|\dot{u}_\rho(s) - \dot{u}(s)\|_V ds + \|\theta_\rho(t) - \theta(t)\|_{L^2(\Omega)} \right). \quad (86)$$

We use (85), the inequality (86) shows that

$$\begin{aligned} & -(\sigma_\rho^R(t) - \sigma^R(t), \varepsilon(\dot{u}_\rho(t)) - \varepsilon(\dot{u}(t)))_{\mathcal{H}} \\ & \leq (B(\rho) + C \int_0^t \|\dot{u}_\rho(s) - \dot{u}(s)\|_V ds) \|\dot{u}_\rho(t) - \dot{u}(t)\|_V \quad \text{a.e. } t \in [0, T]. \end{aligned} \quad (87)$$

We use the definition of  $j$  and  $j_\rho$ , (73)(a) and (24)(b), we find

$$\begin{aligned} & j_\rho(\dot{u}_\rho(t), \dot{u}(t)) - j_\rho(\dot{u}_\rho(t), \dot{u}_\rho(t)) + j(\dot{u}(t), \dot{u}_\rho(t)) - j(\dot{u}(t), \dot{u}(t)) \\ & \leq \int_{\Gamma_3} (p_\nu^\rho(\dot{u}_{\rho\nu}) - p_\nu(\dot{u}_\nu)) (\dot{u}_\nu - \dot{u}_{\rho\nu}) da + \int_{\Gamma_3} (\mu p_\nu^\rho(\dot{u}_{\rho\nu}) - \mu p_\nu(\dot{u}_\nu)) (\|\dot{u}_\tau\| - \|\dot{u}_{\rho\tau}\|) da \\ & \leq \int_{\Gamma_3} |p_\nu^\rho(\dot{u}_{\rho\nu}) - p_\nu(\dot{u}_\nu)| |\dot{u}_\nu - \dot{u}_{\rho\nu}| da + \int_{\Gamma_3} |\mu p_\nu^\rho(\dot{u}_{\rho\nu}) - \mu p_\nu(\dot{u}_\nu)| \|\dot{u}_\tau\| - \|\dot{u}_{\rho\tau}\| da. \end{aligned}$$

Then we use (74) and after some calculations, we get

$$\begin{aligned} & j_\rho(\dot{u}_\rho(t), \dot{u}(t)) - j_\rho(\dot{u}_\rho(t), \dot{u}_\rho(t)) + j(\dot{u}(t), \dot{u}_\rho(t)) - j(\dot{u}(t), \dot{u}(t)) \\ & \leq \text{meas}(\Gamma_3)^{\frac{1}{2}} c_0 (1 + \|\mu\|_{L^\infty(\Gamma_3)}) G_\nu(\rho) \|\dot{u}_\rho(t) - \dot{u}(t)\|_V \\ & \quad + c_0^2 (1 + \|\mu\|_{L^\infty(\Gamma_3)}) L_\nu \|\dot{u}_\rho(t) - \dot{u}(t)\|_V^2. \end{aligned} \quad (88)$$

We use (82), (83), (87) and (88) to obtain

$$\begin{aligned} \|\dot{u}_\rho(t) - \dot{u}(t)\|_V &\leq \frac{1}{m_{\mathcal{A}} - c_0^2(1 + \|\mu\|_{L^\infty(\Gamma_3)})L_\nu} B(\rho) \\ &+ \frac{C}{m_{\mathcal{A}} - c_0^2(1 + \|\mu\|_{L^\infty(\Gamma_3)})L_\nu} \int_0^t \|\dot{u}_\rho(s) - \dot{u}(s)\|_V ds + \frac{\text{meas}(\Gamma_3)^{\frac{1}{2}} c_0(1 + \|\mu\|_{L^\infty(\Gamma_3)})}{m_{\mathcal{A}} - c_0^2(1 + \|\mu\|_{L^\infty(\Gamma_3)})L_\nu} G_\nu(\rho), \end{aligned}$$

this inequality implies that

$$\|\dot{u}_\rho(t) - \dot{u}(t)\|_V \leq \delta (B(\rho) + G_\nu(\rho)) + \frac{C}{m_{\mathcal{A}} - c_0^2(1 + \|\mu\|_{L^\infty(\Gamma_3)})L_\nu} \int_0^t \|\dot{u}_\rho(s) - \dot{u}(s)\|_V ds,$$

where  $\delta = \max \left\{ \frac{1}{m_{\mathcal{A}} - c_0^2(1 + \|\mu\|_{L^\infty(\Gamma_3)})L_\nu}, \frac{\text{meas}(\Gamma_3)^{\frac{1}{2}} c_0(1 + \|\mu\|_{L^\infty(\Gamma_3)})}{m_{\mathcal{A}} - c_0^2(1 + \|\mu\|_{L^\infty(\Gamma_3)})L_\nu} \right\}$ .

Using the Gronwall inequality, we find

$$\|\dot{u}_\rho(t) - \dot{u}(t)\|_V \leq c (B(\rho) + G_\nu(\rho)). \tag{89}$$

We integrate (89) over  $(0, t)$ , using (52), (37) and (72), we get

$$\|u_\rho - u\|_V \leq c \int_0^t \|\dot{u}_\rho(s) - \dot{u}(s)\|_V ds \leq c (B(\rho) + G_\nu(\rho)). \tag{90}$$

It results from (90), (73)(b) and (74)(b) that (75) is satisfied.

It follows from (79) that

$$\sigma_\rho(t) - \sigma = \sigma_\rho^R(t) - \sigma^R(t) + \mathcal{A}\varepsilon(\dot{u}_\rho(t)) - \mathcal{A}\varepsilon(\dot{u}(t)), \quad a.e \ t \in [0, T].$$

We use this inequality, the properties (22) of the operator  $\mathcal{A}$ , (87), (73) and (75), we see that (76) is satisfied. We conclude that (77) is a consequence of (85), (90), (73)(b) and (74)(b).

## 6 Conclusion

Contact problems involving bodies arise in many industrial processes as well as in everyday life. For this reason, they have been widely studied in the recent years, with various constitutive laws and boundary conditions, including the normal compliance condition associated to a version of Coulomb’s friction law. The studies concern the mechanical, mathematical and numerical modeling of the corresponding boundary value problems. In this paper, we consider a mathematical model which describes a quasistatic frictional contact between a body and a foundation. We study an elasto-viscoplastic material with thermal effects. The frictional contact is modeled with a normal damped response condition associated to a version of Coulomb’s law of dry friction. These non standard contact conditions could model the contact with the deformable foundation covered by a lubricant, say oil, as already mentioned. We derive a variational formulation of the problem and prove that the proposed model has a unique weak solution by using evolutionary quasivariational inequality. Also, we study the dependence of the solution on the data and prove a convergence result.

## References

- [1] A. Amassad, K. L. Kuttler, M. Rochdi and M. Shillor. Quasistatic thermoviscoelastic contact problem with slip dependent friction coefficient. *Math. Comput. Model.* **36** (7-8) (2002) 839–854.
- [2] C. Baiocchi and A. Capelo. *Variational and Quasivariational Inequalities: Application to free Boundary Problems*. Wiley-Interscience, Chichester-New York, 1984.
- [3] O. Chau and B. Awbi. Quasistatic thermoviscoelastic frictional contact problem with damped response. *Appl. Anal.* **83** (6) (2004) 635–648.
- [4] M. Frémond. *Non-Smooth Thermomechanics*. Springer, Berlin, 2002.
- [5] I. M. L. Gossa, T. Hadj Ammar and K. Saoudi. A Dynamic Contact Problem between Viscoelastic Piezoelectric Bodies with Friction and Damage. *Nonlinear Dynamics and Systems Theory* **22** (5) (2022) 522–537.
- [6] W. Han and M. Sofonea. Analysis and numerical approximation of an elastic frictional contact problem with normal compliance. *Applicationes Mathematicae* **26** (4) (1999) 415–435.
- [7] W. Han and M. Sofonea. Evolutionary variational inequalities arising in viscoelastic contact problems. *SIAM J. Numer. Anal.* **38** (2000) 556–579.
- [8] K. Kuttler, Y. Renard and M. Shillor. Models and simulations of dynamic frictional contact. *Comput. Meth. Appl. Mech. Eng.* **177** (1999) 259–272.
- [9] N. Kikuchi and J. T. O. Den. *Contact Problems in Elasticity: A Study of Variational Inequalities and Finite Element Methods*. SIAM, Philadelphia, 1988.
- [10] M. Selmani and L. Selmani. Frictional contact problem for elastic-viscoplastic materials with thermal effect *Appl. Math. Mech. (Engl. Ed.)* **34** (6) (2013) 761–776. DOI 10.1007/s10483-013-1705-7.
- [11] M. Selmani and L. Selmani. On a frictional contact problem with adhesion in piezoelectricity. *Bulletin of the Belgian Mathematical Society, Simon Stevin* **23** (2016) 263–284.
- [12] M. Selmani and L. Selmani. Analysis of a frictionless contact problem for elastic-viscoplastic material. *Nonlinear Analysis: Modelling and Control* **17** (1) 2012 99–117.
- [13] M. Shillor, M. Sofonea and J. J. Telega. *Models and Analysis of Quasistatic Contact*. Lecture Notes in Physics Springer, Berlin Heidelberg, 2004. <https://doi.org/10.1007/b99799>.
- [14] S. Smata and N. Lebri. Frictional Contact Problem for Thermoviscoelastic Material with Internal State Variable and Wear. *Nonlinear Dynamics and Systems Theory* **22** (5) (2022) 573–585.
- [15] M. Sofonea, W. Han and M. Shillor. *Analysis and Approximation of Contact Problems with Adhesion or Damage*. Chapman-Hall/ CRC, New York (2006).
- [16] M. Sofonea and A. Matei. *Mathematical Models in Contact Mechanics*. London Mathematical Society Lecture Note Series, Vol. 398, Cambridge University Press, Cambridge, 2012.
- [17] M. Sofonea. Quasistatic processes for Elastic-Viscoplastic Materials with Internal state Variables. *Annales Scientifiques de l'Université Clermont-Ferrand 2, Tome 94, Série Mathématiques*, (1989) 47–60.
- [18] M. Sofonea. *Functional Methods in Thermo-Elasto-Visco-Plasticity*. Ph. D. Thesis, Univ of Bucharest, 1988 (in Romania).
- [19] N. Strömberg. *Thermomechanical modelling of tribological systems*, Ph.D. Thesis, No. 497, Linköping University, Sweden, 1997.
- [20] A. Touzaline. Study of a viscoelastic frictional contact problem with adhesion. *Commentationes Mathematicae Universitatis Carolinae* **52** (2) (2011) 257–272, Persistent URL: <http://dml.cz/dmlcz/141499>.



# Implementation of Infeasible Interior-Point Methods Based on a New Search Direction

L. Derbal

*Department of Mathematics, University of Ferhat Abbas Setif 1.*

Received: March 22, 2023; Revised: May 6, 2023

**Abstract:** In this paper, we present the implementation of infeasible interior-point methods (IIPMs) for linear and nonlinear optimization with the full-Newton step based on an algebraic equivalent transformation (AET). The algorithm was implemented in Matlab language, thus supporting the effectiveness of the method. Numerical tests demonstrate the behavior of the algorithms for different results of parameters.

**Keywords:** *infeasible interior-point methods; nonlinear systems; primal-dual methods; new search direction; nonlinear resonances.*

**Mathematics Subject Classification (2010):** 90C05, 90C51, 93C10, 70K30.

## 1 Introduction

Linear optimization (LO) has numerous applications in different fields such as economics, logistics, engineering, nonlinear dynamics and systems (see, *e.g.*, [6], [7]). The classical method for solving LO problems is the simplex algorithm proposed by Dantzig [2] in 1947. The appearance of interior-point algorithms (IPAs) in LO is the result of a longer process. From the literature, we know that the first result is due to Frisch, who proposed the use of logarithmic barrier functions in LO [8]. Later on Fiacco and McCormick [5] developed the sequential unconstrained minimization technique (SUMT). Since then, the barrier functions have been extensively studied.

The result of Karmarkar obtained in 1984 [9] had a great impact on mathematical optimization from both theoretical and practical point of view. He derived projective scaling IPAs with better complexity than the ellipsoid algorithm and he claimed that his algorithm had better practical performance. Moreover, it turned out that the IPA

---

\* Corresponding author: <mailto:louiza.dербal@univ-setif.dz>.

approach to LO has a natural generalisation to the related field of convex nonlinear optimisation, which resulted in a new stream of research and an excellent monograph of Nesterov and Nemirovski [13]. This study opened the way into other new subfields of optimization such as semidefinite optimization (SDO), convex quadratic optimization (CQO), second-order cone optimization (SOCO), symmetric optimization (SO) and the complementarity problem (CP), with important applications in system theory, discrete optimization, and many other areas. The most important results related to IPAs for LO were summarized in the monographs written by Roos, Terlaky and Vial [16], Wright [19] and Ye [20]. Based on the starting point, two types of IPAs exist; feasible and infeasible algorithm. Feasible IPAs start from a feasible interior point and maintain feasibility during the whole process of the algorithms. Infeasible IPAs start from an infeasible interior point and they use two kinds of steps, feasibility and centering steps in each iteration. The first infeasible algorithms were introduced by Lustig [12] and Tanabe [18]. Kojima et al. [11] analyzed the complexity of these algorithms. In 2005, Roos [14] proposed a new algorithm, which uses only the full-Newton steps and starts from infeasible points. Takács [17] gave an application of infeasible interior-point algorithms. Several implementations of IPAs can be found in state-of-the-art solvers nowadays. The paper presents an implementation of original Roos's infeasible algorithm [2006, 2016], and a short updating algorithm [10], where the AET technique is used with the new function  $\psi(t) = t^2$  to transform the central path equation. Numerical results show that the algorithm with the practical step size is more efficient than that with the fixed (theoretical) step size.

The outline of the paper is as follows. In Section 2, we briefly recall the new search direction based on the type of AET using the new function  $\psi(t) = t^2$ . In Section 3, we report some preliminary numerical results to demonstrate the computational performance of the proposed methods. Finally, some conclusions and remarks are made in Section 4.

We use the following notations throughout the paper:  $\mathbb{R}^n$  is the  $n$ -dimensional Euclidean space with the inner product  $\langle \cdot, \cdot \rangle$  and  $\|\cdot\|$  is the Euclidean norm which denotes the 2-norm,  $\mathbb{R}^{m \times n}$  is the space of matrices of order  $m \times n$ ,  $x_i$  is the  $i$ -th component of  $x$ ,  $xs$  is the component-wise product of vector  $x$  and  $s$ , respectively. The vector of ones is denoted by  $e$ .

## 2 Formulation of the Problem

We consider the LO problem in standard form

$$\min \{c^T x : Ax = b, \quad x \geq 0\}, \quad (P)$$

and its dual form

$$\max \{b^T y : A^T y + s = c, \quad s \geq 0\}, \quad (D)$$

where  $A \in \mathbb{R}^{m \times n}$  with  $\text{rank}(A) = m$ ,  $b \in \mathbb{R}^m$  and  $c \in \mathbb{R}^n$  with  $y \in \mathbb{R}^m$  and  $s \in \mathbb{R}^n$ .

As usual, for IIPMs, we consider the starting point  $(x^0, y^0, s^0) = \xi(e, 0, e)$  such that

$$\|(x^*, s^*)\|_\infty \leq \xi \Leftrightarrow 0 \leq x^* \leq \xi e \text{ and } 0 \leq s^* \leq \xi e. \quad (1)$$

For some primal-dual optimal solution  $(x^*, y^*, s^*)$ ,  $e$  is the all-one vector and  $\xi$  is a positive scalar. The triple  $(x, y, s)$  is the  $\epsilon$ -solution of (P) and (D) if the norms of the residual vectors  $b - Ax$  and  $c - A^T y - s$  do not exceed  $\epsilon$ , and also  $x^T s$ .

For any  $\lambda$  with  $0 < \lambda \leq 1$ , we consider the perturbed problem  $(P_\lambda)$  defined by

$$\{\min(c - \lambda r_c^0)^T x : b - Ax = \lambda r_b^0, \quad x \geq 0\}, \tag{P_\lambda}$$

and its dual form

$$\{\max(b - \lambda r_b^0)^T y : c - A^T y - s = \lambda r_c^0, \quad s \geq 0\}, \tag{D_\lambda}$$

where  $r_b^0$  and  $r_c^0$  denote the primal and dual initial residual vectors, respectively,

$$r_b^0 = b - A\xi e \text{ and } r_c^0 = c - \xi e.$$

Note that if  $\lambda = 1$ , then  $x = x^0$  yields a strictly feasible solution of  $(P_\lambda)$ , and  $(y, s) = (y^0, s^0)$  is a strictly feasible solution of  $(D_\lambda)$ . We conclude that if  $\lambda = 1$ , then  $(P_\lambda)$  and  $(D_\lambda)$  satisfy the interior point condition (IPC), we recall and develop some new results on the scaled search directions.

**Lemma 2.1** (cf. Theorem 5.13 in [20]) *The original problems,  $(P)$  and  $(D)$ , are feasible if and only if for each  $\lambda$  satisfying  $0 < \lambda \leq 1$ , the perturbed problems  $(P_\lambda)$  and  $(D_\lambda)$  satisfy the IPC.*

Let  $(P)$  and  $(D)$  be feasible and  $0 < \lambda \leq 1$ . Then Lemma 2.1 implies that the problems  $(P_\lambda)$  and  $(D_\lambda)$  satisfy the IPC, and hence their central paths exist. This means that the system

$$\begin{cases} b - Ax = \lambda r_b^0, & x \geq 0, \\ c - A^T y - s = \lambda r_c^0, & y \in \mathbb{R}^m, \quad s \geq 0, \\ xs = \mu e \end{cases} \tag{2}$$

has a unique solution for every  $\mu > 0$ . This solution consists of the  $\mu$ -centers of the perturbed problems  $(P_\lambda)$  and  $(D_\lambda)$ . The perturbed central path can be equivalently stated as follows:

$$\begin{cases} b - Ax = \lambda r_b^0, & x \geq 0, \\ c - A^T y - s = \lambda r_c^0, & y \in \mathbb{R}^m, \quad s \geq 0, \\ \frac{xs}{\mu} = \sqrt{\frac{xs}{\mu}}. \end{cases} \tag{3}$$

From [10], we replace the third equation of system (3) by the equivalent equation  $\psi(\frac{xs}{\mu}) = \psi(\sqrt{\frac{xs}{\mu}})$ , where  $\psi$  is a real valued function differentiable on  $(k^2 \rightarrow +\infty)$ , where  $0 \leq k < 1$ , such that  $2t\psi'(t^2) - \psi'(t)$ , we get

$$\begin{cases} b - Ax = \lambda r_b^0, & x \geq 0, \\ c - A^T y - s = \lambda r_c^0, & y \in \mathbb{R}^m, \quad s \geq 0, \\ \psi(\frac{xs}{\mu}) = \psi(\sqrt{\frac{xs}{\mu}}). \end{cases} \tag{4}$$

Let  $(x, y, s)$  be a feasible solution of  $(P_\lambda)$  and  $(D_\lambda)$ . We consider the notation

$$f(x, y, s) = \begin{bmatrix} \lambda^+ r_b^0 - b + Ax \\ \lambda^+ r_c^0 - c + A^T y + s \\ \psi(\frac{xs}{\mu}) - \psi(\sqrt{\frac{xs}{\mu}}) \end{bmatrix} = 0,$$

where  $\lambda^+ = (1 - \theta)\lambda$  and  $\theta \in (0, 1)$ , a new triple

$$(x_+, y_+, s_+) = (x + \Delta x, y + \Delta y, s + \Delta s)$$

is obtained thanks to the Newton method for solving the following system:

$$\begin{cases} A\Delta x = \theta\lambda^+r_b^0, \\ A^T\Delta y + \Delta s = \theta\lambda^+r_c^0 \\ \frac{1}{\mu}(s\Delta x + x\Delta s) = \frac{-\psi\left(\frac{xs}{\mu}\right) + \psi\left(\sqrt{\frac{xs}{\mu}}\right)}{\psi'\left(\frac{xs}{\mu}\right) - \frac{1}{2\sqrt{\frac{xs}{\mu}}}\psi'\left(\sqrt{\frac{xs}{\mu}}\right)}. \end{cases} \quad (5)$$

Define the scaled search directions  $d_x$  and  $d_s$  as follows:

$$v = \sqrt{\frac{xs}{\mu}}, \quad d_x := \frac{v\Delta x}{x}, \quad d_s := \frac{v\Delta s}{s}, \quad (6)$$

then the system reduces to the system

$$\begin{cases} \bar{A}d_x = \theta\lambda^+r_b^0, \\ \bar{A}^T\frac{\Delta y}{\mu} + d_s = \theta v\lambda^+s^{-1}r_c^0, \\ d_x + d_s = p_v, \end{cases} \quad (7)$$

where

$$p_v = \frac{2\psi(v) - 2\psi(v^2)}{2v\psi'(v^2) - 2\psi'(v)} \quad \text{and} \quad \bar{A} = A \operatorname{diag}\left(\frac{x}{v}\right). \quad (8)$$

We consider the proximity measure defined by

$$\delta(v) = \delta(x, s; \mu) = \frac{\|p_v\|}{2} = \frac{1}{2} \left\| \frac{v - v^3}{2v^2 - e} \right\|, \quad (9)$$

suppose that for some  $\mu \in (0, \mu^0)$ , we have a feasible solution  $(x, y, s)$  of the problem  $(P_\lambda)$  and  $(D_\lambda)$  with  $\lambda = \frac{\mu}{\mu^0}$ , such that  $\delta(x, s; \mu) \leq \tau$ ,  $\tau \in (0, 1)$ . Then the algorithm finds the feasible solution  $(x_+, y_+, s_+)$  of  $(P_{\lambda^+})$  and  $(D_{\lambda^+})$ , where  $\lambda^+ = (1 - \theta)\lambda$  and  $\theta \in (0, 1)$ . In this case,  $\mu$  is reduced to  $\mu^+ = (1 - \theta)\mu$  and so  $\delta(x_+, y_+; \mu^+) = \delta(v^+) \leq \tau$ . If necessary, we repeat the procedure until an  $\epsilon$ -solution is found.

Now we can define the generic infeasible interior-point algorithm for LO.

**Algorithm 2.1** *The generic infeasible interior-point algorithm for LO.*

<b>Input :</b>
-Accuracy parameter $\epsilon > 0$ ,
-barrier update parameter $\theta$ barrier update parameter $\theta$ , $0 < \theta < 1$ ,
-threshold parameter $\tau > 0$ ,
<b>Begin</b>
$x = \xi e; y = 0; s = \xi e; \lambda = 1; \mu = \lambda \xi^2$ .
<b>while</b> : $\max(x^T s, \ r_b\ , \ r_c\ ) > \epsilon$ <i>do</i>
<b>Begin</b>
<i>solve the systeme (7) and use (6) to obtain <math>(\Delta x, \Delta y, \Delta s)</math>;</i>
$x = x + \Delta x;$
$y = y + \Delta y;$
$s = s + \Delta s;$
<i>update of <math>\lambda</math> and <math>\mu</math></i>
$\lambda = (1 - \theta)\lambda;$
$\mu = (1 - \theta)\mu;$
<b>end</b>
<b>end</b>

**Lemma 2.2** ([10]) *If  $\tau = \frac{1}{12}$  and  $\theta = \frac{1}{22n}$ ,  $n \geq 4$ , then  $\delta(v) \leq \tau$  implies  $\delta(v^+) \leq \tau$ .*

**Theorem 2.1** (**Theorem 1** [10]) *If (P) and (D) are feasible and  $\xi > 0$  such that  $\|(x^*, s^*)\|_\infty \leq \xi$  for some optimal solutions  $x^*$  of (P) and  $(y^*, s^*)$  of (D), then after at most*

$$22n \log \frac{\max(n\xi^2, \|r_b^0\|, \|r_c^0\|)}{\epsilon}$$

*iterations, the algorithm finds an  $\epsilon$ -optimal solution of (P) and (D).*

### 3 Numerical Results

In this section, we present an implementation of the IIPMs for LO, which demonstrates the influence of the update parameters  $\theta$  and the dimension of the problem on the number of the iterations. The algorithm is coded in MATLAB (R 2014 a) and our experiments are performed on PC with Processor Genuine Intel (R) CPR T2080 @ 1,73 GHZ installed memory (RAM) 2,00GO. In all test problems, the starting point is designated by  $(x^0, y^0, s^0) = \xi(e, 0, e)$  such that  $e = (1, 1, \dots, 1)^T$ , we use  $(m, n)$  as the size of the problem,  $\epsilon = 10^{-6}$  and  $\tau = \frac{1}{12}$  as our default accuracy parameter. The barrier update parameter  $\theta$  is a given constant between 0 and 1, while in the theoretical version of the algorithm,  $\theta = \frac{1}{22n}$ . We denote by iter the number of iterations and by CPU the computing time in seconds. The primal and dual optimal solutions are denoted by  $x^*$ ,  $(y^*, s^*)$ , we tested the above mentioned algorithms in two different cases of the test: the full Newton step ( $\alpha = 1$ ) and the practice step size  $\alpha_{\max}$ , which guarantees that the new iterates

$$\begin{cases} x_+ = x + \alpha_{\max} \Delta x, \\ s_+ = s + \alpha_{\max} \Delta s \end{cases}$$

remain nonnegative. To ensure the strict feasibility of the new iterates, we used a factor  $\rho = 0.95$  to shorten the step length, thus the used step length is  $\alpha_p = \rho\alpha_{\max}$  with  $\alpha_{\max} = \min(\alpha_x, \alpha_s)$ , or  $\alpha_x$  and  $\alpha_s$  are given by

$$\alpha_x = \begin{cases} \min\left(-\frac{x_i}{\Delta x_i}\right) & \text{if } \Delta x_i < 0, \\ 1 & \text{if } \Delta x_i \geq 0, \end{cases}$$

$$\alpha_s = \begin{cases} \min\left(-\frac{s_i}{\Delta s_i}\right) & \text{if } \Delta s_i < 0, \\ 1 & \text{if } \Delta s_i \geq 0. \end{cases}$$

### 3.1 Cases of full Newton step ( $\alpha = 1$ ) with $\theta = \frac{1}{22n}$

#### 3.1.1 Examples with fixed size

**Example 3.1**  $m = 2, n = 4$ ,

$$A = \begin{pmatrix} 1 & 1 & 1 & 1 \\ 1 & 1 & 0 & -3 \end{pmatrix}, b = (1 \ 0.5)^T, c = (1 \ 2 \ 3 \ 2 \ 4)^T.$$

The optimal solution is

$$x^* = (0.875, 0, 0, 0.125)^T, y^* = (1.75, -0.75)^T, s^* = (0, 1, 1.25, 0)^T.$$

<i>iter</i>	<i>CPU</i>
1332	0.3279

Table 1: Number of iterations and computation time.

**Example 3.2**  $m = 3, n = 6$ ,

$$A = \begin{pmatrix} 2 & 1 & 0 & -1 & 0 & 0 \\ 0 & 0 & 1 & 0 & 1 & -1 \\ 1 & 1 & 1 & 1 & 1 & 1 \end{pmatrix}, b = (0 \ 0 \ 1)^T, c = (3 \ -1 \ 1 \ 0 \ 0 \ 0)^T.$$

The optimal solution is

$$x^* = (0.0000, 0.5000, 0.0000, 0.5000, 0.0000, 0.0000)^T,$$

$$y^* = (-0.5000, -0.0383, -0.5000)^T,$$

$$s^* = (4.5000, 0.0000, 1.4617, 0.0000, 0.4617, 0.5383)^T.$$

<i>iter</i>	<i>CPU</i>
2054	0.5914

Table 2: Number of iterations and computation time.

**Example 3.3**  $m = 5, n = 9,$

$$A = \begin{pmatrix} 0 & 1 & 2 & -1 & 1 & 1 & 0 & 0 & 0 \\ 1 & 2 & 3 & 4 & -1 & 0 & 1 & 0 & 0 \\ -1 & 0 & -2 & 1 & 2 & 0 & 0 & 1 & 0 \\ 1 & 2 & 0 & -1 & -2 & 0 & 0 & 0 & 1 \\ 1 & 3 & 4 & 2 & 1 & 0 & 0 & 0 & 0 \end{pmatrix},$$

$$b = ( 1 \ 2 \ 3 \ 2 \ 1 )^T, \quad c = ( 1 \ 0 \ -2 \ 1 \ 1 \ 0 \ 0 \ 0 \ 0 )^T.$$

The optimal solution is

$$x^* = ( 0 \ 0 \ 0.25 \ 0 \ 0 \ 0.5 \ 1.25 \ 3.5 \ 2 )^T, \quad y^* = ( 0 \ 0 \ 0 \ 0 \ -0.5 )^T,$$

$$s^* = ( 1.5 \ 1.5 \ 0 \ 2 \ 1.5 \ 0 \ 0 \ 0 \ 0 )^T.$$

<i>iter</i>	<i>CPU</i>
3241	1.5285

Table 3: Number of iterations and computation time.

### 3.1.2 Examples with variable size

**Example 3.4** We consider the following example:  $n = 2m,$

$$A(i, j) = \begin{cases} 0 & \text{if } i \neq j \text{ and } i \neq j + m \\ 1 & \text{if } i = j \text{ and } i = j + m \end{cases}, \quad c(i) = -1, \quad c(i + m) = 0 \text{ and } b(i) = 2 \text{ for } i = 1, \dots, m.$$

The optimal solutions is obtained as follows:

$$x^* = \begin{cases} 2 & \text{for } i = 1, \dots, m, \\ 0 & \text{for } i = m + 1, \dots, n, \end{cases}, \quad y^* = -1 \text{ for } i = 1, \dots, n,$$

and  $s^* = \begin{cases} 0 & \text{for } i = 1, \dots, m, \\ 1 & \text{for } i = m + 1, \dots, n. \end{cases}$

We have the following results:

$(m, n)$	<i>iter</i>	<i>CPU</i>
(10, 20)	7390	6.2958
(15, 30)	11356	13.8918
(25, 50)	19493	45.4140
(50, 100)	40518	226.3179
(100, 200)	84093	1856.1149
(200, 400)	174293	61443.8710

Table 4: Number of iterations and computation time.

### 3.2 Cases of practice step size ( $\alpha_{\max}$ ) with $\theta \in (0, 1)$

In this part, to improve the numerical results, we take  $\theta \in (0, 1)$ . Then we obtain the numerical results in the following tables.

### 3.2.1 Examples with fixed size

$\theta$	<i>iter</i>	<i>CPU</i>
0.01	1514	0.3941
0.02	754	0.2678
0.05	298	0.1895
0.1	146	0.1646
0.2	70	0.1575
0.8	11	0.1868

Table 5: Number of iterations and computation time in Example 1.

$\theta$	<i>iter</i>	<i>CPU</i>
0.01	1554	0.438790
0.02	774	0.283944
0.05	306	0.190252
0.1	150	0.167571
0.2	72	0.180073
0.4	32	0.184932

Table 6: Number of iterations and computation time in Example 2.

$\theta$	<i>iter</i>	<i>CPU</i>
0.01	1633	0.7102
0.05	320	0.2167
0.02	813	0.4256
0.1	156	0.1827
0.7	15	0.2377
0.8	11	0.2349

Table 7: Number of iterations and computation time in Example 3.

### 3.2.2 Examples with variable size

$\theta$	0.01		0.05		0.1	
$(m, n)$	<i>iter</i>	<i>CPU</i>	<i>iter</i>	<i>CPU</i>	<i>iter</i>	<i>CPU</i>
(10, 20)	1664	1.0255	329	0.3340	161	0.2524
(15, 30)	1715	1.7057	337	0.4459	165	0.2990
(25, 50)	1765	2.7304	347	0.6487	170	0.4376
(50, 100)	1834	8.4164	361	1.5884	176	0.86035
(100, 200)	1903	38.0307	374	7.0592	176	4.5225
(200, 400)	1972	182.1165	388	36.1221	183	29.9616

$\theta$	0.2		0.3	
$(m, n)$	<i>iter</i>	<i>CPU</i>	<i>iter</i>	<i>CPU</i>
(10, 20)	74	0.2840	47	0.6049
(15, 30)	76	1.2352	48	0.6665
(25, 50)	78	2.1898	49	1.3937
(50, 100)	81	4.3522	–	–
(100, 200)	84	16.9204	–	–
(200, 400)	–	–	–	–

Table 8: Number of iterations and computation time in Example 4.

#### 4 Concluding Remarks

In this paper, we have proposed an implementation of the IIPMs for linear and nonlinear optimization based on the AET proposed in [10]. Some preliminary numerical results are provided to reveal the influence of the update parameters  $\theta$  and the dimension of the problem on the number of iterations. Through these results, we notice that the number of iterations and the computation time to reach the optimal solution are a bit large. To improve these results, we proposed other choices of the parameter  $\theta$  and the step size  $\alpha$  different from the theoretical values. It was found that these values decreased the number of iterations and the computation time. For further research, it is necessary to think of a simple strategy to determine the appropriate values of the parameter  $\theta$  which keeps the iteration in the interior of the feasible domain. Furthermore, this algorithm may be possible to extend to the semidefinite linear optimization, quadratic programming and linear complementarity problem with these choices of the step size.

#### Acknowledgment

The author thanks the anonymous referees and editors for their constructive comments and suggestions for improving the presentation. This work has been supported by: The General Directorate of Scientific Research and Technological Development (DGRSDT-MESRS), under project PRFU number C00L03UN190120190004. Algeria.

#### References

- [1] M. Achache. A new primal-dual path-following method for convex quadratic programming. *Comp. Appl. Math.* **25** (1) (2006) 97–110.
- [2] G. B. Dantzig. *Linear Programming and Extension*. Princeton University Press, Princeton, NJ, 1963.
- [3] L. Derbal and Z. Kebbiche. Theoretical and Numerical Result for Linear Optimization Problem Based on a New Kernel Function. *Journal of Siberian Federal University. Mathematics & Physics* **12** (2) (2019) 160–172.
- [4] L. Derbal. Implementation of Interior-point Methods for P\*(k)-LCP Based on New Search Direction. *International Journal of Informatics and Applied Mathematics* **4** (2) (2021) 35–42.
- [5] A. V. Fiacco and G. P. McCormick. *Nonlinear Programming: Sequential Unconstrained Minimization Techniques*. John Wiley & Sons, New York, 1968.

- [6] Firman, Syamsuddin Toaha and Muh Nur. Asymptotic Stability of Some Class of Affine Nonlinear Control Systems through Partial Feedback Linearization. *Nonlinear Dynamics and Systems Theory* **21** (3) (2021) 238–245.
- [7] Firman, Syamsuddin Toaha and Kasbawati. Modification of the Trajectory Following Method for Asymptotic Stability in a System Nonlinear Control. *Nonlinear Dynamics and Systems Theory* **22** (2) (2022) 169–177.
- [8] K. R. Frisch. The multiplex method for linear programming. *Sankhya. The Indian Journal of Statistics* **18** (1957) 329–362.
- [9] N. K. Karmarkar. A new polynomial-time algorithm for linear programming. In: *Proceedings of the 16th Annual ACM Symposium on Theory of Computing* **4** (1984) 373–395.
- [10] B. Kheirfam. A new search direction for full-Newton step infeasible interior-point method in linear optimization. <https://doi.org/10.48550/arXiv.2102.07223>.
- [11] M. Kojima, N. Megiddo and S. Mizuno. A primal-dual infeasible-interior-point algorithm for linear programming. *Mathematical Programming* **4** (1993) 263–280.
- [12] I. J. Lustig. Feasibility issues in a primal-dual interior-point method for linear programming. *Mathematical Programming* **49** (1-3) (1991) 145–162.
- [13] Y. Nesterov and A. Nemirovskii. *Interior Point Polynomial Methods in Convex Programming. Theory and Algorithm*, SIAM Publication, Philadelphia, USA, 1993.
- [14] C. Roos. A full-newton step  $O(n)$  infeasible interior-point algorithm for linear optimization. *SIAM J. Optim.* **16** (4) (2006) 1110–1136.
- [15] C. Roos. An improved and simplified full-Newton step  $O(n)$  infeasible interior point method for linear optimization. *SIAM J. Optim.* **25** (1) (2015) 102–114.
- [16] C. Roos, T. Terlaky and J. P. Vial. *Theory and Algorithms for Linear Optimization. An Interior-Point Approach*. John Wiley and Sons, Chichester, UK, 1997.
- [17] P.-R. Takács. Applications of infeasible interior-point algorithms. In: K. Havrelk and V. allas, eds., *A Magyar Tudomány Ünnepe 2013 Konferencia, Acta Periodica*, 175–183.
- [18] K. Tanabe. Centered newton method for linear programming: Interior and ‘exterior’ point method. In: K. Tone, ed., *New Methods for Linear Programming 3*, Institute of Statistical Mathematics, Tokyo, Japan, 1990, 98–100. [In Japanese.]
- [19] S. J. Wright. *Primal-Dual Interior-Point Methods*. SIAM, Philadelphia, USA, 1997.
- [20] Y. Ye. *Interior Point Algorithms: Theory and Analysis*. Wiley-Interscience. Series in Discrete Mathematics and Optimization, Wiley, New York, 1997.



# A Frictional Contact Problem with Wear for Two Electro-Viscoelastic Bodies

A. Djabi

*Laboratory of Applied Mathematics, Department of Basic Education, Faculty of Economic Commerce and Management Sciences, University of Ferhat Abbas-Setif 1, Setif 19000, Algeria*

Received: January 6, 2023; Revised: March 13, 2023

**Abstract:** We consider a mathematical problem for the quasistatic contact between two electro-viscoelastic bodies. The contact is modelled with a version of normal compliance and the evolution of the wear function is described by Archard's law. We derive a variational formulation for the model and prove an existence and uniqueness result of the weak solution. The proof is based on the arguments of evolutionary variational inequalities, a classical existence and uniqueness result for parabolic inequalities and the Banach fixed point theorem.

**Keywords:** *electro-viscoelastic; fixed point; friction contact; piezoelectric; wear.*

**Mathematics Subject Classification (2010):** 74H20, 74H25, 49J40, 74M15.

## 1 Introduction

A considerable progress has been achieved recently in applied mathematics and mechanics for dynamic and quasistatic problems, the recent advances in the formulation of these problems are articulated around two main components, one devoted to the laws of behavior and the other devoted to the boundary conditions imposed on the body. The boundary conditions reflect the binding of the body with the outside world. The laws of behavior are stipulated by the nature of the materials under study, The authors utilize composite laws of behavior that combine materials with varying thermal and mechanical characteristics. These materials are referred to as thermo-mechanical materials. Alternatively, the authors also consider materials with combined mechanical and electrical behavior, which are known as piezoelectric materials. For the boundary conditions, the authors investigate the real processes such as adhesion, friction and wear to describe new

---

\* Corresponding author: <mailto:djabi.zaki@yahoo.fr>

problems, these processes can be described by several types of the models with normal compliance or a normal damped response version.

The piezoelectric effect is characterized by the coupling between the mechanical and electrical behavior of the materials.

Materials undergoing piezoelectric effects are called piezoelectric materials; their study requires techniques and results from electromagnetic theory and continuum mechanics. However, there are very few mathematical results concerning contact problems involving piezoelectric materials and therefore, there is a need to extend the results to the models for contact with deformable bodies which include coupling between mechanical and electrical properties. General models for elastic materials with piezoelectric effects can be found in [4, 6, 12, 13, 15, 16]. A static frictional contact problem for electric-elastic materials was considered in [4, 15]. A frictional contact problem for electro-viscoelastic materials was studied in [13]. Contact problems with friction and adhesion for electro-elastic-viscoplastic materials were studied recently in [1].

Wear is one of the processes which reduce the lifetime of modern machine elements. It represents the unwanted removal of materials from the surfaces of contacting bodies occurring in relative motion. Wear arises when a hard rough surface slides against a softer surface, digs into it, and its asperities plough a series of grooves. When two surfaces come into contact, rearrangement of the surface asperities takes place. When they are in relative motion, some of the peaks break, and therefore, the harder surface removes the softer material. This phenomenon involves the wear of the contacting surfaces. The material loss by the wearing solids, the generation and circulation of free wear debris are the main effects of the wear process. The loose particles form a thin layer on the body surface. Tribological experiments show that this layer has a great influence on contact phenomena and the wear particles between sliding surfaces affect the frictional behavior. Realistically, wear cannot be totally eliminated.

Wear is a major problem for materials when two bodies come into contact with friction and sliding, the contact surfaces are found worn-out, the more rigid one wears out the other. The particles lost by contact surfaces form a thin layer between the two bodies, this layer can improve the sliding, it may get one body enters in the other.

Generally, a mathematical theory of friction and wear should be a generalization of experimental facts and it must be in agreement with the laws of thermodynamics of irreversible processes. The first attempts of a thermodynamical description of the friction and wear processes were provided in [3]. A bilateral frictional problem with wear for multidisciplinary bodies and foundation was studied in [6, 8, 9]. General models of quasi-static frictional contact with wear between deformable bodies were derived in [18] from thermodynamic considerations.

The goal of this paper is to analyse the coupling of two electro-viscoelastic materials and a frictional contact problem with wear. We study a quasistatic problem of frictional contact with wear. We model the materials behavior by an electro-viscoelastic constitutive law and the contact is frictional.

The paper is organized as follows. In Section 2, we introduce the notation and give some preliminaries. In Section 3, we describe the mathematical models for the frictional contact problem between two electro-viscoelastic bodies. The contact is modelled with normal compliance and wear, we introduce the list the assumptions on the problem's data and the variational formulation of the model. In Section 4, we state our main existence and uniqueness result, Theorem 4.1. The proof of the theorem is based on the arguments of evolutionary variational inequalities, a classical existence and uniqueness result on

parabolic inequalities, differential equations and the Banach fixed point theorem.

## 2 Notation and Preliminaries

In this short section, we present the notation we shall use and some preliminary material. For more details, we refer the reader to [5, 10, 17]. We denote by  $\mathbb{S}^d$  the space of second order symmetric tensors on  $\mathbb{R}^d$  ( $d = 2, 3$ ), while  $\|\cdot\|$  represents the Euclidean norm if it is applied to a vector on  $\mathbb{S}^d$  and  $\mathbb{R}^d$ , respectively. Let  $\Omega^k \subset \mathbb{R}^d$  be a bounded domain with the outer Lipschitz boundary  $\Gamma$  and let  $\nu$  denote the unit outer normal on  $\partial\Omega^k = \Gamma^k$ . We shall use the following notation.

We recall that the inner products and the corresponding norms on  $\mathbb{S}^d$  and  $\mathbb{R}^d$  are given by

$$\begin{aligned} \mathbf{u}^k \cdot \mathbf{v}^k &= u_i^k \cdot v_i^k, \quad \|\mathbf{v}^k\| = (\mathbf{v}^k \cdot \mathbf{v}^k)^{\frac{1}{2}}, \quad \forall \mathbf{u}^k, \mathbf{v}^k \in \mathbb{R}^d, \\ \boldsymbol{\sigma}^k \cdot \boldsymbol{\tau}^k &= \sigma_{ij}^k \cdot \tau_{ij}^k, \quad \|\boldsymbol{\tau}^k\| = (\boldsymbol{\tau}^k \cdot \boldsymbol{\tau}^k)^{\frac{1}{2}}, \quad \forall \boldsymbol{\sigma}^k, \boldsymbol{\tau}^k \in \mathbb{S}^d. \end{aligned}$$

Here and below, the indices  $i$  and  $j$  run between 1 and  $d$  and the summation convention over repeated indices is adopted. Now, to proceed with the variational formulation, we need the following function spaces:

$$\begin{aligned} H^k &= \{v^k = (v_i^k); v_i^k \in L^2(\Omega^k)\}, \quad H_1^k = \{v^k = (v_i^k); v_i^k \in H^1(\Omega^k)\}, \\ Q^k &= \{\boldsymbol{\tau}^k = (\tau_{ij}^k); \tau_{ij}^k = \tau_{ji}^k \in L^2(\Omega^k)\}, \quad Q_1^k = \{\boldsymbol{\tau}^k = (\tau_{ij}^k) \in Q^k; \text{div } \boldsymbol{\tau}^k \in H^k\}. \end{aligned}$$

The spaces  $H^k$ ,  $H_1^k$ ,  $Q^k$  and  $Q_1^k$  are the real Hilbert spaces endowed with the canonical inner products given by

$$\begin{aligned} (\mathbf{u}^k, \mathbf{v}^k)_{H^k} &= \int_{\Omega^k} \mathbf{u}^k \cdot \mathbf{v}^k dx, \quad (\mathbf{u}^k, \mathbf{v}^k)_{H_1^k} = \int_{\Omega^k} \mathbf{u}^k \cdot \mathbf{v}^k dx + \int_{\Omega^k} \nabla \mathbf{u}^k \cdot \nabla \mathbf{v}^k dx, \\ (\boldsymbol{\sigma}^k, \boldsymbol{\tau}^k)_{Q^k} &= \int_{\Omega^k} \boldsymbol{\sigma}^k \cdot \boldsymbol{\tau}^k dx, \quad (\boldsymbol{\sigma}^k, \boldsymbol{\tau}^k)_{Q_1^k} = \int_{\Omega^k} \boldsymbol{\sigma}^k \cdot \boldsymbol{\tau}^k dx + \int_{\Omega^k} \text{div } \boldsymbol{\sigma}^k \cdot \text{Div } \boldsymbol{\tau}^k dx \end{aligned}$$

and the associated norms  $\|\cdot\|_{H^k}$ ,  $\|\cdot\|_{H_1^k}$ ,  $\|\cdot\|_{Q^k}$ , and  $\|\cdot\|_{Q_1^k}$ , respectively. Here and below we use the notation

$$\begin{aligned} \nabla \mathbf{u}^k &= (u_{i,j}^k), \quad \varepsilon(\mathbf{u}^k) = (\varepsilon_{ij}(\mathbf{u}^k)), \quad \varepsilon_{ij}(\mathbf{u}^k) = \frac{1}{2}(u_{i,j}^k + u_{j,i}^k), \quad \forall u^k \in H_1^k, \\ \text{Div } \boldsymbol{\sigma}^k &= (\sigma_{ij,j}^k), \quad \forall \boldsymbol{\sigma}^k \in Q_1^k. \end{aligned}$$

For every element  $\mathbf{v}^k \in H_1^k$ , we also use the notation  $\mathbf{v}^k$  for the trace of  $\mathbf{v}^k$  on  $\Gamma^k$  and we denote by  $v_\nu^k$  and  $\mathbf{v}_\tau^k$  the *normal* and the *tangential* components of  $\mathbf{v}^k$  on the boundary  $\Gamma^k$  given by

$$v_\nu^k = \mathbf{v}^k \cdot \boldsymbol{\nu}^k, \quad \mathbf{v}_\tau^k = \mathbf{v}^k - v_\nu^k \boldsymbol{\nu}^k.$$

Let  $H'_{\Gamma^k}$  be the dual of  $H_{\Gamma^k} = H^{\frac{1}{2}}(\Gamma^k)^d$  and let  $(\cdot, \cdot)_{-\frac{1}{2}, \frac{1}{2}, \Gamma^k}$  denote the duality pairing between  $H'_{\Gamma^k}$  and  $H_{\Gamma^k}$ . For every element  $\boldsymbol{\sigma}^k \in Q_1^k$ , let  $\boldsymbol{\sigma}^k \boldsymbol{\nu}^k$  be the element of  $H'_{\Gamma^k}$  given by

$$(\boldsymbol{\sigma}^k \boldsymbol{\nu}^k, \mathbf{v}^k)_{-\frac{1}{2}, \frac{1}{2}, \Gamma^k} = (\boldsymbol{\sigma}^k, \varepsilon(\mathbf{v}^k))_{Q^k} + (\text{Div } \boldsymbol{\sigma}^k, \mathbf{v}^k)_{H^k}, \quad \forall \mathbf{v}^k \in H_1^k.$$

Denote by  $\sigma_\nu^k$  and  $\sigma_\tau^k$  the *normal* and the *tangential* traces of  $\boldsymbol{\sigma}^k \in Q_1^k$ , respectively. If  $\boldsymbol{\sigma}^k$  is continuously differentiable on  $\Omega^k \cup \Gamma^k$ , then

$$\begin{aligned}\sigma_\nu^k &= (\boldsymbol{\sigma}^k \boldsymbol{\nu}^k) \cdot \boldsymbol{\nu}^k, & \sigma_\tau^k &= \boldsymbol{\sigma}^k \boldsymbol{\nu}^k - \sigma_\nu^k \boldsymbol{\nu}^k, \\ (\boldsymbol{\sigma}^k \boldsymbol{\nu}^k, \mathbf{v}^k)_{-\frac{1}{2}, \frac{1}{2}, \Gamma^k} &= \int_{\Gamma^k} \boldsymbol{\sigma}^k \boldsymbol{\nu}^k \cdot \mathbf{v}^k da\end{aligned}$$

for all  $\mathbf{v}^k \in H_1^k$ , where  $da$  is the surface measure element.

For the displacement field, we need the closed subspace of  $H_1^k$  defined by

$$V^k = \{\mathbf{v}^k \in H_1^k; \mathbf{v}^k = 0 \text{ on } \Gamma_1^k\}.$$

Since  $\text{meas } \Gamma_1^k > 0$ , the following Korn's inequality holds:

$$\|\varepsilon(\mathbf{v}^k)\|_{Q^k} \geq c_K \|\mathbf{v}^k\|_{H_1^k}, \quad \forall \mathbf{v}^k \in V^k, \quad (1)$$

where the constant  $c_K$  denotes a positive constant which may depend only on  $\Omega^k$ ,  $\Gamma_1^k$  (see [17]).

Over the space  $V^k$ , we consider the inner product given by

$$(\mathbf{u}^k, \mathbf{v}^k)_{V^k} = (\varepsilon(\mathbf{u}^k), \varepsilon(\mathbf{v}^k))_{Q^k}, \quad \forall \mathbf{u}^k, \mathbf{v}^k \in V^k, \quad (2)$$

and let  $\|\cdot\|_{V^k}$  be the associated norm. It follows from Korn's inequality (1) that the norms  $\|\cdot\|_{H_1^k}$  and  $\|\cdot\|_{V^k}$  are equivalent on  $V^k$ . Then  $(V^k, \|\cdot\|_{V^k})$  is a real Hilbert space. Moreover, by the Sobolev trace theorem and (2), there exists a constant  $c_0 > 0$  depending only on  $\Omega^k$ ,  $\Gamma_1^k$  and  $\Gamma_3$  such that

$$\|\mathbf{v}^k\|_{L^2(\Gamma_3)^d} \leq c_0 \|\mathbf{v}^k\|_{V^k}, \quad \forall \mathbf{v}^k \in V^k. \quad (3)$$

We also introduce the spaces

$$\begin{aligned}W^k &= \{\psi^k \in E_1^k; \psi^k = 0 \text{ on } \Gamma_a^k\}, \\ W_1^k &= \{\mathbf{D}^k = (D_i^k); D_i^k \in L^2(\Omega^k), \text{div } \mathbf{D}^k \in L^2(\Omega^k)\}.\end{aligned}$$

Since  $\text{meas } \Gamma_a^k > 0$ , the following Friedrichs-Poincaré inequality holds:

$$\|\nabla \psi^k\|_{W^k} \geq c_F \|\psi^k\|_{H^1(\Omega^k)}, \quad \forall \psi^k \in W^k, \quad (4)$$

where  $c_F > 0$  is a constant which depends only on  $\Omega^k$ ,  $\Gamma_a^k$ . In the space  $W^k$ , we consider the inner product

$$(\varphi^k, \psi^k)_{W^k} = \int_{\Omega^k} \nabla \varphi^k \cdot \nabla \psi^k dx, \quad (5)$$

and let  $\|\cdot\|_{W^k}$  be the associated norm. It follows from (4) that  $\|\cdot\|_{H^1(\Omega^k)}$  and  $\|\cdot\|_{W^k}$  are equivalent norms on  $W^k$  and therefore  $(W^k, \|\cdot\|_{W^k})$  is a real Hilbert space. Moreover, by the Sobolev trace theorem, there exists a constant  $\mathbf{c}_0$  depending only on  $\Omega^k$ ,  $\Gamma_a^k$  and  $\Gamma_3$  such that

$$\|\zeta^k\|_{L^2(\Gamma_3)} \leq c_0 \|\zeta^k\|_{W^k}, \quad \forall \zeta^k \in W^k. \quad (6)$$

The space  $W_1^k$  is a real Hilbert space with the inner product

$$(\mathbf{D}^k, \mathbf{\Phi}^k)_{W_1^k} = \int_{\Omega^k} \mathbf{D}^k \cdot \mathbf{\Phi}^k dx + \int_{\Omega^k} \operatorname{div} \mathbf{D}^k \cdot \operatorname{div} \mathbf{\Phi}^k dx,$$

where  $\operatorname{div} \mathbf{D}^k = (\mathbf{D}_{i,i}^k)$ , and the associated norm  $\|\cdot\|_{W_1^k}$ .

To simplify the notation, we define the product spaces

$$\begin{aligned} \mathbb{V} &= V^1 \times V^2, \mathbb{H} = H^1 \times H^2, \quad \mathbb{H}_1 = H_1^1 \times H_1^2, \\ \mathbb{Q} &= Q^1 \times Q^2, \quad \mathbb{Q}_1 = Q_1^1 \times Q_1^2, \quad \mathbb{W} = W^1 \times W^2, \mathbb{W}_1 = W_1^1 \times W_1^2. \end{aligned}$$

The spaces  $\mathbb{V}$ ,  $\mathbb{W}$  and  $\mathbb{W}_1$  are the real Hilbert spaces endowed with the canonical inner products denoted by  $(\cdot, \cdot)_{\mathbb{V}}$ ,  $(\cdot, \cdot)_{\mathbb{W}}$  and  $(\cdot, \cdot)_{\mathbb{W}_1}$ . The associate norms will be denoted by  $\|\cdot\|_{\mathbb{V}}$ ,  $\|\cdot\|_{\mathbb{W}}$  and  $\|\cdot\|_{\mathbb{W}_1}$ , respectively.

Finally, for any real Hilbert space  $X$ , we use the classical notation for the spaces  $L^p(0, T; X)$ ,  $W^{k,p}(0, T; X)$ , where  $1 \leq p \leq \infty$ ,  $k \geq 1$ . We denote by  $\mathcal{C}(0, T; X)$  and  $\mathcal{C}^1(0, T; X)$  the space of continuous and continuously differentiable functions from  $[0, T]$  to  $X$ , respectively, with the norms

$$\begin{aligned} \|f\|_{\mathcal{C}(0, T; X)} &= \max_{t \in [0, T]} \|f(t)\|_X, \\ \|f\|_{\mathcal{C}^1(0, T; X)} &= \max_{t \in [0, T]} \|f(t)\|_X + \max_{t \in [0, T]} \|\dot{f}(t)\|_X. \end{aligned}$$

### 3 The Model and Variational Problem

Let us consider two electro-viscoelastic bodies occupying two bounded domains  $\Omega^1, \Omega^2$  of the space  $\mathbb{R}^d (d = 2, 3)$ . For each domain  $\Omega^k$ , the boundary  $\Gamma^k$  is assumed to be Lipschitz continuous, and is partitioned into three disjoint measurable parts  $\Gamma_1^k, \Gamma_2^k$  and  $\Gamma_3^k$  on one hand, and into two measurable parts  $\Gamma_a^k$  and  $\Gamma_b^k$  on the other hand, such that  $\operatorname{meas} \Gamma_1^k > 0$ ,  $\operatorname{meas} \Gamma_a^k > 0$ . Let  $T > 0$  and let  $[0, T]$  be the time interval of interest. The body  $\Omega^k$  is subjected to  $\mathbf{f}_0^k$  forces and volume electric charges of density  $q_0^k$ . The bodies are assumed to be clamped on  $\Gamma_1^k \times [0, T]$ . The surface tractions  $\mathbf{f}_2^k$  act on  $\Gamma_2^k \times [0, T]$ . We also assume that the electrical potential vanishes on  $\Gamma_a^k \times [0, T]$  and a surface electric charge of density  $q_2^k$  is prescribed on  $\Gamma_b^k \times [0, T]$ . The two bodies can enter in contact along the common part  $\Gamma_3^1 = \Gamma_3^2 = \Gamma_3$ , the bodies are in contact with wear.

We denote by  $\mathbf{u}^k$  the displacement field, by  $\boldsymbol{\sigma}^k$  the stress tensor field and by  $\boldsymbol{\varepsilon}(\mathbf{u}^k)$  the linearized strain tensor. We use an electro-viscoelastic constitutive law given by

$$\boldsymbol{\sigma}^k(t) = \mathcal{A}^k \boldsymbol{\varepsilon}(\dot{\mathbf{u}}^k(t)) + \mathcal{G}^k \boldsymbol{\varepsilon}(\mathbf{u}^k(t)) + (\mathcal{E}^k)^* \nabla \varphi^k(t). \tag{7}$$

Here  $\mathcal{A}^k$  is a given nonlinear operator,  $\mathcal{G}^k$  represents the elasticity operator.  $E(\varphi^k) = -\nabla \varphi^k$  is the electric field,  $\mathcal{E}^k$  represents the third order piezoelectric tensor,  $(\mathcal{E}^k)^*$  is its transposition. In (7) and everywhere in this paper, the dot above a variable represents the derivative with respect to the time variable  $t$ .

We now briefly describe the boundary conditions on the contact surface  $\Gamma_3$  based on the model derived in [18]. We introduce the wear function  $w : \Gamma_3 \times [0, T] \rightarrow \mathbb{R}^+$  which measures the wear of the surface.

The wear is identified as the normal depth of the material that is lost. Let  $g$  be the initial gap between the two bodies and let  $p_\nu$  and  $p_\tau$  denote the normal and tangential

compliance functions. We denote by  $\mathbf{v}^*$  and  $\alpha^* = \|\mathbf{v}^*\|$  the tangential velocity and the tangential speed of the contact surface, respectively. We use the modified version of Archard's law  $\dot{w} = -k_w \alpha^* \sigma_\nu$  to describe the evolution of wear, where  $k_w > 0$  is a wear coefficient. We introduce the unitary vector  $\delta : \Gamma_3 \rightarrow \mathbb{R}^d$  defined by  $\delta = \mathbf{v}^* / \|\mathbf{v}^*\|$ . In the reference configuration, there is a gap between  $\Gamma_3$  of the two bodies, measured along the direction of  $\nu$ , denoted by  $g$ . When the contact occurs, some material of the contact surface is worn out and immediately removed from the system. This process is measured by the wear function  $w$ .

Then, the classical formulation of the mechanical problem of a frictional contact with wear between two electro-viscoelastic bodies may be stated as follows.

### Problem $\mathcal{P}$

For  $k = 1, 2$ , find a displacement field  $\mathbf{u}^k : \Omega^k \times [0, T] \rightarrow \mathbb{R}^d$ , a stress field  $\boldsymbol{\sigma}^k : \Omega^k \times [0, T] \rightarrow \mathbb{S}^d$ , an electric potential  $\varphi^k : \Omega^k \times [0, T] \rightarrow \mathbb{R}$ , a wear function  $w : \Gamma_3 \times [0, T] \rightarrow \mathbb{R}_+$  and an electric displacement field  $\mathbf{D}^k : \Omega^k \times [0, T] \rightarrow \mathbb{R}^d$  such that

$$\boldsymbol{\sigma}^k = \mathcal{A}^k \boldsymbol{\varepsilon}(\dot{\mathbf{u}}^k) + \mathcal{G}^k \boldsymbol{\varepsilon}(\mathbf{u}^k) + (\mathcal{E}^k)^* \nabla \varphi^k, \text{ in } \Omega^k \times [0, T], \quad (8)$$

$$\mathbf{D}^k = \mathcal{E}^k \boldsymbol{\varepsilon}(\mathbf{u}^k) - \mathcal{B}^k \nabla \varphi^k \quad \text{in } \Omega^k \times [0, T], \quad (9)$$

$$\text{Div } \boldsymbol{\sigma}^k + \mathbf{f}_0^k = 0 \quad \text{in } \Omega^k \times [0, T], \quad (10)$$

$$\text{div } \mathbf{D}^k - q_0^k = 0 \quad \text{in } \Omega^k \times [0, T], \quad (11)$$

$$\mathbf{u}^k = 0 \quad \text{on } \Gamma_1^k \times [0, T], \quad (12)$$

$$\boldsymbol{\sigma}^k \boldsymbol{\nu}^k = \mathbf{f}_2^k \quad \text{on } \Gamma_2^k \times [0, T], \quad (13)$$

$$\left. \begin{array}{l} \sigma_\nu^1 = \sigma_\nu^2 \equiv \sigma_\nu, \\ \sigma_\nu = p_\nu (u_\nu - w - g), \end{array} \right\} \quad \text{on } \Gamma_3 \times [0, T], \quad (14)$$

$$\left. \begin{array}{l} \sigma_\tau^1 = -\sigma_\tau^2 \equiv \sigma_\tau, \\ \sigma_\tau = -p_\tau (u_\nu - w - g) \frac{\mathbf{v}^*}{\|\mathbf{v}^*\|}, \end{array} \right\} \quad \text{on } \Gamma_3 \times [0, T], \quad (15)$$

$$u_\nu^1 + u_\nu^2 = 0, \quad \text{on } \Gamma_3 \times [0, T], \quad (16)$$

$$\dot{w} = -k_w \alpha^* \sigma_\nu = k_w \alpha^* p_\nu (u_\nu - w - g), \quad \text{on } \Gamma_3 \times [0, T], \quad (17)$$

$$\varphi^k = 0 \quad \text{on } \Gamma_a^k \times [0, T], \quad (18)$$

$$\mathbf{D}^k \cdot \boldsymbol{\nu}^k = q_2^k \quad \text{on } \Gamma_b^k \times [0, T], \quad (19)$$

$$\mathbf{u}^k(0) = \mathbf{u}_0^k, \quad \text{in } \Omega^k, \quad (20)$$

$$w(0) = w_0 \quad \text{on } \Gamma_3. \quad (21)$$

First, equations (8) and (9) represent the electro-viscoelastic constitutive law. Equations (10) and (11) are the equilibrium equations for the stress and electric-displacement fields, respectively, in which “*Div*” and “*div*” denote the divergence operator for the tensor and vector valued functions, respectively. Next, the equations (12) and (13) represent the displacement and traction boundary condition, respectively. Conditions (14), (15) represent the frictional contact with the wear described above. Equation (16) means that the two bodies are inseparable.

Next, the equation (17) represents the ordinary differential equation which describes the evolution of the wear function. Equations (18) and (19) represent the electric bound-

ary conditions. (20) represents the initial displacement field. Finally, (21) represents the initial condition in which  $w_0$  is the given initial wear field.

We now list the assumptions on the problem’s data.

The *viscosity function*  $\mathcal{A}^k : \Omega^k \times \mathbb{S}^d \rightarrow \mathbb{S}^d$  satisfies the following conditions:

$$\left\{ \begin{array}{l} \text{(a) There exists } L_{\mathcal{A}^k} > 0 \text{ such that} \\ \quad \|\mathcal{A}^k(\mathbf{x}, \boldsymbol{\varepsilon}_1) - \mathcal{A}^k(\mathbf{x}, \boldsymbol{\varepsilon}_2)\| \leq L_{\mathcal{A}^k} \|\boldsymbol{\varepsilon}_1 - \boldsymbol{\varepsilon}_2\| \text{ for all } \boldsymbol{\varepsilon}_1, \boldsymbol{\varepsilon}_2 \in \mathbb{S}^d, \text{ a.e. } \mathbf{x} \in \Omega^k. \\ \text{(b) There exists } m_{\mathcal{A}^k} > 0 \text{ such that} \\ \quad (\mathcal{A}^k(\mathbf{x}, \boldsymbol{\varepsilon}_1) - \mathcal{A}^k(\mathbf{x}, \boldsymbol{\varepsilon}_2)) \cdot (\boldsymbol{\varepsilon}_1 - \boldsymbol{\varepsilon}_2) \geq m_{\mathcal{A}^k} \|\boldsymbol{\varepsilon}_1 - \boldsymbol{\varepsilon}_2\|^2 \\ \quad \text{for all } \boldsymbol{\varepsilon}_1, \boldsymbol{\varepsilon}_2 \in \mathbb{S}^d, \text{ a.e. } \mathbf{x} \in \Omega^k. \\ \text{(c) The mapping } \mathbf{x} \mapsto \mathcal{A}^k(\mathbf{x}, \boldsymbol{\varepsilon}) \text{ is Lebesgue measurable on } \Omega^k \\ \quad \text{for any } \boldsymbol{\varepsilon} \in \mathbb{S}^d. \\ \text{(d) The mapping } \mathbf{x} \mapsto \mathcal{A}^k(\mathbf{x}, \mathbf{0}) \text{ belongs to } \mathbb{Q}. \end{array} \right. \quad (22)$$

The *elasticity operator*  $\mathcal{G}^k : \Omega^k \times \mathbb{S}^d \rightarrow \mathbb{S}^d$  satisfies the following conditions:

$$\left\{ \begin{array}{l} \text{(a) There exists a constant } L_{\mathcal{G}^k} > 0 \text{ such that} \\ \quad \|\mathcal{G}^k(\mathbf{x}, \boldsymbol{\varepsilon}_1) - \mathcal{G}^k(\mathbf{x}, \boldsymbol{\varepsilon}_2)\| \leq L_{\mathcal{G}^k} \|\boldsymbol{\varepsilon}_1 - \boldsymbol{\varepsilon}_2\| \\ \quad \text{for all } \boldsymbol{\varepsilon}_1, \boldsymbol{\varepsilon}_2 \in \mathbb{S}^d \text{ a.e. } \mathbf{x} \in \Omega^k. \\ \text{(b) The mapping } \mathbf{x} \rightarrow \mathcal{G}^k(\mathbf{x}, \boldsymbol{\varepsilon}) \text{ is Lebesgue measurable on } \Omega^k \\ \quad \text{for all } \boldsymbol{\varepsilon} \in \mathbb{S}^d. \\ \text{(c) The mapping } \mathbf{x} \rightarrow \mathcal{G}^k(\mathbf{x}, \mathbf{0}) \in \mathbb{Q}. \end{array} \right. \quad (23)$$

The *piezoelectric tensor*  $\mathcal{E}^k : \Omega^k \times \mathbb{S}^d \rightarrow \mathbb{R}^d$  satisfies the following conditions:

$$\left\{ \begin{array}{l} \text{(a) } \mathcal{E}^k(\mathbf{x}, \boldsymbol{\tau}) = (e_{ijk}^k(\mathbf{x})\tau_{jk}) \text{ for all } \boldsymbol{\tau} = (\tau_{ij}) \in \mathbb{S}^d \text{ a.e. } \mathbf{x} \in \Omega^k. \\ \text{(b) } e_{ijk}^k = e_{ikj}^k \in L^\infty(\Omega^k), 1 \leq i, j, k \leq d. \end{array} \right. \quad (24)$$

Recall also that the transposed operator  $(\mathcal{E}^k)^*$  is given by  $(\mathcal{E}^k)^* = (e_{ijk}^{k,*})$ , where  $e_{ijk}^{k,*} = e_{kij}^k$  and the following equality holds:

$$\mathcal{E}^k \boldsymbol{\sigma} \cdot \mathbf{v} = \boldsymbol{\sigma} \cdot (\mathcal{E}^k)^* \mathbf{v} \quad \forall \boldsymbol{\sigma} \in \mathbb{S}^d, \forall \mathbf{v} \in \mathbb{R}^d.$$

The *electric permittivity operator*  $\mathcal{B}^k = (b_{ij}^k) : \Omega^k \times \mathbb{R}^d \rightarrow \mathbb{R}^d$  satisfies the following conditions:

$$\left\{ \begin{array}{l} \text{(a) } \mathcal{B}^k(\mathbf{x}, \mathbf{E}) = (b_{ij}^k(\mathbf{x})E_j) \text{ for all } \mathbf{E} = (E_i) \in \mathbb{R}^d, \text{ a.e. } \mathbf{x} \in \Omega^k. \\ \text{(b) } b_{ij}^k = b_{ji}^k, b_{ij}^k \in L^\infty(\Omega^k), 1 \leq i, j \leq d. \\ \text{(c) There exists } m_{\mathcal{B}^k} > 0, \text{ such that } \mathcal{B}^k \mathbf{E} \cdot \mathbf{E} \geq m_{\mathcal{B}^k} |\mathbf{E}|^2 \text{ for all } \mathbf{E} = (E_i) \in \mathbb{R}^d, \\ \quad \text{a.e. } \mathbf{x} \in \Omega^k. \end{array} \right. \quad (25)$$

The *normal compliance function*  $p_\nu : \Gamma_3 \times \mathbb{R} \rightarrow \mathbb{R}_+$  satisfies the following conditions:

$$\left\{ \begin{array}{l} \text{(a) There exists } \mathcal{L}_\nu > 0 \text{ such that} \\ \quad |p_\nu(\mathbf{x}, r_1) - p_\nu(\mathbf{x}, r_2)| \leq \mathcal{L}_\nu |r_1 - r_2| \text{ for all } r_1, r_2 \in \mathbb{R}, \text{ a.e. } \mathbf{x} \in \Gamma_3. \\ \text{(b) The mapping } \mathbf{x} \mapsto p_\nu(\mathbf{x}, r) \text{ is measurable on } \Gamma_3 \text{ for all } r \in \mathbb{R}. \\ \text{(c) } p_\nu(\mathbf{x}, r) = 0 \text{ for all } r \leq 0, \text{ a.e. } \mathbf{x} \in \Gamma_3. \end{array} \right. \quad (26)$$

The *tangential contact function*  $p_\tau : \Gamma_3 \times \mathbb{R} \rightarrow \mathbb{R}_+$  satisfies the following conditions:

$$\left\{ \begin{array}{l} \text{(a) There exists } \mathcal{L}_\tau > 0 \text{ such that} \\ \quad |p_\tau(\mathbf{x}, r_1) - p_\tau(\mathbf{x}, r_2)| \leq \mathcal{L}_\tau |r_1 - r_2| \text{ for all } r_1, r_2 \in \mathbb{R}, \text{ a.e. } \mathbf{x} \in \Gamma_3. \\ \text{(b) The mapping } \mathbf{x} \mapsto p_\tau(\mathbf{x}, r) \text{ is measurable on } \Gamma_3 \text{ for all } r \in \mathbb{R}. \\ \text{(c) } p_\tau(\mathbf{x}, r) = 0 \text{ for all } r \leq 0, \text{ a.e. } \mathbf{x} \in \Gamma_3. \end{array} \right. \quad (27)$$

We also suppose the following regularities:

$$\begin{aligned} \mathbf{f}_0^k \in C(0, T; L^2(\Omega^k)^d), \quad \mathbf{f}_2^k \in C(0, T; L^2(\Gamma_2^k)^d), \\ q_0^k \in C(0, T; L^2(\Omega^k)), \quad q_2^k \in C(0, T; L^2(\Gamma_b^k)), \end{aligned} \quad (28)$$

$$\mathbf{u}_0^k \in \mathbf{V}^k, \quad (29)$$

$$w_0 \in L^2(\Gamma_3), \quad (30)$$

$$p_\nu(\cdot, r) \in L^2(\Gamma_3), p_\tau(\cdot, r) \in L^2(\Gamma_3), \forall r \in \mathbb{R} \quad (31)$$

$$g \in L^2(\Gamma_3), g \geq 0 \text{ a.e on } \Gamma_3. \quad (32)$$

Using the Riesz representation theorem, we define the linear mappings  $\mathbf{f} = (\mathbf{f}^1, \mathbf{f}^2) : [0, T] \rightarrow \mathbb{V}$  and  $q = (q^1, q^2) : [0, T] \rightarrow \mathbb{W}$  as follows:

$$(\mathbf{f}(t), \mathbf{v})_{\mathbb{V}} = \sum_{k=1}^2 \int_{\Omega^k} \mathbf{f}_0^k(t) \cdot \mathbf{v}^k dx + \sum_{k=1}^2 \int_{\Gamma_2^k} \mathbf{f}_2^k(t) \cdot \mathbf{v}^k da \quad \forall \mathbf{v} \in \mathbb{V}, \quad (33)$$

$$(q(t), \zeta)_{\mathbb{W}} = \sum_{k=1}^2 \int_{\Omega^k} q_0^k(t) \zeta^k dx - \sum_{k=1}^2 \int_{\Gamma_b^k} q_2^k(t) \zeta^k da \quad \forall \zeta \in \mathbb{W}. \quad (34)$$

The use of (33) permits to verify that

$$\mathbf{f} \in \mathcal{C}(0, T; \mathbb{V}). \quad (35)$$

Next, we define the mappings  $j : L^2(\Gamma_3) \times \mathbb{V} \times \mathbb{V} \rightarrow \mathbb{R}$  by

$$\begin{aligned} j(w, \mathbf{u}, \mathbf{v}) = \int_{\Gamma_3} (p_\nu(u_\nu - w - g) v_\nu) da + \int_{\Gamma_3} p_\tau(u_\nu - w - g) \cdot \delta \cdot \mathbf{v}_\tau da, \\ \text{for all } \mathbf{u}, \mathbf{v} \in \mathbb{V}, w \in L^2(\Gamma_3). \end{aligned} \quad (36)$$

Now, we give the following variational formulation of the mechanical problem (8)–(21).

### Problem $\mathcal{PV}$

Find a displacement field  $\mathbf{u} = (\mathbf{u}^1, \mathbf{u}^2) : [0, T] \rightarrow \mathbb{V}$ , a stress field  $\boldsymbol{\sigma} = (\boldsymbol{\sigma}^1, \boldsymbol{\sigma}^2) : [0, T] \rightarrow \mathbb{Q}$ , an electric potential  $\varphi = (\varphi^1, \varphi^2) : [0, T] \rightarrow \mathbb{W}$ , a wear  $w : [0, T] \rightarrow L^2(\Gamma_3)$  and an electric displacement field  $\mathbf{D} = (\mathbf{D}^1, \mathbf{D}^2) : [0, T] \rightarrow \mathbb{W}_1$  such that

$$\boldsymbol{\sigma}^k = \mathcal{A}^k \boldsymbol{\varepsilon}(\mathbf{u}^k) + \mathcal{G}^k \boldsymbol{\varepsilon}(\mathbf{u}^k) + (\mathcal{E}^k)^* \nabla \varphi^k \text{ in } \Omega^k \times [0, T], \quad (37)$$

$$\mathbf{D}^k = \mathcal{E}^k \boldsymbol{\varepsilon}(\mathbf{u}^k) - \mathcal{B}^k \nabla \varphi^k \text{ in } \Omega^k \times [0, T], \quad (38)$$

$$\sum_{k=1}^2 (\boldsymbol{\sigma}^k, \boldsymbol{\varepsilon}(\mathbf{v}^k))_{Q^k} + j(w(t), \mathbf{u}(t), \mathbf{v}) = (\mathbf{f}(t), \mathbf{v})_{\mathbb{V}} \quad (39)$$

$$\forall \mathbf{v} \in \mathbb{V}, \text{ a.e. } t \in (0, T),$$

$$\sum_{k=1}^2 (\mathcal{B}^k \nabla \varphi^k(t), \nabla \phi^k)_{H^k} - \sum_{k=1}^2 (\mathcal{E}^k \boldsymbol{\varepsilon}(\mathbf{u}^k(t)), \nabla \phi^k)_{H^k} = (q(t), \phi)_{\mathbb{W}}, \quad (40)$$

$$\forall \phi \in \mathbb{W}, \text{ a.e. } t \in (0, T),$$

$$\dot{w} = k_w \alpha^* p_\nu(u_\nu - w - g), \quad \text{a.e. } (0, T), \quad (41)$$

$$\mathbf{u}(0) = \mathbf{u}_0, \quad w(0) = w_0. \quad (42)$$

We notice that the variational Problem  $\mathcal{PV}$  is formulated in terms of a displacement field, a stress field, an electrical potential, a wear and an electric displacement field. The existence of the unique solution of Problem  $\mathcal{PV}$  is stated and proved in the next section.

#### 4 Existence and Uniqueness of a Solution

Our main existence and uniqueness result is the following.

**Theorem 4.1** *Assume that (22)–(32) hold and also assume the smallness assumption:*

$$(\mathcal{L}_\nu + \mathcal{L}_\tau) < \alpha_0, \tag{43}$$

where  $\alpha_0 = \frac{m_{\mathcal{A}^k}}{c_0^2}$  such that  $m_{\mathcal{A}^k}$  is defined in (22) and  $c_0$  is defined in (3). Then there

exists a unique solution of Problem  $\mathcal{PV}$ . Moreover, the solution satisfies the following conditions

$$\mathbf{u} \in \mathcal{C}^1(0, T; \mathbb{V}), \tag{44}$$

$$\boldsymbol{\sigma} \in \mathcal{C}(0, T; \mathbb{Q}_1), \tag{45}$$

$$w \in \mathcal{C}^1(0, T; L^2(\Gamma_3)), \tag{46}$$

$$\varphi \in \mathcal{C}(0, T; \mathbb{W}), \tag{47}$$

$$\mathbf{D} \in \mathcal{C}(0, T; \mathbb{W}_1). \tag{48}$$

Then  $\{\mathbf{u}, \boldsymbol{\sigma}, w, \varphi, \mathbf{D}\}$  which satisfy (37)–(42) are called a weak solution of the contact Problem  $\mathcal{P}$ . We conclude that, under the assumptions (22)–(32), the mechanical problem (8)–(21) has a unique weak solution satisfying (44)–(48).

The proof of Theorem (4.1) is carried out in several steps and is based on the following abstract result for evolutionary variational inequalities.

We turn now to the proof of Theorem (4.1) which will be carried out in several steps and is based on the arguments of nonlinear equations with monotone operators, a classical existence and uniqueness result on parabolic inequalities and fixed-point arguments. To this end, we assume in what follows that (22)–(32) hold, and we consider that  $C$  is a generic positive constant which depends on  $\Omega^k, \Gamma_1^k, \Gamma_3, p_\nu, p_\tau, \mathcal{A}^k, \mathcal{G}^k, \mathcal{E}^k$  but does not depend on  $t$  or the rest of input data, and whose value may change from place to place.

**First step.**

Let  $\eta = (\eta^1, \eta^2) \in \mathcal{C}(0, T; \mathbb{V})$ .

We consider the following variational problem.

**Problem  $\mathcal{PV}_\eta^u$ .**

Find a displacement field  $\mathbf{u}_\eta = (\mathbf{u}_\eta^1, \mathbf{u}_\eta^2) : [0, T] \rightarrow \mathbb{V}$  such that

$$\sum_{k=1}^2 (\mathcal{A}^k \boldsymbol{\varepsilon}(\dot{\mathbf{u}}^k), \boldsymbol{\varepsilon}(\mathbf{v}^k))_{Q^k} + (\eta(t), \mathbf{v})_{\mathbb{V}} = (\mathbf{f}(t), \mathbf{v})_{\mathbb{V}}, \tag{49}$$

$$\mathbf{u}_\eta(0) = \mathbf{u}_0 \tag{50}$$

for all  $\mathbf{v} \in \mathbb{V}$  a.e  $t \in (0, T)$ .

We have the following result for  $\mathcal{PV}_\eta^u$ .

**Lemma 4.1** *There exists a unique solution  $\mathbf{u}_\eta = (\mathbf{u}_\eta^1, \mathbf{u}_\eta^2) \in \mathcal{C}^1(0, T; \mathbb{V})$  to the problem (49) and (50).*

**Proof.** Let  $A : \mathbb{V} \rightarrow \mathbb{V}$  be a semi-continuous and monotone operator which satisfies the condition

$$(A\mathbf{u}, \mathbf{v})_{\mathbb{V} \times \mathbb{V}} = \sum_{k=1}^2 (\mathcal{A}^k \varepsilon(\mathbf{u}^k), \varepsilon(\mathbf{v}^k))_{Q^k}. \quad (51)$$

It follows from hypothesis (22) that

$$\|A\mathbf{u} - A\mathbf{v}\|_{\mathbb{V}} \leq L_{\mathcal{A}^k} \|\mathbf{u} - \mathbf{v}\|_{\mathbb{V}} \quad \forall \mathbf{u}, \mathbf{v} \in \mathbb{V}.$$

This proves that  $A$  is bounded and semi-continuous on  $\mathbb{V}$ .

On the other hand, by (22) and Korn's inequality, we find, for every  $\mathbf{v} \in \mathbb{V}$ ,

$$\frac{(A\mathbf{v}, \mathbf{v})_{\mathbb{V} \times \mathbb{V}}}{\|\mathbf{v}\|_{\mathbb{V}}} \geq c_0^2 m_{\mathcal{A}^k} \|\mathbf{v}\|_{\mathbb{V}}.$$

The passage to the limit in this inequality when  $\|\mathbf{v}\|_{\mathbb{V}} \rightarrow +\infty$  implies that  $A$  is coercive in  $\mathbb{V}$ .

Next, by the definition of  $A$ , the use of (22) and Korn's inequality permits also to obtain

$$(A\mathbf{u} - A\mathbf{v}, \mathbf{u} - \mathbf{v})_{\mathbb{V} \times \mathbb{V}} > c_0^2 m_{\mathcal{A}^k} \|\mathbf{u} - \mathbf{v}\|_{\mathbb{V}} \quad \text{if } \mathbf{u} \neq \mathbf{v}.$$

Then  $A$  is strict monotone. Therefore, we put

$$\mathbf{f}_\eta(t) = \mathbf{f}(t) - \eta(t) \in \mathcal{C}(0, T; \mathbb{V}).$$

From (33) and the condition  $\eta \in \mathcal{C}(0, T; \mathbb{V})$ , we have  $\mathbf{f}_\eta \in \mathcal{C}(0, T; \mathbb{V})$ . Then, from the Cauchy-Lipschitz theorem, there exists a unique function  $\mathbf{v}_\eta$  satisfying the relations

$$A\mathbf{v}_\eta(t) = \mathbf{f}_\eta(t) \quad \text{a.e } t \in (0, T),$$

$$\mathbf{u}_\eta = \int_0^t \mathbf{v}_\eta(s) ds + \mathbf{u}_0, \quad \forall t \in [0, T].$$

We recall that by (35), we have  $\mathbf{F}_\eta \in \mathcal{C}(0, T; \mathbb{V})$ . Keeping in mind that the operator  $A$  is strict monotone, semi-continuous, bounded and coercive, and by using the classical arguments of functional analysis concerning parabolic equations [5, 14], we can easily prove the existence and uniqueness of  $\mathbf{u}_\eta$  satisfying (49)–(50) and the regularity (44).

### Second step.

In the second step, we consider the following variational problem.

**4.1 Problem  $\mathcal{PV}_\eta^w$**

Find the wear function  $w_\eta : [0, T] \rightarrow L^2(\Gamma_3)$  such that

$$\dot{w}_\eta(t) = k_w \alpha^* p_\nu (u_\nu - w - g), \tag{52}$$

$$w_\eta(0) = w_0 \text{ in } \Gamma_3. \tag{53}$$

We have the following result for  $\mathcal{PV}_\eta^w$ .

**Lemma 4.2** *There exists a unique solution  $w_\eta \in C^1(0, T; L^2(\Gamma_3))$  to the problem  $\mathcal{PV}_\eta^w$ .*

**Proof.** We use a version of the classical Cauchy–Lipschitz theorem when considering the mapping  $\mathcal{F}_\eta : [0, T] \times L^2(\Gamma_3) \rightarrow L^2(\Gamma_3)$  defined by

$$\mathcal{F}_\eta(t, w_\eta) = k_w \alpha^* p_\nu (u_\nu - w_\eta - g), \quad \forall w_\eta \in L^2(\Gamma_3), t \in [0, T].$$

It is easy to see that  $\mathcal{F}_\eta$  is Lipschitz continuous with respect to the second variable, uniformly in time. Thus, by the Cauchy–Lipschitz theorem, there exists a unique solution  $w_\eta$  which satisfies (52)–(53).

**Third step.**

In the third step, we consider the following variational problem.

**4.2 Problem  $\mathcal{PV}_\eta^\varphi$**

Find the electric potential  $\varphi_\eta : [0, T] \rightarrow \mathbb{W}$  such that

$$\sum_{k=1}^2 (\mathcal{B}^k \nabla \varphi_\eta^k(t), \nabla \phi^k)_{H^k} - \sum_{k=1}^2 (\mathcal{E}^k \varepsilon(\mathbf{u}_\eta^k(t)), \nabla \phi^k)_{H^k} = (q(t), \phi)_\mathbb{W} \tag{54}$$

for all  $\phi \in \mathbb{W}$ , a.e.  $t \in (0, T)$ . We have the following result.

**Lemma 4.3** *There exists a unique solution  $\varphi_\eta \in C(0, T; \mathbb{W})$  to the problem  $\mathcal{PV}_\eta^\varphi$ .*

**Proof.** We define a bilinear form  $b(\cdot, \cdot) : \mathbb{W} \times \mathbb{W} \rightarrow \mathbb{R}$  such that

$$b(\varphi, \phi) = \sum_{k=1}^2 (\mathcal{B}^k \nabla \varphi^k, \nabla \phi^k)_{H^k} \quad \forall \varphi, \phi \in \mathbb{W}. \tag{55}$$

We use (4), (5), (25) and (55) to show that the bilinear form  $b(\cdot, \cdot)$  is continuous, symmetric and coercive on  $\mathbb{W}$ , moreover, using (34) and the Riesz representation theorem, we may define an element  $q_\eta : [0, T] \rightarrow \mathbb{W}$  such that

$$(q_\eta(t), \phi)_\mathbb{W} = (q(t), \phi)_\mathbb{W} + \sum_{k=1}^2 (\mathcal{E}^k \varepsilon(\mathbf{u}_\eta^k(t)), \nabla \phi^k)_{H^k} \quad \forall \phi \in \mathbb{W}, t \in [0, T].$$

We apply the Lax-Milgram theorem to deduce that there exists a unique element  $\varphi_\eta(t) \in \mathbb{W}$  such that

$$b(\varphi_\eta(t), \phi) = (q_\eta(t), \phi)_\mathbb{W} \quad \forall \phi \in \mathbb{W}. \tag{56}$$

We conclude that  $\varphi_\eta$  is a solution of Problem  $\mathcal{PV}_\eta^\varphi$ . Let  $t_1, t_2 \in [0, T]$ , it follows from (54) that

$$\|\varphi_\eta(t_1) - \varphi_\eta(t_2)\|_{\mathbb{W}} \leq C(\|\mathbf{u}_\eta(t_1) - \mathbf{u}_\eta(t_2)\|_{\mathbb{V}} + \|q(t_1) - q(t_2)\|_{\mathbb{W}}). \quad (57)$$

We also note that assumptions (28),  $\mathbf{u}_\eta \in C^1(0, T; \mathbb{V})$  and inequality (57) imply that  $\varphi_\eta \in C(0, T; \mathbb{W})$ .

Finally, as a consequence of these results, and using the properties of the operator  $\mathcal{E}^k$  and the functional  $j$ , for  $t \in [0, T]$ , we consider the element

$$\Lambda : \mathcal{C}(0, T; \mathbb{V}) \rightarrow \mathcal{C}(0, T; \mathbb{V}) \quad (58)$$

defined by the equations

$$\begin{aligned} (\Lambda\eta(t), \mathbf{v})_{\mathbb{V}} &= \sum_{k=1}^2 (\mathcal{G}^k \boldsymbol{\varepsilon}(\mathbf{u}_\eta^k(t)), \mathbf{v})_{\mathbb{V}} + j(w_\eta(t), \mathbf{u}_\eta(t), \mathbf{v}) \\ &+ \sum_{k=1}^2 ((\mathcal{E}^k)^* \nabla \varphi_\eta^k(t), \boldsymbol{\varepsilon}(\mathbf{v}^k))_{Q^k}, \forall \mathbf{v} \in \mathbb{V}. \end{aligned} \quad (59)$$

Here, for every  $\eta \in \mathcal{C}(0, T; \mathbb{V})$ ,  $\mathbf{u}_\eta$ ,  $w_\eta$  and  $\varphi_\eta$  represent the displacement field, wear field and the potential electric field obtained in Lemmas 4.1, 4.2 and 4.3, respectively, and  $\boldsymbol{\sigma}_\eta^k$  is denoted by

$$\boldsymbol{\sigma}_\eta^k(t) = \mathcal{A}^k \boldsymbol{\varepsilon}(\dot{\mathbf{u}}_\eta^k(t)) + \mathcal{G}^k \boldsymbol{\varepsilon}(\mathbf{u}_\eta^k(t)) + (\mathcal{E}^k)^* \nabla \varphi_\eta^k(t) \text{ in } \Omega^k \times [0, T]. \quad (60)$$

We have the following result.

**Lemma 4.4** *There exists a unique  $\eta^* \in \mathcal{C}(0, T; \mathbb{V})$  such that  $\Lambda\eta^* = \eta^*$ .*

**Proof.** Let  $\eta_1, \eta_2 \in \mathcal{C}(0, T; \mathbb{V})$  and denote by  $\mathbf{u}_i$ ,  $w_i$ ,  $\varphi_i$  and  $\boldsymbol{\sigma}_i$  the functions obtained in Lemmas 4.1, 4.2, 4.3 and the relation (60), respectively, for  $\eta = \eta_i$ ,  $i = 1, 2$ . Let  $t \in [0, T]$ , we have

$$\begin{aligned} \|\Lambda\eta_1(t) - \Lambda\eta_2(t)\|_{\mathbb{V}} &\leq \sum_{k=1}^2 \|\mathcal{G}^k \boldsymbol{\varepsilon}(\mathbf{u}_1^k(t)) - \mathcal{G}^k \boldsymbol{\varepsilon}(\mathbf{u}_2^k(t))\|_{Q^k} \\ &+ |j(w_1(t), \mathbf{u}_1(t), \mathbf{v}) - j(w_2(t), \mathbf{u}_2(t), \mathbf{v})| \\ &+ \sum_{k=1}^2 \|(\mathcal{E}^k)^* \nabla \varphi_1^k(t) - (\mathcal{E}^k)^* \nabla \varphi_2^k(t)\|_{Q^k}. \end{aligned}$$

We use (23) and (24), we have

$$\begin{aligned} \|\Lambda\eta_1(t) - \Lambda\eta_2(t)\|_{\mathbb{V}} &\leq C \left( \|\mathbf{u}_1(t) - \mathbf{u}_2(t)\|_{\mathbb{V}} + \|\varphi_1(t) - \varphi_2(t)\|_{\mathbb{W}} \right. \\ &\left. + |j(w_1(t), \mathbf{u}_1(t), \mathbf{v}) - j(w_2(t), \mathbf{u}_2(t), \mathbf{v})| \right). \end{aligned} \quad (61)$$

From (3),(26),(36) and (27), we get

$$\begin{aligned} &\|j(w_1(t), \mathbf{u}_1(t), \mathbf{v}) - j(w_2(t), \mathbf{u}_2(t), \mathbf{v})\|_{L^2(\Gamma_3)} \\ &\leq c_0 (\mathcal{L}_\nu + \mathcal{L}_\tau) \left( c_0 \|\mathbf{u}_1(t) - \mathbf{u}_2(t)\|_{\mathbb{V}} + \|w_1(t) - w_2(t)\|_{L^2(\Gamma_3)} \right) \|\mathbf{v}\|_{\mathbb{V}}. \\ &\forall \mathbf{u}_1, \mathbf{u}_2, \mathbf{v} \in \mathbb{V}, w_1, w_2 \in L^2(\Gamma_3). \end{aligned}$$

Recall that  $u_{\eta\nu}^k$  and  $\mathbf{u}_{\eta\tau}^k$  denote the normal and the tangential component of the function  $\mathbf{u}_\eta^k$ , respectively.

Also, since

$$\mathbf{u}_i^k(t) = \int_0^t \dot{\mathbf{u}}_i^k(s) ds + \mathbf{u}_0^k(t), \quad t \in [0, T], \quad k = 1, 2,$$

we have

$$\|\mathbf{u}_1(t) - \mathbf{u}_2(t)\|_{\mathbb{V}} \leq \int_0^t \|\dot{\mathbf{u}}_1(s) - \dot{\mathbf{u}}_2(s)\|_{\mathbb{V}} ds. \tag{62}$$

Using now (22),(26),(27), (59) and (60), we get

$$(m_{\mathcal{A}^k} - (\mathcal{L}_\nu + \mathcal{L}_\tau)) \|\dot{\mathbf{u}}_1(t) - \dot{\mathbf{u}}_2(t)\|_{\mathbb{V}} \leq \|\eta_1(s) - \eta_2(s)\|_{\mathbb{V}}.$$

It follows from (49) that

$$\|\dot{\mathbf{u}}_1(t) - \dot{\mathbf{u}}_2(t)\|_{\mathbb{V}}^2 \leq C \|\eta_1(s) - \eta_2(s)\|_{\mathbb{V}}^2,$$

and using this inequality in (62) yields

$$\|\mathbf{u}_1(t) - \mathbf{u}_2(t)\|_{\mathbb{V}}^2 \leq C \int_0^t \|\eta_1(s) - \eta_2(s)\|_{\mathbb{V}}^2 ds. \tag{63}$$

On the other hand, from the Cauchy problem (52)–(53), we can write

$$w_i(t) = w_0 - \int_0^t k_w \alpha^* p_\nu (u_\nu(s) - w_i(s) - g(s)) ds,$$

and then

$$\begin{aligned} \|w_1(t) - w_2(t)\|_{L^2(\Gamma_3)} &\leq C \left( \int_0^t \|k_w \alpha^* p_\nu (u_\nu(s) - w_1(s) - g(s))\|_{L^2(\Gamma_3)} ds \right. \\ &\quad \left. + \int_0^t \|k_w \alpha^* p_\nu (u_\nu(s) - w_2(s) - g(s))\|_{L^2(\Gamma_3)} ds \right). \end{aligned}$$

Using (26),(27), and writing  $w_1 = w_1 - w_2 + w_2$ , we obtain

$$\begin{aligned} \|w_1(t) - w_2(t)\|_{L^2(\Gamma_3)} &\leq C \left( \int_0^t \|w_1(s) - w_2(s)\|_{L^2(\Gamma_3)} ds \right. \\ &\quad \left. + \int_0^t \|\mathbf{u}_1(s) - \mathbf{u}_2(s)\|_{\mathbb{V}} ds \right). \end{aligned}$$

Next, we apply Gronwall’s inequality to deduce

$$\|w_1(t) - w_2(t)\|_{L^2(\Gamma_3)} \leq C \int_0^T \|\mathbf{u}_1(s) - \mathbf{u}_2(s)\|_{\mathbb{V}} ds,$$

and from the relation (3), we obtain

$$\|w_1(t) - w_2(t)\|_{L^2(\Gamma_3)}^2 \leq C \int_0^T \|\mathbf{u}_1(s) - \mathbf{u}_2(s)\|_{\mathbb{V}}^2 ds. \tag{64}$$

We use now (4), (24),(25) and (54) to find

$$\|\varphi_1(t) - \varphi_2(t)\|_W^2 \leq C \|\mathbf{u}_1(t) - \mathbf{u}_2(t)\|_{\mathbb{V}}^2. \quad (65)$$

We substitute (63), (64) and (65) in (61) to obtain

$$\|\Lambda\eta_1(t) - \Lambda\eta_2(t)\|_{\mathbb{V}}^2 \leq C \int_0^T \|\eta_1(s) - \eta_2(s)\|_{\mathbb{V}}^2 ds.$$

Reiterating this inequality  $m$  times, we obtain

$$\|\Lambda^m \eta_1 - \Lambda^m \eta_2\|_{\mathcal{C}(0,T;\mathbb{V})}^2 \leq \frac{C^m T^m}{m!} \|\eta_1 - \eta_2\|_{\mathcal{C}(0,T;\mathbb{V})}^2.$$

Thus, for  $m$  sufficiently large, the operator  $\Lambda^m$  is a contraction on the Banach space  $\mathcal{C}(0, T; \mathbb{V})$ , and so  $\Lambda$  has a unique fixed point.

Now, we have all the ingredients to prove Theorem 4.1.

**Proof.** [Proof of Existence] Let  $\eta^* \in \mathcal{C}(0, T; \mathbb{V})$  be the fixed point of  $\Lambda$  defined by (59), and if  $\{\mathbf{u}_*, w_*, \varphi_*\}$  are the solutions of  $\mathcal{PV}_\eta^u, \mathcal{PV}_\eta^w$  and  $\mathcal{PV}_\eta^\varphi$ , for  $\eta = \eta^*$ , we use the following notations:

$$\mathbf{u}_* = \mathbf{u}_{\eta^*}, \quad \varphi_* = \varphi_{\eta^*}, \quad w_* = w_{\eta^*}. \quad (66)$$

Let  $\boldsymbol{\sigma}$  and  $\mathbf{D}$  be the functions defined by

$$\boldsymbol{\sigma}_*^k = \mathcal{A}^k \boldsymbol{\varepsilon}(\dot{\mathbf{u}}_*^k) + \mathcal{G}^k \boldsymbol{\varepsilon}(\mathbf{u}_*^k) + (\mathcal{E}^k)^* \nabla \varphi_*^k, \quad (67)$$

$$\mathbf{D}_*^k = \mathcal{E}^k \boldsymbol{\varepsilon}(\mathbf{u}_*^k) - \mathcal{B}^k \nabla \varphi_*^k. \quad (68)$$

We prove that  $\{\mathbf{u}_*, \boldsymbol{\sigma}_*, w_*, \varphi_*, \mathbf{D}_*\}$  satisfies (37)–(42) and the regularities (44)–(48). Clearly, (37), (41) and (42) are satisfied. We use now the equality  $\Lambda\eta^* = \eta^*$ , it follows that

$$(\Lambda\eta^*(t), \mathbf{v})_{\mathbb{V}} = (\eta^*(t), \mathbf{v})_{\mathbb{V}}. \quad (69)$$

From the problem  $\mathcal{PV}_\eta^u$ , we get

$$(\eta^*(t), \mathbf{v})_{\mathbb{V}} = - \sum_{k=1}^2 (\mathcal{A}^k \boldsymbol{\varepsilon}(\dot{\mathbf{u}}_*^k(t)), \boldsymbol{\varepsilon}(\mathbf{v}^k(t)))_{Q^k} + (\mathbf{f}(t), \mathbf{v})_{\mathbb{V}}, \forall \mathbf{v} \in \mathbb{V}, \text{ a.e. } t \in (0, T). \quad (70)$$

From the definition of  $\Lambda$ , we have

$$\begin{aligned} (\Lambda\eta^*(t), \mathbf{v})_{\mathbb{V}} &= \sum_{k=1}^2 (\mathcal{G}^k \boldsymbol{\varepsilon}(\mathbf{u}_*^k(t)), \boldsymbol{\varepsilon}(\mathbf{v}^k(t)))_{\mathbb{V}} + j(w_*(t), \mathbf{u}_*(t), \mathbf{v}) \\ &\quad + \sum_{k=1}^2 ((\mathcal{E}^k)^* \nabla \varphi_*^k(t), \boldsymbol{\varepsilon}(\mathbf{v}^k(t)))_{Q^k}, \\ &\quad \forall \mathbf{v} \in \mathbb{V}, \text{ a.e. } t \in (0, T), k = 1, 2. \end{aligned} \quad (71)$$

From (69), (70) and (71), we deduce that

$$\begin{aligned} (\mathbf{f}(t), \mathbf{v})_{\mathbb{V}} &= \sum_{k=1}^2 (\mathcal{A}^k \boldsymbol{\varepsilon}(\dot{\mathbf{u}}_*^k(t)), \boldsymbol{\varepsilon}(\mathbf{v}^k(t)))_{Q^k} + \sum_{k=1}^2 (\mathcal{G}^k \boldsymbol{\varepsilon}(\mathbf{u}_*^k(t)), \boldsymbol{\varepsilon}(\mathbf{v}^k))_{\mathbb{V}} \\ &\quad + j(w_*(t), \mathbf{u}_*(t), \mathbf{v}) + \sum_{k=1}^2 ((\mathcal{E}^k)^* \nabla \varphi_*^k(t), \boldsymbol{\varepsilon}(\mathbf{v}^k))_{Q^k}, \\ &\quad \forall \mathbf{v} \in \mathbb{V}, \text{ a.e. } t \in (0, T), k = 1, 2. \end{aligned} \quad (72)$$

We use (67) and (72), we get

$$(\mathbf{f}(t), \mathbf{v})_{\mathbb{V}} = \sum_{k=1}^2 (\boldsymbol{\sigma}_*^k(t), \varepsilon(\mathbf{v}^k))_{Q^k} + j(w_*(t), \mathbf{u}_*(t), \mathbf{v}). \tag{73}$$

We deduce that (39) is satisfied. Additionally, we use  $\mathbf{u}_{\eta^*}$  in (52) and (66) to find

$$\dot{w}_*(t) = k_w \alpha^* p_{*\nu} (u_{*\nu} - w_* - g), \text{ a.e. } t \in (0, T). \tag{74}$$

Now, relations (66), (67), (68), (73) and (74) allow us to conclude that  $\{\mathbf{u}_*, \boldsymbol{\sigma}_*, w_*, \varphi_*, \mathbf{D}_*\}$  satisfies (37)–(42).

Next, (42) and the regularities (44), (46)–(47) follow from Lemmas 4.1, 4.2 and 4.3.

Since  $\mathbf{u}_*, w_*$  and  $\varphi_*$  satisfy (44), (46) and (47), respectively, it follows from (66) and (67) that

$$\boldsymbol{\sigma}_* \in C(0, T; \mathbb{Q}). \tag{75}$$

For  $k = 1, 2$ , we choose  $\mathbf{v} = \dot{\mathbf{u}} \pm \phi$  in (73), with  $\phi = (\phi^1, \phi^2)$ ,  $\phi^k \in D(\Omega^k)^d$  and  $\phi^{3-k} = 0$  in (54), to obtain

$$\text{Div } \boldsymbol{\sigma}_*^k(t) = -\mathbf{f}_0^k(t) \quad \forall t \in [0, T], \quad k = 1, 2, \tag{76}$$

where  $D(\Omega^k)$  is the space of infinitely differentiable real functions with a compact support in  $\Omega^k$ . The regularity (45) follows from (28), (75) and (76). Let now  $t_1, t_2 \in [0, T]$ , by (4), (24), (25) and (68), we deduce that

$$\|\mathbf{D}_*(t_1) - \mathbf{D}_*(t_2)\|_{\mathbb{H}} \leq C (\|\varphi_*(t_1) - \varphi_*(t_2)\|_{\mathbb{W}} + \|\mathbf{u}_*(t_1) - \mathbf{u}_*(t_2)\|_{\mathbb{V}}).$$

The regularity of  $\mathbf{u}_*$  and  $\varphi_*$  given by (44) and (47) implies

$$\mathbf{D}_* \in C(0, T; \mathbb{H}). \tag{77}$$

For  $k = 1, 2$ , we choose  $\phi = (\phi^1, \phi^2)$  with  $\phi^k \in D(\Omega^k)^d$  and  $\phi^{3-k} = 0$  in (54) and using (34), we find

$$\text{div } \mathbf{D}_*^k(t) = q_0^k(t) \quad \forall t \in [0, T], \quad k = 1, 2. \tag{78}$$

Property (48) follows from (28), (77) and (78).

Finally, we conclude that the weak solution  $\{\mathbf{u}_*, \boldsymbol{\sigma}_*, w_*, \varphi_*, \mathbf{D}_*\}$  of the Problem  $\mathcal{PV}$  has the regularities (44)–(48), which concludes the existence part of Theorem 4.1.

**Proof.** [Proof of Uniqueness] The uniqueness of the solution is a consequence of the uniqueness of the fixed point of the operator  $\Lambda$  defined by (59) and the unique solvability of the Problems  $\mathcal{PV}_\eta^u, \mathcal{PV}_\eta^w$  and  $\mathcal{PV}_\eta^\varphi$ .

**References**

[1] A. Aissaoui and N. Hemic. A frictional contact problem with damage and adhesion for an electro elastic-viscoplastic body. *Electronic Journal of Differential Equations* **2014** (11) (2014) 1–19.  
 [2] R.C. Batra and J. S. Yang. Analysis and numerical approach of a piezoelectric contact problem. *Annals of the Academy of Romanian Scientists* **1** (2009) 7–30.  
 [3] J. J. Bikerman. Thermodynamics, adhesion, and sliding friction. *Journal of lubrication technology* **92** (1970) 243–247.

- [4] P. Bisenga, F. Lebon and F. Maceri. The unilateral frictional contact of a piezoelectric body with a rigid support. In: *Contact Mechanics*, J. A. C. Martins and Manuel D. P. Monteiro Marques (Eds), Kluwer, Dordrecht, 2002, 347–354.
- [5] H. Brézis. Equations et inéquations non linéaires dans les espaces vectoriels en dualité. *Ann. Inst. Fourier* **18** (1968) 115–175. [French]
- [6] A. Djabi. *Etude Mathématique de systèmes modélisant des phénomènes mécaniques*. Editions universitaires européennes, 2018, ISBN: 6138396545 [French]
- [7] A. Djabi and A. Merouani. A fixed point method for a class of nonlinear evolution systems modeling a mechanical phenomenon. *International Journal of Open Problems in Computer Science and Mathematics* **8** (1) (2015) 1–13.
- [8] A. Djabi and A. Merouani. Bilateral contact problem with friction and wear for an electro elastic-viscoplastic materials with damage. *Taiwanese Journal of Mathematics* **19** (4) (2015) 1161–1182.
- [9] A. Djabi, A. Merouani and A. Aissaoui. A frictional contact problem with wear involving elastic-viscoplastic materials with damage and thermal effects. *Electronic Journal of Qualitative Theory of Differential Equations* **27** (2015) 1–18.
- [10] G. Duvaut and J. Lions. *Les inéquations en mécanique et en physique*. Springer, Berlin 1976. [French]
- [11] C. Eck, J. Jarušek, M. and Krbeč. Unilateral Contact Problems: Variational Methods and Existence Theorems. *Pure and Applied Mathematics*. **270**, Chapman/CRC Press, New York, 2005.
- [12] T. Ikeda. *Fundamentals of Piezoelectricity*. Oxford University Press, Oxford, 1990.
- [13] Z. Lerguet, Z. Zellagui, H. Benseridi and S. Drabla. Variational analysis of an electro viscoelastic contact problem with friction. *Journal of the Association of Arab Universities for Basic and Applied Sciences* **14** (1) (2013) 93–100.
- [14] J. L. Lions. *Quelques Méthodes de Résolution des Problèmes Aux Limites Non Linéaires*. Dunod, 1969. [French]
- [15] F. Maceri and P. Bisegna. The unilateral frictionless contact of a piezoelectric body with a rigid support. *Mathematical and Computer Modelling* **28** (1998) 19–28.
- [16] R. D. Mindlin. Elasticity piezoelectricity and crystal lattice dynamics. *Journal of Elasticity* **4** (1972) 217–280.
- [17] J. Nečas and I. Hlaváček. *Mathematical Theory of Elastic and Elasto-plastic Bodies, An Introduction*. Elsevier, Amsterdam, 1981.
- [18] N. Strömberg, L. Johansson and A. Klarbring. Derivation and analysis of a generalized standard model for contact friction and wear. *International Journal of Solids and Structures* **33** (1996) 1817–1836.



# Global Optimization Method of Multivariate non-Lipschitz Functions Using Tangent Minorants

Djaouida Guettal \*, Chahinez Chenouf and Mohamed Rahal

*Laboratory of Fundamental and Numerical Mathematics (LMFN),  
Department of Mathematics, University of Ferhat Abbas Setif 1, Algeria.*

Received: January 12, 2023; Revised: March 20, 2023

**Abstract:** This paper deals with the multidimensional global optimization problem where the objective function  $f$  is non-Lipschitz over a hyper-rectangle of  $\mathbb{R}^n$ . The generalization of Piyavskii’s algorithm to the multivariate case requires finding the intersection of many non-linear hyper-surfaces. In this paper, we propose an algorithm which is composed of two steps. The first one is to transform the multivariate function  $f$  into a single variable function  $\mathbf{f}(t)$  using the  $\alpha$ -dense curves and the second one is to apply the extended version of Piyavskii’s algorithm to  $\mathbf{f}(t)$ . For minimizing  $\mathbf{f}(t)$ , we construct a sequence of lower bounding piecewise tangent functions. A convergence result is proved and the numerical experiments on some test functions are given and compared with the existing methods.

**Keywords:** *global optimization; non-Lipschitz multivariate functions; lower bounding function; Piyavskii’s algorithm.*

**Mathematics Subject Classification (2010):** 93-03, 93A30, 93B40, 93C35, 90C26.

## 1 Introduction

Let us consider the box constrained global optimization problem

$$\min_{x \in \mathbf{P} = \prod_{i=1}^n [a_i, b_i]} f(x), \quad (\text{P})$$

where  $f$  is a real continuous multi-extremal function defined on the hyper-rectangle  $\mathbf{P}$  and satisfies the following condition:

$$|f(x) - f(y)| \leq h \|x - y\|^{1/m}, \quad \forall x, y \in \mathbf{P}, \quad (1)$$

---

\* Corresponding author: <mailto:djaouida.guettal@univ-setif.dz>

with two parameters  $h > 0$  and  $1/m$  ( $m > 1$ ), where  $\|\cdot\|$  stands for the Euclidean norm. The last condition is called the Hölder condition (it is clear that if  $m = 1$ , we have the Lipschitz case) [7]. Global optimization is of interest in many complex industrial applications. But it can also be applied to a variety of other multidimensional problems such as the resolution of systems of nonlinear functional equations [6] involving objective functions, which are only continuous and do not possess strong mathematical proprieties such as convexity or differentiability, and which should be optimized [1]. The kind of problem (P) arises in several applications, for instance, the simple plant location problem under a uniform delivered price policy, see Hanjoul et al. [10], infinite horizon optimization problems, see Kiatsupaibul et al. [12], etc. The local irregularity of the objective function, particularly when the value of  $m$  is large, is what causes the problem to be complex to solve in this case. When applied to higher dimensions, the traditional multidimensional global optimization methods present significant challenges. Some researchers have considered reducing the dimension of certain problems to convert them into others that are simpler [5], [17]. There are numerous methods for reducing a multidimensional global optimization problem to one or more optimization problems with a smaller dimension, especially with one dimension. Many authors have explored the strategy based on filling the feasible region with a curve, see, for example, Butz [4], Strongin [18], and Sergeev et al. [17]. For this, they take into account the Peano-type curve approximations. These curves, known as space-filling curves, were first presented by Peano (1890), subsequently by Hilbert (1891), and have the property of passing through all points of a hyper-rectangle of  $\mathbb{R}^n$ . On the other hand, Cherruault [5], Guettal and Ziadi [9], [15], [16] and their collaborators have consistently improved the reducing transformation method in recent years, their method depends on reducing a multidimensional problem to a unidimensional one by using the space-filling curves like  $\alpha$ -dense type curves to fill the feasible domain, and then, using a one-dimensional global optimization algorithm, to approximate the global minimizer. Gourdin et al. [8] have suggested solving this problem by the generalization of Piyavskii's algorithm to the multivariate situation [8]. Indeed, Piyavskii's approach cannot be directly generalized since finding the intersection of many parabolic hyper-surfaces is necessary to find the local minima of the sub-estimators of the objective function on  $\mathbf{P}$ . The authors in [8] proposed a procedure for partitioning and eliminating (Branch-and-Bound) hyper-rectangles of no interest by constructing piecewise constant sub-estimator functions. Here, we present a novel method for deterministic global optimization that relies on a methodology for reducing the dimension of the problem (P) and is referred to as the "method of the reducing transformation". Finding the global minima of multivariate functions with a lot of local minima has proven to be quite effective with the Alienor method coupled with some covering one-dimensional methods. The concept is to densify the hyper-rectangle  $\mathbf{P}$  as accurately as we need, using pretty regular so-called " $\alpha$ -dense curves", and then approach the objective function  $f$  with  $n$  variables defined on the hyper-rectangle  $\mathbf{P}$ , by a function  $\mathbf{f}$  with a single variable  $t$  on a real interval  $A$  of  $\mathbb{R}$ , which will be specified later. This allows the multidimensional optimization problem to be reduced to a one-dimensional optimization problem, which can then be solved using one-dimensional methods that are well-known for their effectiveness and performance. This coupling has proved to be efficient for solving diverse non-Lipschitz global optimization problems. For minimizing the function  $\mathbf{f}$  on  $A$ , we construct a sequence of lower bounding piecewise tangent functions.

The remainder of the work is organized as follows. Section 2 contains the Alienor

reducing transformation method. Section 3 presents some covering methods to find the global minima of univariate functions. Section 4 shows the modified mixed Alienor method with covering methods and their convergence. Section 5 gives some numerical experiments confirming theoretical results and showing a reliable performance of the proposed method and Section 6 concludes the paper.

## 2 A Multivariate non-Lipschitz Method

### 2.1 The Alienor reducing transformation method

Global optimization is essentially the purpose of the Alienor reducing transformation approach [5], [19], [20]. But it can also be applied to a variety of other multidimensional problems such as the resolution of systems of non-linear functional equations and the approximation of functions of many variables by functions of a single variable. The essential idea behind this approach is to perform a transformation that turns multidimensional optimization problems into single-variable ones before using an effective algorithm for one-dimensional optimization problems. The transformation is thus based on the creation of a specific  $\alpha$ -dense parametrized curve  $\zeta(t) = (\zeta_1(t), \zeta_2(t), \dots, \zeta_n(t))$  in the feasible set  $\mathbf{P}$ .

**Definition 2.1** Let  $A$  be an interval of  $\mathbb{R}$ . We say that a parametrized curve of  $\mathbb{R}^n$  defined by  $\zeta : A \rightarrow \mathbf{P}$  is  $\alpha$ -dense in  $\mathbf{P}$  if for all  $x \in \mathbf{P}$ ,  $\exists t \in A$  such that

$$d(x, \zeta(t)) \leq \alpha,$$

where  $d$  stands for the Euclidean distance in  $\mathbb{R}^n$ .

### 2.2 Building $\alpha$ -dense curves

In order to create  $\alpha$ -dense curves in  $\mathbf{P}$ , let us assume that the function  $\zeta(t)$  is defined on the closed and bounded interval  $A = [0, T]$  of  $\mathbb{R}$  with values in  $\mathbf{P}$ , where  $T$  is the upper bound of the domain of definition of  $\zeta$ . The number  $\alpha$  is supposed strictly positive and extremely small the dimension of the hyper-rectangle  $\mathbf{P} = \prod_{i=1}^n [a_i, b_i]$ . We define by a constructive way an  $\alpha$ -dense curve in an arbitrary hyper-rectangle of  $\mathbb{R}^n$  thanks to the following results.

**Theorem 2.1** Let  $\zeta(t) = (\zeta_1(t), \zeta_2(t), \dots, \zeta_n(t))$  be a function defined from  $[0, T]$  into the hyper-rectangle  $\mathbf{P}$ ,  $\alpha > 0$ , and  $\mu$  be the Lebesgue measure such that

- (1)  $(\zeta_i)_{1 \leq i \leq n}$  are continuous and surjective.
- (2)  $(\zeta_i)_{2 \leq i \leq n}$  are periodic, respectively, of periods  $(t_i)_{2 \leq i \leq n}$ .
- (3) For any interval  $I$  of  $[0, T]$  and for any  $i \in \{2, \dots, n\}$ , we have

$$\mu(I) \leq t_i \Rightarrow \mu(\zeta_{i-1}(I)) < \alpha.$$

Then for  $t \in [0, T]$ , the function  $\zeta(t)$  represents a parametrized  $\sqrt{n-1}\alpha$ -dense curve in  $\mathbf{P}$ . (The proof can be found in [20]).

**Corollary 2.1** [20] Let  $\zeta(t) = (\zeta_1(t), \zeta_2(t), \dots, \zeta_n(t)) : \left[0, \frac{\pi}{\alpha_1}\right] \rightarrow \prod_{i=1}^n [a_i, b_i]$  be a function defined by

$$\zeta_i(t) = \frac{a_i - b_i}{2} \cos(\alpha_i t) + \frac{a_i + b_i}{2}, \quad i = 1, 2, \dots, n,$$

where  $\alpha_1, \alpha_2, \dots, \alpha_n$  are given strictly positive constants satisfying the relationships

$$\alpha_i \geq \frac{\pi}{\alpha} (b_{i-1} - a_{i-1}) \alpha_{i-1}, \quad \forall i = 2, \dots, n.$$

Then the curve defined by the parametric curve  $\zeta(t)$ , is  $\sqrt{n-1}\alpha$ -dense in  $\mathbf{P}$ .

When using the reducing transformation approach, we first explicitly provide a parametric representation  $x_i = \zeta_i(t)$ , where  $i = 1, \dots, n$ , of the  $\alpha$ -dense curve in the hyper-rectangle  $\mathbf{P}$ , for  $t \in \left[0, \frac{\pi}{\alpha_1}\right]$ . Let us specify the following function:

$$\zeta(t) = (\zeta_1(t), \zeta_2(t), \dots, \zeta_n(t)) : \left[0, \frac{\pi}{\alpha_1}\right] \rightarrow \mathbf{P}$$

with

$$\zeta_i(t) = \frac{a_i - b_i}{2} \cos(\alpha_i t) + \frac{a_i + b_i}{2}, \quad i = 1, \dots, n,$$

where  $\alpha$  and  $(\alpha_i)_{1 \leq i \leq n}$  are provided by

$$\alpha = \left(\frac{\varepsilon}{2h}\right)^m \frac{1}{\sqrt{n-1}}, \quad \alpha_1 = 1 \text{ and } \alpha_i = \frac{\pi}{\alpha} (b_{i-1} - a_{i-1}) \alpha_{i-1}, \quad i = 2, \dots, n.$$

According to Corollary 2.1, the parametrized curve  $\zeta(t)$  is  $\alpha$ -dense in the hyper-rectangle  $\mathbf{P}$ . Moreover, the function  $\zeta$  is Lipschitzian on  $\left[0, \frac{\pi}{\alpha_1}\right]$  with the constant

$$L = \frac{1}{2} \left( \sum_{i=1}^n (b_i - a_i)^2 \alpha_i^2 \right)^{\frac{1}{2}}.$$

Then the objective function  $f$  is approximated by the function of a single variable defined by  $\mathbf{f}(t) = f(\zeta(t))$ . The minimization problem (P) is then approximated by the one-dimensional minimization problem

$$\min_{t \in \left[0, \frac{\pi}{\alpha_1}\right]} \mathbf{f}(t).$$

**Theorem 2.2** *The function  $\mathbf{f}(t) = f(\zeta(t))$  for  $t \in \left[0, \frac{\pi}{\alpha_1}\right]$  satisfies the condition (1) with the constant  $\mathbf{h}$  and exponent  $1/m$ , where  $\mathbf{h}$  is given by  $\mathbf{h} = hL^{1/m}$ .*

**Proof.** For  $t_1$  and  $t_2$  in  $\left[0, \frac{\pi}{\alpha_1}\right]$ , we have

$$|\mathbf{f}(t_1) - \mathbf{f}(t_2)| = |f(\zeta(t_1)) - f(\zeta(t_2))| \leq h \|\zeta(t_1) - \zeta(t_2)\|^{1/m}.$$

As the function  $\zeta$  is Lipschitzian on  $\left[0, \frac{\pi}{\alpha_1}\right]$  with the constants  $L$ , we have

$$\|\zeta(t_1) - \zeta(t_2)\| \leq L |t_1 - t_2|,$$

then

$$|\mathbf{f}(t_1) - \mathbf{f}(t_2)| \leq h (L |t_1 - t_2|)^{1/m},$$

whence

$$|\mathbf{f}(t_1) - \mathbf{f}(t_2)| \leq hL^{1/m} |t_1 - t_2|^{1/m}.$$

This permits us to use one of the unidimensional algorithms to solve the multidimensional problem (P) shown in Section 3.

### 3 A Single Variable non-Lipschitz Method

The following unidimensional optimization problem will be defined by

$$\min_{t \in \left[0, \frac{\pi}{\alpha_1}\right]} \mathbf{f}(t), \tag{P'}$$

where  $\mathbf{f}$  is defined on the interval  $\left[0, \frac{\pi}{\alpha_1}\right]$  and satisfies the condition (1) with the constant  $\mathbf{h}$  and exponent  $1/m$ , ( $m > 1$ ). When minimizing a non-convex function  $\mathbf{f}$ , the general principle behind most deterministic global optimization methods is to relax the original non-convex problem in order to make the relaxed problem convex by utilizing an under-estimator of the objective function [11], [14].

**Definition 3.1** A function  $F$  is said to be an under-estimator of a function  $\mathbf{f}$  on a set  $X$  if

$$F(t) \leq \mathbf{f}(t), \quad \forall t \in X,$$

with the possibility that  $F$  may not reach  $\mathbf{f}$  at any point in  $X$ .

#### 3.1 Constructing a sequence of under-estimators

The idea is to build an increasing sequence of piecewise functions that minorize the objective function  $\mathbf{f}$  and are constructed in such a way that their global minima converge to the desired global minimum. From the condition (1), if a point  $t' \in \left[0, \frac{\pi}{\alpha_1}\right]$  is fixed, then we have

$$F(t) = \mathbf{f}(t') - \mathbf{h} |t - t'|^{1/m} \leq \mathbf{f}(t), \quad \forall t \in \left[0, \frac{\pi}{\alpha_1}\right],$$

i.e.,  $F$  is an under-estimator of  $\mathbf{f}$  on  $\left[0, \frac{\pi}{\alpha_1}\right]$ . Let us define the first under-estimator by

$$F_1(t) = \mathbf{f}(t_1) - \mathbf{h} |t - t_1|^{1/m} \leq \mathbf{f}(t), \quad \forall t \in \left[0, \frac{\pi}{\alpha_1}\right],$$

where  $t_1$  is chosen arbitrarily, we then determine a point  $t_2 = \arg \min_{t \in \left[0, \frac{\pi}{\alpha_1}\right]} F_1(t)$ , we thus

obtain a new under-estimator of  $\mathbf{f}$ ,

$$F_2(t) = \max_{1 \leq i \leq 2} \left\{ \mathbf{f}(t_i) - \mathbf{h} |t - t_i|^{1/m} \right\}.$$

At step  $k$ , the function

$$F_k(t) = \max_{1 \leq i \leq k} \left\{ \mathbf{f}(t_k) - \mathbf{h} |t - t_k|^{1/m} \right\}.$$

In the search interval  $\left[0, \frac{\pi}{\alpha_1}\right]$ , the restriction of  $F_k$  on each sub-interval  $[t_{i-1}, t_i]$ ,  $i = 2, \dots, k$ , can be expressed as

$$F_i(t) = \max_i \left\{ \underbrace{\mathbf{f}(t_{i-1}) - \mathbf{h} (t - t_{i-1})^{1/m}}_{\Phi_{i-1}(t)}, \underbrace{\mathbf{f}(t_i) - \mathbf{h} (t_i - t)^{1/m}}_{\Phi_i(t)} \right\}.$$

The function  $F_i(t)$  is convex and non-differentiable in  $[t_{i-1}, t_i]$  and its global minimum value can be computed by locating the point where the two parabolic curves intersect, i.e., it necessitates solving a non-linear algebraic equation on  $[0, \frac{\pi}{\alpha_1}]$ ,

$$\mathbf{f}(t_{i-1}) - \mathbf{h}(t - t_{i-1})^{1/m} = \mathbf{f}(t_i) - \mathbf{h}(t_i - t)^{1/m}. \tag{2}$$

Determining the unique point of intersection of two parabolic curves is generally easy only for certain cases of  $m$ . Gourdin et al. [8] give the analytical expression for the intersection point when  $m$  is the integers 2, 3, 4 and  $\mathbf{h}$  is known. Lera and Sergeyev proposed the secant method (SM) [13] when they utilized a different concept based on changing the intersection point of the parabolic curves at each sub-interval  $[t_{i-1}, t_i]$  to the intersection point  $\bar{t}_i$  of two linked linear interpolations  $l_{i-1}$  (resp.  $l_i$ ) of the parabolas  $\Phi_{i-1}$  (resp.  $\Phi_i$ ). Then the constant lower bound of the objective function on  $[t_{i-1}, t_i]$  is defined by

$$\mathbf{w}_i = \min \{ \Phi_{i-1}(\bar{t}_i), \Phi_i(\bar{t}_i) \}.$$

Here we suggest another technique noted *TM*, when changing the solution of the equation (2) by an intersection point  $\omega_i$  of two tangents  $T_{i-1}$  (resp.  $T_i$ ) at the same middle point of the interval  $[t_{i-1}, t_i]$ , related to these two parabolas  $\Phi_{i-1}$  (resp.  $\Phi_i$ ) and defined by

$$\begin{cases} T_{i-1}(t) = -(\mathbf{h}/m)e_i^{(1/m)-1}t + \mathbf{h}e_i^{1/m}(\frac{v_i}{me_i} - 1) + \mathbf{f}(t_{i-1}), \\ T_i(t) = (\mathbf{h}/m)e_i^{(1/m)-1}t - \mathbf{h}e_i^{1/m}(\frac{v_i}{me_i} + 1) + \mathbf{f}(t_i) \end{cases} \tag{3}$$

such as  $v_i = \frac{t_i+t_{i-1}}{2}$  and  $e_i = \frac{t_i-t_{i-1}}{2}$ .

In this case, the point  $\omega_i$  can be calculated even if  $m$  is large enough or not integer, by

$$\omega_i = v_i + \frac{m(\mathbf{f}(t_{i-1}) - \mathbf{f}(t_i))}{2\mathbf{h}e_i^{(1/m)-1}}. \tag{4}$$

**Proposition 3.1** *Let  $\mathbf{f}$  be a real univariate function satisfying the condition (1) with the constant  $\mathbf{h} > 0$  and exponent  $1/m$  defined on the interval  $[0, \frac{\pi}{\alpha_1}]$ . Let the value  $\mathbf{T}_i = \min \{ \Phi_{i-1}(\omega_i), \Phi_i(\omega_i) \}$  as a constant lower bound of  $\mathbf{f}$  on  $[t_{i-1}, t_i] \subset [0, \frac{\pi}{\alpha_1}]$ , then we have*

$$\mathbf{T}_i = \min \left\{ \mathbf{f}(t_{i-1}) - \mathbf{h} \left( e_i + \frac{m(\mathbf{f}(t_{i-1}) - \mathbf{f}(t_i))}{2\mathbf{h}e_i^{(1/m)-1}} \right)^{1/m}, \mathbf{f}(t_i) - \mathbf{h} \left( e_i + \frac{m(\mathbf{f}(t_i) - \mathbf{f}(t_{i-1}))}{2\mathbf{h}e_i^{(1/m)-1}} \right)^{1/m} \right\}$$

and

$$\mathbf{T}_i < \mathbf{f}(t), \quad \forall t \in [t_{i-1}, t_i]. \tag{5}$$

**Proof.** The value  $\mathbf{T}_i$  is given by replacing the variable  $t$  in the two functions  $\Phi_{i-1}(t)$  and  $\Phi_i(t)$  by the expression (4). Since  $F_i(t) < \mathbf{f}(t), \forall t \in ]t_{i-1}, t_i[$ , where  $F_i(t) = \max \{ \Phi_{i-1}(t), \Phi_i(t) \}$ , we have

$$\min \{ \Phi_{i-1}(t), \Phi_i(t) \} \leq \min_{[t_{i-1}, t_i]} F_i(t) \leq \mathbf{f}(t), \quad \forall t \in [t_{i-1}, t_i].$$

In particular, for  $t = \omega_i$ , it then follows

$$\mathbf{T}_i = \min \{ \Phi_{i-1}(\omega_i), \Phi_i(\omega_i) \} < \mathbf{f}(t), \quad \forall t \in ]t_{i-1}, t_i[.$$

#### 4 The Modified Mixed Alienor-*TM* Method

In order to determine the global minimum of  $f(x)$ , the modified mixed Alienor-*TM* Method consists of two steps: the reducing transformation step and the application of the *TM* algorithm to the function  $\mathbf{f}(t) = f(\zeta(t))$ , which satisfies the condition (1) with the constant  $\mathbf{h} = hL^{1/m}$ .

---

**Algorithm 4.1** (Alienor-*TM*)

---

**Input:**  $\mathbf{P} = \prod_{i=1}^n [a_i, b_i]$  is the search domain,  $f$  is the objective function (multivariate non-Lipschitz function). The parameters  $h, m, \varepsilon$  and the dimension  $n$ .

**Output:** **Part 1 :**  $\zeta(t)$  is the parametric curve,  
 $\mathbf{f}$  is the univariate non-Lipschitz function.

**Part 2 :**  $\mathbf{f}_{opt}$  is the best global minimum of  $\mathbf{f}$ .

**Part 1 :**

$$\alpha = \left(\frac{\varepsilon}{2h}\right)^m, \quad \alpha_1 = 1.$$

**for**  $i = 2$  to  $n$  **do**

$$\alpha_i = \frac{\pi}{\alpha} (b_i - a_i) \alpha_{i-1}.$$

**end for**

**for**  $i = 1$  to  $n$  **do**

$$\zeta_i(t) = \frac{a_i - b_i}{2} \cos(\alpha_i t) + \frac{a_i + b_i}{2}.$$

**end for**

$$\zeta(t) = (\zeta_1(t), \zeta_2(t), \dots, \zeta_n(t)) \text{ and } \mathbf{f}(t) = f(\zeta(t)).$$

**Part 2 :**

**Initialization:**  $k \leftarrow 2, \mu \leftarrow 2, t_1 \leftarrow 0, t_2 \leftarrow \frac{\pi}{\alpha_1}$ .

**Step  $k$ :**  $t_1, t_2, \dots, t_k$  are ordered such that  $0 = t_1 < t_2 < \dots < t_k = \frac{\pi}{\alpha_1}$ .

**for**  $i = 2$  to  $k$  **do**

$$\omega_i = v_i + \frac{m(\mathbf{f}(t_{i-1}) - \mathbf{f}(t_i))}{2he_i^{(1/m)-1}},$$

$$\mathbf{T}_i = \min \{ \mathbf{f}(t_{i-1}) - \mathbf{h}(\omega_i - t_{i-1})^{1/m}, \mathbf{f}(t_i) - \mathbf{h}(t_i - \omega_i)^{1/m} \}.$$

**end for**

$$\mathbf{T}_\mu \leftarrow \min \{ \mathbf{T}_i, 2 \leq i \leq k \}, \tag{6}$$

$$t_\mu \leftarrow \omega_\mu.$$

**if**  $|t_\mu - t_{\mu-1}| > \varepsilon = \left(\frac{\varepsilon}{2h}\right)^m$ , **then**

$$t_{k+1} \leftarrow \omega_\mu \tag{7}$$

$$k \leftarrow k + 1$$

Go to Step  $k$

**else**

$$\mathbf{f}_{opt} = \min \{ \mathbf{f}(t_i) : 1 \leq i \leq k \} \text{ and Stop.}$$

**end if**

return  $\mathbf{f}_{opt}$

---

## 5 Convergence Results of $TM$ and Alienor- $TM$ Algorithms

**Theorem 5.1** *Let  $\mathbf{f}(t)$  be a real non-Lipschitz function defined on a closed interval  $[0, \frac{\pi}{\alpha_1}]$ , with  $\mathbf{h} > 0$  and  $1/m$ , ( $m > 1$ ). Let  $t^*$  be a global minimizer of  $\mathbf{f}(t)$ . Then the sequence  $(t_k)_{k \geq 1}$  generated by the  $TM$  algorithm converges to  $t^*$ , i.e.,*

$$\lim_{k \rightarrow +\infty} \mathbf{f}(t_k) = \mathbf{f}(t^*).$$

**Proof.** Let  $t_1, t_2, t_3, \dots$  be the sampling sequence satisfying (4), (6), (7). Let us consider that  $t_s \neq t_{s'}$  for all  $s \neq s'$ , the set of the elements of the sequence  $(t_k)_{k \geq 1}$  is then infinite and therefore has at least one limit point in  $[0, \frac{\pi}{\alpha_1}]$ . Let  $\mathbf{z}$  be any limit point of  $(t_k)_{k \geq 1}$  such that  $\mathbf{z} \neq 0$ ,  $\mathbf{z} \neq \frac{\pi}{\alpha_1}$ , then the convergence to  $\mathbf{z}$  is bilateral (one can see [13]). Consider now an interval  $[t_{\rho(k)-1}, t_{\rho(k)}]$  which contains  $\mathbf{z}$ , using (4), (6) and (7), we obtain

$$\lim_{k \rightarrow +\infty} (t_{\rho(k)-1} - t_{\rho(k)}) = 0. \quad (8)$$

In addition, the value  $\mathbf{T}_{\rho(k)}$  that corresponds to  $[t_{\rho(k)-1}, t_{\rho(k)}]$ , is given by

$$\mathbf{T}_{\rho(k)} = \min \left\{ \mathbf{f}(t_{\rho(k)-1}) - \mathbf{h}(\omega_\rho - t_{\rho(k)-1})^{1/m}, \mathbf{f}(t_{\rho(k)}) - \mathbf{h}(t_{\rho(k)} - \omega_\rho)^{1/m} \right\}, \quad (9)$$

where  $z_\rho$  is obtained by replacing  $i$  by  $\rho$  in (4). As  $\mathbf{z} \in [t_{\rho(k)-1}, t_{\rho(k)}]$  and from (8), we have

$$\lim_{k \rightarrow +\infty} \mathbf{T}_{\rho(k)} = \mathbf{f}(\mathbf{z}). \quad (10)$$

On the other hand, according to (5),

$$\mathbf{T}_{j(k)} \leq \mathbf{f}(t), \quad \forall t \in [t_{j(k)-1}, t_{j(k)}]. \quad (11)$$

From (6),  $\mathbf{T}_{\rho(k)} = \min \{\mathbf{T}_j, j = 2, \dots, k\}$ , then

$$\mathbf{T}_{\rho(k)} \leq \mathbf{T}_{j(k)}, \quad \forall t \in [t_{j(k)-1}, t_{j(k)}],$$

and since  $[0, \frac{\pi}{\alpha_1}] = \bigcup_{j=2}^k [t_{j(k)-1}, t_{j(k)}]$ , we have

$$\lim_{k \rightarrow +\infty} \mathbf{T}_{\rho(k)} \leq \mathbf{T}_{j(k)}, \quad \forall t \in [0, \frac{\pi}{\alpha_1}], \quad (12)$$

and from (11), (12) we get

$$\lim_{k \rightarrow +\infty} \mathbf{T}_{\rho(k)} \leq \mathbf{f}(t), \quad \forall t \in [0, \frac{\pi}{\alpha_1}].$$

Since  $t^*$  is the global minimizer of  $\mathbf{f}$  over  $[0, \frac{\pi}{\alpha_1}]$ ,

$$\lim_{k \rightarrow +\infty} \mathbf{T}_{\rho(k)} \leq \mathbf{f}(t^*) \leq \mathbf{f}(\mathbf{z}),$$

from (10), we have

$$0 \leq \mathbf{f}(\mathbf{z}) - \mathbf{f}(t^*) \leq \mathbf{f}(\mathbf{z}) - \lim_{k \rightarrow +\infty} \mathbf{T}_{\rho(k)} = 0,$$

then

$$\mathbf{f}(\mathbf{z}) = \mathbf{f}(t^*).$$

The function  $\mathbf{f}$  is non-Lipschitz on  $[0, \frac{\pi}{\alpha_1}]$ , so  $\mathbf{f}$  must be continuous so that

$$\mathbf{f}(\mathbf{z}) = \mathbf{f}\left(\lim_{k \rightarrow +\infty} t_k\right) = \lim_{k \rightarrow +\infty} \mathbf{f}(t_k) = \mathbf{f}(t^*).$$

**Theorem 5.2** *Let  $f$  be a non-Lipschitz function satisfying the condition (1) over  $\mathbf{P}$  and  $M$  be the global minimum of  $f$  on  $\mathbf{P}$ . Then the mixed Alienor-TM algorithm converges to the global minimum with an accuracy at least equal to  $\varepsilon$ .*

**Proof.** Denote by  $M^*$  the global minimum of  $\mathbf{f}$  on  $[0, \frac{\pi}{\alpha_1}]$ , where  $\mathbf{f}(t) = f(\zeta(t))$ . On the other hand, let us designate by  $\mathbf{f}_\varepsilon$  the global minimum of the problem ( $\mathbf{P}'$ ) obtained by the Alienor-TM method.

Let us show that

$$\mathbf{f}_\varepsilon - M \leq \varepsilon.$$

a) As  $f$  is continuous on  $\mathbf{P}$ , there exists a point  $\mathbf{x} \in \mathbf{P}$  such that  $M = f(\mathbf{x})$ . Moreover, there exists  $t_0 \in [0, \frac{\pi}{\alpha_1}]$  such that  $\|\mathbf{x} - \zeta(t_0)\| \leq (\frac{\varepsilon}{2h})^m$  so that  $\|f(\mathbf{x}) - f(\zeta(t_0))\| \leq \frac{\varepsilon}{2}$ . And therefore

$$f(\zeta(t_0)) - M \leq \frac{\varepsilon}{2}.$$

But from  $M \leq M^* \leq f(\zeta(t_0))$ , we deduce that

$$M^* - M \leq \frac{\varepsilon}{2}. \tag{13}$$

b) As  $\mathbf{f}$  is continuous on  $[0, \frac{\pi}{\alpha_1}]$ , there exists a point  $t^* \in [0, \frac{\pi}{\alpha_1}]$  such that  $M^* = \mathbf{f}(t^*)$ , involving  $t^*$  as a global minimizer of  $\mathbf{f}$ . Then  $t^*$  is a limit point of the sequence  $(t_k)_{k \geq 1}$  obtained by the mixed algorithm.

Hence  $t^* \in [t_{\rho(k)-1}, t_{\rho(k)}]$  and  $\lim_{k \rightarrow +\infty} (t_{\rho(k)} - t_{\rho(k)-1}) = 0$ , i.e.,

$$\exists t_\varepsilon \in [t_{s-1}, t_s] : |t_s - t_{s-1}| \leq \left(\frac{\varepsilon}{2h}\right)^m \text{ and } \mathbf{f}_\varepsilon = \mathbf{f}(t_\varepsilon)$$

so that

$$\begin{cases} \mathbf{T}_s = \min \left\{ \mathbf{f}(t_{s-1}) - h |t - t_{s-1}|^{1/m}, \mathbf{f}(t_s) - h |t - t_s|^{1/m} \right\}, \\ \mathbf{T}_s \leq \mathbf{f}(t^*) \leq \mathbf{f}(t_\varepsilon) \text{ and } t^* \in [t_{s-1}, t_s]. \end{cases}$$

Consequently,

$$\mathbf{f}_\varepsilon - M^* = \mathbf{f}(t_\varepsilon) - \mathbf{f}(t^*) \leq h |t_\varepsilon - t^*|^{1/m} \leq \frac{\varepsilon}{2}. \tag{14}$$

Finally, from (13) and (14), the result of Theorem 5.2 is proved.

## 6 Computational Experiments

In this section, we present a series of numerical results concerning two mixed Alienor-SM and Alienor-TM algorithms, applied to a set of non-Lipschitz test functions given in the literature. The analytical expressions of the objective functions are reported in Table 1 below including their sources.

Problem No.	Non-Lipschitz test functions.	Domain	$h$	$m$	Ref.
1	$\max \left\{ \sqrt{ x }, \sqrt{ y } \right\}$	$[-1, 1]^2$	1	2	[2]
2	$\sqrt{ x  +  y }$	$[-1, 1]^2$	$(\sqrt{2})^{\frac{1}{2}}$	2	[2]
3	$\sqrt{ x } + \sqrt{ y }$	$[-1, 1]^2$	2	2	[2]
4	$ x + y - 0.25 ^{2/3} - 3 \cos(\frac{x}{2})$	$[\frac{-1}{2}, \frac{1}{2}]^2$	2.42	$\frac{3}{2}$	[15]
5	$\sum_{k=1}^3 \frac{1}{2k} \left  \cos \left( \left( \frac{3}{2k} + 1 \right) x + \frac{1}{2k} \right) \right   x - y ^3$	$[0, 3]^2$	15.8	3	[15]
6	$-\cos(x) \cos(y) \exp \left( 1 - \frac{\sqrt{x^2 + y^2}}{\pi} \right)$	$[-6, 6]^2$	45.265	2	[3]
7	$-10 \exp \left( -\sqrt{0.5( x  +  y )} \right)$	$[-2, 12]^2$	$\frac{10}{\sqrt{2}}$	2	[3]

**Table 1:** The non-Lipschitz test functions.

The experiments have been carried out on PC with Intel(R) Core(TM)i5-7200U CPU 2.50 GHz and 8.00 RAM. The codes are implemented in MATLAB R2017a, with the parameter  $\alpha = 0.1$ . We give, in Table 2, the numerical results obtained by each method to solve the problem (P) and the comparison is made with respect to the number of evaluations  $Ev$  and the calculation time  $CPU$ . In Table 2, the bold form indicates the best results in terms of  $CPU$  and  $Ev$ .

Problem No.	Alienor- $SM$		Alienor- $TM$	
	$Ev$	$CPU$	$Ev$	$CPU$
1	<b>207</b>	<b>0.0655</b>	212	0.1506
2	<b>192</b>	<b>0.0901</b>	196	0.1731
3	283	0.1738	<b>248</b>	<b>0.0783</b>
4	214	0.1063	<b>206</b>	<b>0.0899</b>
5	4905	1.6163	<b>4865</b>	<b>1.6039</b>
6	65549	308.5771	<b>65546</b>	<b>307.6463</b>
7	<b>4792</b>	13.5927	4862	<b>12.9657</b>

**Table 2:** The numerical results.

According to Table 1, all the test functions satisfy the condition (1) with  $m > 1$  and even for non-integer  $m$ . The results given in Table 2 show that the Alienor-TM mixed method gives relatively satisfactory results, either in terms of the calculation time  $CPU$  or the number of evaluations  $Ev$ . The dimensionality reduction Alienor method is rather effective for dealing with difficult problems and its numerical implementation is very simple. The number of evaluations  $Ev$  of  $\mathbf{f}(t)$  depends on the length of the  $\alpha$ -dense curve. This raises a particular interest when choosing other curves. In general, for a fixed value of  $\alpha$ , the shorter the curve, the shorter the calculation time. It is therefore natural to look for other  $\alpha$ -dense curves having a shorter length.

## 7 Conclusion

In this paper, we report a method for solving a multidimensional global optimization problem, where the objective function is non-Lipschitz over a hyper-rectangle of  $\mathbb{R}^n$ . The concept relies on using the  $\alpha$ -dense curve for reducing the size of the space  $\mathbb{R}^n$  to 1, then we apply the one-dimensional version of Piyavskii's algorithm based on constructing tangent minorant functions. This method is simple and easy to implement on any multivariate non-Lipschitz function even if  $m$  is not an integer. We suggested a series of numerical applications, followed by a comparative study of two mixed algorithms applied to the proposed problem. We see that the mixed Alienor-*TM* and Alienor-*SM* methods offer interesting prospects for reducing the computation time and the number of evaluations. Finally, we want to elaborate on these investigations in cases where the constant  $h$  is a priori unknown.

## Acknowledgment

This work is funded by the General Directorate of Scientific Research and Technological Development (DGRSDT) of Algeria.

## References

- [1] M. H. Almomani, M. H. Alrefaei and M. H. Almomani. Stopping Rules for Selecting the Optimal Subset. *Nonlinear Dynamics and Systems Theory* **21** (1) (2021) 13–27.
- [2] N. K. Arutynova, A. M. Dulliev and V. I. Zaboltn. Algorithms for projecting a point into a level surface of a continuous function on a compact set. *Computational Mathematics and Mathematical Physics* **54** (9) (2014) 1395–1401.
- [3] N. K. Arutynova, A. M. Dulliev and V. I. Zaboltn. Global optimization of multi-variable functions satisfying the Vanderbei condition. *Journal of Applied Mathematics and Computing* **68** (2022) 1135–1161.
- [4] A. R. Butz. Space filling curves and mathematical programming. *Information and control* **12** (4) (1968) 313–330.
- [5] Y. Cherruault. A new reducing transformation for global optimization with Alienor method. *Kybernetes* **34** (2005) 1084–1089.
- [6] A. Djaout, T. Hamaizia and F. Derouiche. Performance Comparison of Some Two-Dimensional Chaotic Maps for Global Optimization. *Nonlinear Dynamics and Systems Theory* **22** (2) (2022) 144–154.
- [7] R. Fiorenza. *Hölder and Locally Hölder Continuous Functions, and Open Sets of Class  $C^k, C^{k,\lambda}$* . Springer International Publishing, 2016.
- [8] E. Gourdin, B. Jaumard and R. Ellaia. Global Optimization of Hölder functions. *Journal of Global Optimization* **8** (4) (1996) 323–348.
- [9] D. Guettal and A. Ziadi. Reducing Transformation and Global Optimization. *Applied Mathematics and Computation* **218** (10) (2012) 5848–5860.
- [10] P. Hanjoul, P. Hansen, D. Peeters, and J. F., Thisse. Uncapacitated plant location under alternative space price policies. *Management Science* **36** (1) (1990) 41–47.
- [11] R. Horst and P. M. Pardalos. *Handbook of Global Optimization*. Kluwer Academic Publishers, Dordrecht, London, 1995.

- [12] S. Kiatsupaibul, R. L. Smith and Z. B. Zabinsky. Solving infinite horizon optimization problems through analysis of a one-dimensional global optimization problem. *Journal of Global Optimization* **66** (2016) 711–727.
- [13] D. Lera and Y. D. Sergeyev. Global Minimization Algorithms for Hölder functions. *BIT Numerical mathematics* **42** (2002) 119–133.
- [14] S. A. Piyavskii. An algorithm for finding the absolute minimum for a function. *Theory of Optimal Solution* **2** (1967) 13–24.
- [15] M. Rahal and A. Ziadi. A new extension of Piyavskii’s method to Hölder functions of several variables. *Applied mathematics and Computation* **197** (2) (2008) 478–488.
- [16] M. Rahal, A. Ziadi and R. Ellaia. Generating  $\alpha$ -dense curves in non-convex sets to solve a class of non-smooth constrained global optimization. *Croatian Operational Research Review* **10** (2) (2019) 289–314.
- [17] Y. D. Sergeyev, R. G. Strongin and D. Lera. *Introduction to Global Optimization Exploiting Space-Filling-Curves*. Springer Science & Business Media, 2013.
- [18] R. G. Strongin. Algorithms for multi-extremal programming problems employing the set of joint space-filling curves. *Journal of Global Optimization* **2** (1992) 357–378.
- [19] A. Ziadi, Y. Cherruault and G. Mora. Global optimization: A new variant of the Alienor method. *Computers & Mathematics with Applications* **41** (1-2) (2001) 63–71.
- [20] A. Ziadi, D. Guettal and Y. Cherruault. Global optimization: The Alienor mixed method with Piyavskii-Shubert technique. *Kybernetes* **34** (7/8) (2005) 1049–1058.



## Analysis of Solutions to Equations with a Generalized Derivative and Delay

O. D. Kichmarenko<sup>1\*</sup>, I. V. Chepovskyi<sup>2</sup>, Y. Platonova<sup>1</sup>  
and S. Dashkovskiy<sup>3</sup>

<sup>1</sup> *Department of Optimal Control and Economical Cybernetics, Faculty of Mathematics, Physics and Information Technologies, Odesa I. I. Mechnikov National University, 2 Dvoryanska Str., 65082, Odesa, Ukraine.*

<sup>2</sup> *The Development Department, LLC “Dengroup”, 19 Velyka Arnavtska str., 19, 65048, Odesa, Ukraine.*

<sup>3</sup> *Institute of Mathematics, University of Würzburg, Emil-Fischer-Str. 40, 97074, Würzburg, Germany.*

Received: December 16, 2021; Revised: May 5, 2023

**Abstract:** This paper is concerned with the set-valued differential equations with a generalized derivative and constant delay. We introduce the notion of the initial problem solutions and establish conditions for their existence and uniqueness, also we provide a result on the continuous dependence of the solution of this problem on the initial function. It is found that the solutions of such equations can expand and contract, depending on the initial conditions. Also, in this paper we develop a numerical algorithm to calculate solutions to such problem approximately. By means of examples, we demonstrate how this algorithm works when solving different nonlinear differential equations with generalized derivative with constant delay under different initial conditions.

**Keywords:** *set-valued differential equations; generalized derivative; delay; existence and uniqueness of solution; numerical algorithm.*

**Mathematics Subject Classification (2010):** 34A06, 34K05, 34K06, 93C10, 93C35.

---

\* Corresponding author: <mailto:olga.kichmarenko@gmail.com>

## 1 Introduction

The study of the properties of a trajectory set and the construction of a reachability set for control systems plays an important role in the investigation of optimal control problems. Let the equation of motion of the control object have the form

$$\dot{x} = f(t, x, u), \quad u \in U, \quad x(t_0) = x_0, \quad (1)$$

where  $x \in R^n$  is a phase vector,  $t > t_0$ ,  $u(t) \in U \in \text{comp}(R^k)$  is a control vector. Problem (1) can be replaced by the following problem [23]:

$$\dot{x} \in F(t, x), \quad x(t_0) = x_0, \quad (2)$$

where  $F(t, x) = \{z \in R^n | z = f(t, x, u), u \in U\}$  is a multivalued mapping. It is also mentioned in [23] that the sets of solutions of equation (1) and inclusion (2) coincide. In the same book, it is mentioned that the solution of the corresponding equation with the Hukuhara derivative, in which the right-hand side contains the same multi-valued mapping from (2), bounds the solution of the differential inclusion (2).

Thus, differential equations with a set-valued right-hand side can be used to study solutions to the optimal control problem.

The first analysis of differential equations with a multivalued right-hand side was conducted by S. Zaremba [28] and A. Marchaud [12], [13], [14]. The main results were also presented in the works of T. Wazewski [26], [27], V.A. Plotnikov [22], [23], J.-P. Aubin [1], K. Deimling [7], M. Kisielewicz [9], [10] and others. The development of the theory of multivalued mappings has led to the clarification of the question of what is meant by a derivative of multivalued mappings. This is stated in the works of M. Hukuhara [8], T.F. Bridgland [4], H.T. Banks, M.Q. Jacobs [2], A.V. Plotnikov, N.V. Skripnik [19], [21], B. Bede, S.G. Gal [3], O. Carja, T. Donchev and A.I. Lazu [6].

Differential equations with set-valued right-hand side and generalized derivative appeared first in the works of A.V. Plotnikov, N.V. Skripnik [19], [21]. The existence and uniqueness of solutions to the Cauchy problems with such equations were studied there.

Let us note that the notion of generalized derivatives for multivalued maps was first introduced in [17], where the corresponding Cauchy problem was stated and the notion of solutions to such problems was provided. The initial condition in this Cauchy problem was given at a time point and the right-hand side of the equation depends on a time point rather than on a time interval. In contrary to [17], in the current paper, we consider the equations and initial states which depend on prehistory, that is, are defined on a time interval. Hence we consider equations with time delay which make the problems considered here essentially different from [17]. Hence our work extends the results of [17] to the case of equations with time delays. The presence of a time delay leads to essential changes in the approach of [17] and to other properties of solutions.

In this paper, the differential equation with a generalized derivative with a constant delay is considered, the theorem on the existence and uniqueness of solution of such equations is formulated and proved, the numerical algorithm for construction of these solutions is developed, and examples of the application of the numerical algorithm for construction of solutions of differential equations with a constant delay are given.

## 2 Main Results

### 2.1 Concept of solution

Consider a nonlinear differential equation with a generalized derivative with a constant delay:

$$DX = F(t, X(t), X(t - \Delta)), \quad X(s) = \rho(s), \quad s \in [-\Delta, t_0], \quad (3)$$

where  $t \in I = [t_0, T]$ ,  $F : I \times \text{conv}(\mathbb{R}^n) \times \text{conv}(\mathbb{R}^n) \rightarrow \text{conv}(\mathbb{R}^n)$  is a multivalued mapping,  $t_0 = 0$ ,  $\Delta > 0$  is a constant delay,  $\rho(\cdot) : [-\Delta, t_0] \rightarrow \text{conv}(\mathbb{R}^n)$ .

**Definition 2.1** A multivalued mapping  $X(\cdot) : [t_0, T] \rightarrow \text{conv}(\mathbb{R}^n)$  is called a solution of differential equation (3) if it is absolutely continuous and satisfies (3) almost everywhere on  $[t_0, T]$ .

But similarly to a differential equation with a generalized derivative without delay, in this case, it is impossible to ensure the unity of the solution [21]. Next, consider the differential equation of the form

$$\begin{aligned} DX \stackrel{h}{=} \Phi(-\varphi(t)) F_1(t, X(t), X(t - \Delta)) &= \Phi(\varphi(t)) F_2(t, X(t), X(t - \Delta)), \\ X(s) = \rho(s), \quad s \in [-\Delta, t_0], \end{aligned} \quad (4)$$

where  $t \in [t_0, T]$ ,  $X(\cdot) : [t_0, T] \rightarrow \text{conv}(\mathbb{R}^n)$ ,  $t_0 = 0$ ,  $\Delta > 0$  is a constant delay,  $\rho(\cdot) : [-\Delta, t_0] \rightarrow \text{conv}(\mathbb{R}^n)$ ,  $F_1, F_2(\cdot, \cdot, \cdot) : [t_0, T] \times \text{conv}(\mathbb{R}^n) \times \text{conv}(\mathbb{R}^n) \rightarrow \text{conv}(\mathbb{R}^n)$  is a multivalued mappings,  $\varphi(\cdot) : [t_0, T] \rightarrow \mathbb{R}$  is a continuous function.

$$\Phi(\varphi) = \begin{cases} 1, & \varphi > 0, \\ 0, & \varphi \leq 0. \end{cases}$$

**Definition 2.2** A multivalued mapping  $X(\cdot) : [t_0, T] \rightarrow \text{conv}(\mathbb{R}^n)$  is called a solution of differential equation (4) if it is absolutely continuous and on any segment  $[\tau_i, \tau_{i+1}] \subset [t_0, T]$ , where the function  $\varphi(\cdot)$  on the interval  $(t_i, t_{i+1})$  has a constant sign, satisfies the integral equation

$$\begin{aligned} X(t) + \int_{\tau_i}^t \Phi(-\varphi(s)) F_1(s, X(s), X(s - \Delta)) \, ds &= \\ = X(\tau_i) + \int_{\tau_i}^t \Phi(\varphi(s)) F_2(s, X(s), X(s - \Delta)) \, ds. \end{aligned} \quad (5)$$

If on the interval  $(\tau_i, \tau_{i+1})$ , a function  $\varphi(t) > 0$ , then  $X(\cdot)$  satisfies the integral equation

$$X(t) = X(\tau_i) + \int_{\tau_i}^t F_2(s, X(s), X(s - \Delta)) \, ds$$

for  $t \in [\tau_i, \tau_{i+1}]$  and  $\text{diam}(X(t))$  is a growing function.

If on the interval  $(\tau_i, \tau_{i+1})$ , a function  $\varphi(t) < 0$ , then  $X(\cdot)$  satisfies the integral equation

$$X(\tau_i) = X(t) + \int_{\tau_i}^t F_1(s, X(s), X(s - \Delta)) \, ds,$$

that is,

$$X(t) = X(\tau_i) - \int_{\tau_i}^t F_1(s, X(s), X(s - \Delta)) ds$$

for  $t \in [\tau_i, \tau_{i+1}]$  and  $\text{diam}(X(t))$  is a decreasing function.

If on the interval  $(\tau_i, \tau_{i+1})$ , a function  $\varphi(t) = 0$ , then  $X(t) = X(\tau_i)$  for  $t \in [\tau_i, \tau_{i+1}]$  and  $\text{diam}(X(t))$  is a constant function.

We will also introduce another equivalent definition of the solution of the equation (4).

**Definition 2.3** A multivalued mapping  $X(\cdot) : [t_0, T] \rightarrow \text{conv}(\mathbb{R}^n)$  is called a solution of differential equation (4) if it is absolutely continuous, satisfying (4) almost everywhere on  $[t_0, T]$ , and

$$\text{diam}(X(t)) = \begin{cases} \text{increase,} & \varphi(t) > 0, \\ \text{constant,} & \varphi(t) = 0, \\ \text{decrease,} & \varphi(t) < 0. \end{cases}$$

In the equation (4), the multivalued mappings  $F_1$  and  $F_2$  determine the rate of change ("compression" and "expansion") of the multivalued mapping  $X(t)$  and how it changes in the space  $\text{conv}(\mathbb{R}^n)$ , and a function  $\varphi(t)$  determines when a diameter  $X(t)$  increases, decreases or is constant. These mappings are considered different because the laws of "compression" and "expansion" may be different.

## 2.2 A condition for the existence of a unique solution.

Based on [24], we can formulate and prove the following theorems.

**Theorem 2.1** Let  $F_1$  and  $F_2$  be continuous mappings and, in some neighborhood, points  $(t_0, \rho(t_0), \rho(t_0 - \Delta))$  satisfy the Lipschitz condition with respect to the 2nd and 3rd variables with a constant  $\lambda$ . Let the initial function  $\rho(s)$  be continuous and the delay  $\Delta$  be non-negative. Then there is a unique solution  $X(t)$  of equation (4) for  $t_0 \leq t \leq t_0 + \sigma$ , where  $\sigma$  is arbitrarily small.

**Proof.** Consider the function  $\varphi(t)$  on the segment  $t \in [t_0; t_0 + \sigma]$ . As mentioned above, it can take a negative, positive and zero value.

1.  $\varphi(t) = 0$ . Then

$$X(t) = \rho(t). \quad (6)$$

2.  $\varphi(t) > 0$ . Then we obtain a differential equation with the Hukuhara derivative with a constant delay, which has a unique solution [24].

3.  $\varphi(t) < 0$ . Then we transform the system (4) into the integral equation

$$X(t) = \rho(t) - \int_{t_0}^t F_1(s, X(s), X(s - \Delta)) ds \quad (7)$$

and prove that it has a unique solution on the segment  $[t_0; t_0 + d]$ .

Suppose the opposite. Let the equation (7) have at least two solutions  $X(t)$  and  $Y(t)$  such that

$$\bar{\omega} = \max_{t \in [t_0; t_0 + d]} h(X(t), Y(t)) > 0,$$

where  $[t_0; t_0 + d]$  is the total period of existence of solutions  $X(t)$  and  $Y(t)$ . We have

$$X(t) \equiv \rho(t) - \int_{t_0}^t F_1(s, X(s), X(s - \Delta)) ds,$$

$$Y(t) \equiv \rho(t) - \int_{t_0}^t F_1(s, Y(s), Y(s - \Delta)) ds,$$

whence, using the Lipschitz condition and the Hausdorff distance properties, we obtain

$$\begin{aligned} & h(X(t), Y(t)) = \\ & = h\left(\rho(t) - \int_{t_0}^t F_1(s, X(s), X(s - \Delta)) ds, \rho(t) - \int_{t_0}^t F_1(s, Y(s), Y(s - \Delta)) ds\right) = \\ & = h\left(\int_{t_0}^t F_1(s, X(s), X(s - \Delta)) ds, \int_{t_0}^t F_1(s, Y(s), Y(s - \Delta)) ds\right) \leq \\ & \leq \int_{t_0}^t h(F_1(s, X(s), X(s - \Delta)), F_1(s, Y(s), Y(s - \Delta))) ds \leq \\ & \leq \lambda \left(\int_{t_0}^t h(X(s), Y(s)) ds + \int_{t_0}^t h(X(s - \Delta), Y(s - \Delta)) ds\right). \end{aligned}$$

So we get

$$h(X(t), Y(t)) \leq \lambda \int_{t_0}^t \bar{\omega} ds = \lambda \bar{\omega} (t - t_0) \leq \lambda \bar{\omega} d,$$

$$h(X(t), Y(t)) \leq \lambda \int_{t_0}^t \bar{\omega} (s - t_0) ds = \frac{\lambda^2 \bar{\omega} (t - t_0)^2}{2} \leq \frac{\lambda^2 \bar{\omega} d^2}{2} \dots$$

Using the method of complete mathematical induction, we have that for any natural  $m$  on the segment  $[t_0; t_0 + d]$ , there is an inequality

$$h(X(t), Y(t)) \leq \frac{\lambda^m \bar{\omega} d^m}{m!}.$$

Then

$$\bar{\omega} = \max_{t \in [t_0; t_0 + d]} h(X(t), Y(t)) \leq \frac{\lambda^m \bar{\omega} d^m}{m!},$$

from here, by virtue of the positivity  $\bar{\omega}$ , we have that for any natural  $m$ ,

$$1 \leq \frac{(\lambda d)^m}{m!}. \quad (8)$$

In view of the sign of the d'Alembert series,  $\sum_{m=1}^{\infty} \frac{(\lambda d)^m}{m!}$  converges and from here, the necessity of the condition  $\lim_{m \rightarrow \infty} \frac{(\lambda d)^m}{m!} = 0$ . This means that for  $\varepsilon = \frac{1}{2}$ , there exists  $m \in \mathbb{N}$  such that  $\frac{(\lambda d)^m}{m!} < \frac{1}{2}$ . Then, by virtue of (8), we get that  $1 < \frac{1}{2}$ . We have obtained a contradiction, and so we have that the equation (7) and the equivalent equation (4) have a unique solution.

4. In the case when the function  $\varphi(t)$  changes the sign on the segment  $[t_0; t_0 + d]$ , the existence of a unique solution is proved by the combination of cases 1) – 3).

The theorem is proved.

**Theorem 2.2** *Let all conditions of Theorem 2.1 be satisfied. Then the solution of the equation (4) continuously in the space  $\text{comp}(\mathbb{R}^n)$  depends on the initial function, and at  $h(\rho_1(s), \rho_2(s)) \leq \delta$ ,  $\delta > 0$ ,  $s \in [-\Delta; t_0]$ , we have*

$$h(X_1(t), X_2(t)) \leq \delta e^{2\lambda(t-t_0)}, t \geq t_0. \quad (9)$$

**Proof.** Similarly to the previous theorem, consider 3 cases for the function  $\varphi(t)$ .

1.  $\varphi(t) = 0$ . We have

$$h(\rho_1(s), \rho_2(s)) < \delta \leq \delta e^{2\lambda(t-t_0)},$$

which implies (9).

2.  $\varphi(t) > 0$ . We have

$$\begin{aligned} h \left( \int_{t_0}^t F_2(s, X_1(s), X_1(s-\Delta)) ds, \int_{t_0}^t F_2(s, X_2(s), X_2(s-\Delta)) ds \right) &\leq \\ &\leq \int_{t_0}^t h(F_2(s, X_1(s), X_1(s-\Delta)), F_2(s, X_2(s), X_2(s-\Delta))) ds \leq \\ &\leq \lambda \int_{t_0}^t [h(X_1(s), X_2(s)) + h(X_1(s-\Delta), X_2(s-\Delta))] ds. \end{aligned} \quad (10)$$

Let

$$z(t) = \max \left\{ \delta, \max_{t_0 \leq s \leq t} h(X_1(s), X_2(s)) \right\}.$$

From (10), we get

$$z(t) \leq \delta + 2\lambda \int_{t_0}^t z(s) ds. \quad (11)$$

From (11), by the Gronwall-Bellman lemma, we get (9).

3.  $\varphi(t) < 0$ . Similar to the previous case, we have

$$h \left( \int_{t_0}^t F_2(s, X_1(s), X_1(s - \Delta)) ds, \int_{t_0}^t F_2(s, X_2(s), X_2(s - \Delta)) ds \right) \leq \leq \lambda \int_{t_0}^t [h(X_1(s), X_2(s)) + h(X_1(s - \Delta), X_2(s - \Delta))] ds.$$

Next, from (11) and by the Gronwall-Bellman lemma, we get (9).

The theorem is proved.

**2.3 A numerical algorithm for construction of solutions of differential equations with a generalized derivative with a constant delay**

Based on Definitions 2.2 and 2.3, Theorems 2.1, and 2.2 and [21], we can formulate a numerical algorithm for constructing a solution of a differential equation with a generalized derivative with delay.

Consider the equation (4)

$$DX \stackrel{h}{=} \Phi(-\varphi(t)) F_1(t, X(t), X(t - \Delta)) = \Phi(\varphi(t)) F_2(t, X(t), X(t - \Delta)), \\ X(s) = \rho(s), s \in [-\Delta, t_0],$$

where  $t \in [t_0, T], X(\cdot) : [t_0, T] \rightarrow conv(\mathbb{R}^n), t_0 = 0, \Delta > 0$  is a constant delay,  $\rho(\cdot) : [-\Delta, t_0] \rightarrow conv(\mathbb{R}^n), F_1, F_2(\cdot, \cdot, \cdot) : [t_0, T] \times conv(\mathbb{R}^n) \times conv(\mathbb{R}^n) \rightarrow conv(\mathbb{R}^n)$  are multivalued mappings,  $\varphi(\cdot) : [t_0, T] \rightarrow \mathbb{R}$  is a continuous function.

$$\Phi(\varphi) = \begin{cases} 1, & \varphi > 0, \\ 0, & \varphi \leq 0. \end{cases}$$

Let the dimension of the space  $n = 2$ . Next, we write the formula for a counterpart of Euler’s method in the case of differential equation (4)

$$X_m(t) = \begin{cases} X_m(t_k) + (t - t_k) F_2(t_k, X(t_k), X(t_k - \Delta)), & \varphi(t) > 0, \\ X_m(t_k) \stackrel{h}{=} (t - t_k) F_1(t_k, X(t_k), X(t_k - \Delta)), & \varphi(t) < 0, \\ X_m(t_k), & \varphi(t) = 0. \end{cases} \\ t \in [t_k, t_{k+1}], k = \overline{0, m - 1}, X_m(s) = \rho(s), s \in [-\Delta, t_0].$$

Using the apparatus of support functions, we obtain

$$C(X_m(t), \psi) = \begin{cases} C(X_m(t_k) + (t - t_k) F_2(t_k, X(t_k), X(t_k - \Delta)), \psi), \\ C(X_m(t_k) \stackrel{h}{=} (t - t_k) F_1(t_k, X(t_k), X(t_k - \Delta)), \psi), \\ C(X_m(t_k), \psi). \end{cases} = \\ = \begin{cases} C(X_m(t_k), \psi) + (t - t_k) C(F_2(t_k, X(t_k), X(t_k - \Delta)), \psi), \\ C(X_m(t_k), \psi) - (t - t_k) C(F_1(t_k, X(t_k), X(t_k - \Delta)), \psi), \\ C(X_m(t_k), \psi), \end{cases}$$

where  $\psi$  is a unit vector.

For  $t = t_{k+1}$  we have formulas:

$$C(X_m(t_{k+1}), \psi) = \begin{cases} C(X_m(t_k), \psi) + \delta C(F_2(t_k, X(t_k), X(t_k - \Delta)), \psi), \\ C(X_m(t_k), \psi) - \delta C(F_1(t_k, X(t_k), X(t_k - \Delta)), \psi), \\ C(X_m(t_k), \psi). \end{cases} \quad (12)$$

To construct an external approximation of the set  $X_m(t_{k+1})$ , we find

$$C(X_m(t_{k+1}), \psi_i), \text{ where } \psi_i = \begin{pmatrix} \cos \gamma_i \\ \sin \gamma_i \end{pmatrix}, \gamma_i = \frac{2\pi i}{p}, i = \overline{0, p-1}.$$

It follows from (12) that

$$\begin{aligned} C(X_m(t_{k+1}), \psi) &= \begin{cases} C(X_m(t_k) + \delta F_2(t_k, X(t_k), X(t_k - \Delta)), \psi_i), \\ C\left(X_m(t_k) - \delta F_1(t_k, X(t_k), X(t_k - \Delta)), \psi_i\right), \\ C(X_m(t_k), \psi_i). \end{cases} = \\ &= \begin{cases} C(X_m(t_k), \psi) + \delta C(F_2(t_k, X(t_k), X(t_k - \Delta)), \psi_i), \\ C(X_m(t_k), \psi) - \delta C(F_1(t_k, X(t_k), X(t_k - \Delta)), \psi_i), \\ C(X_m(t_k), \psi_i). \end{cases} \end{aligned}$$

Thus, we can get the values of the support functions  $C(X_m(t_k), \psi_i)$ ,  $k = \overline{0, m}$ ,  $i = \overline{0, p-1}$ .

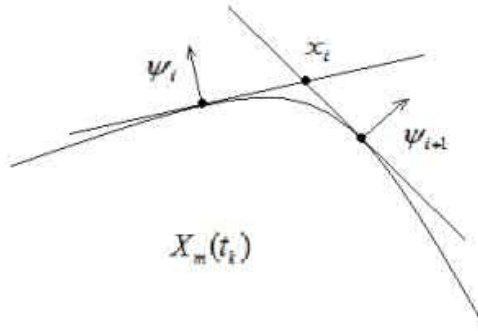


**Figure 1:** Construction of boundary points of the numerical approximation of a convex set.

To construct the approximation (Fig. 1), find the points of intersection of the support hyperplanes to the set  $X_m(t_k)$  in the directions of the vectors  $\psi_i$  and  $\psi_{i+1}$ ,  $i = \overline{0, p-1}$ ,  $\psi_p = \psi_0$ :

$$\begin{cases} (x, \psi_i) = C(X_m(t_k), \psi_i), \\ (x, \psi_{i+1}) = C(X_m(t_k), \psi_{i+1}). \end{cases}$$

This is a linear system relatively unknown vector  $x \in \mathbb{R}^2$  with determinant

$$\Delta = \begin{pmatrix} \cos \gamma_i & \sin \gamma_i \\ \cos \gamma_{i+1} & \sin \gamma_{i+1} \end{pmatrix} = \sin(\gamma_{i+1} - \gamma_i) = \sin \frac{2\pi}{p} \neq 0.$$

Let us denote the solution of the system by  $x_i, i = \overline{0, p-1}$ . Construct a polygon with vertices at points  $x_0, x_1, \dots, x_{p-1}$ , which we denote  $Q_k^p$ . The criterion for account termination is

$$\left| \text{square } Q_{k+1}^{p+1} - \text{square } Q_k^p \right| < \varepsilon,$$

where  $\varepsilon$  is a predefined number.

### 2.4 Construction of solutions of differential equation with a generalized derivative with a constant delay

Using the Octave package, we constructed a solution of differential equations with a generalized derivative with a delay with different initial sets  $X_0$ , a partition  $m$ , the Euler number of "broken lines"  $p$  and a constant delay  $\Delta$  on the time interval  $t \in [0; T]$ . It should be noted that the delay  $\Delta$  must be a multiple of the time step  $h = \frac{T-t_0}{m}$ . The following examples show how this program works.

Consider the equation of the form

$$DX \stackrel{h}{-} \Phi(t-a) \frac{1}{2} X(t-\Delta) = \Phi(a-t) X(t), X(s) = X_0(s), s \in [-\Delta, 0]. \quad (13)$$

1. Let  $X_0 = S_{100} \begin{pmatrix} 0 \\ t \end{pmatrix}$ , then  $c(X_0, \psi) = t\psi_2 + 100 \|\psi\|$ .

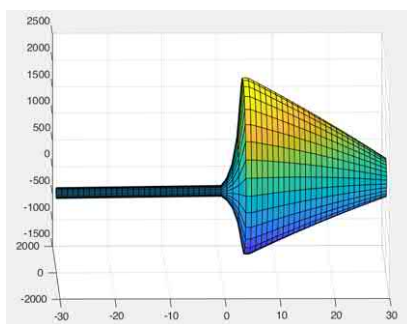


**Figure 2:** Equation (13) sol. graph for  $m = 30, p = 30, \Delta = 30, a = 5, T = 30$ , init. conditions (1).

2. Let  $X_0 = K_{10000} \begin{pmatrix} t \\ 2t^2 \end{pmatrix}$ , then  $c(X_0, \psi) = t\psi_1 + 2t^2\psi_2 + 10000 |\psi_1| + 10000 |\psi_2|$ .

Consider the equation with a generalized derivative with a delay of the form

$$\begin{aligned} DX \stackrel{h}{-} \Phi(\text{diam}(X(t)) - \text{diam}(X_0) - 100) \frac{1}{2} X(t-\Delta) = \\ = \Phi(\text{diam}(X_0) + 100 - \text{diam}(X(t))) X(t), \\ X(s) = X_0(s), s \in [-\Delta, 0]. \end{aligned} \quad (14)$$

There are no proved theorems on the existence and uniqueness of the solution for this equation, so we will consider it as an experiment.

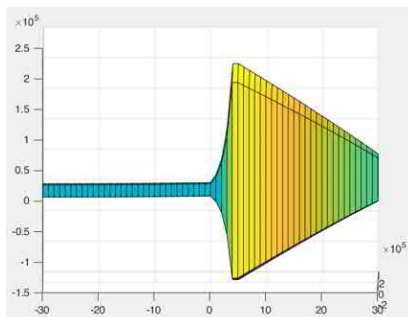


**Figure 3:** Equation (13) sol. graph for  $m = 30$ ,  $p = 30$ ,  $\Delta = 30$ ,  $a = 5$ ,  $T = 30$ , init. conditions (2).

- Let  $X_0 = \begin{pmatrix} 10 & 0 \\ 0 & 20 \end{pmatrix} S_1 \begin{pmatrix} sint \\ 2cost \end{pmatrix}$ , then  $c(X_0, \psi) = sint\psi_1 + 2cost\psi_2 + \left\| \begin{pmatrix} 10 & 0 \\ 0 & 20 \end{pmatrix} \psi \right\|$ .

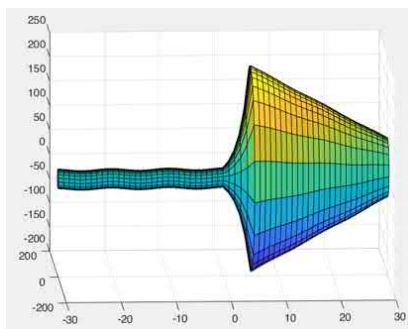


**Figure 4:** Equation (14) sol. graph for  $m = 30$ ,  $p = 30$ ,  $\Delta = 30$ ,  $T = 30$ , init. conditions (1).

- Let  $X_0 = \left( \begin{array}{l} \text{rectangle with half sides } 100 \text{ and } 300 \\ \text{and the center at the point } \begin{pmatrix} sint \\ 2cost \end{pmatrix} \end{array} \right)$ , then  $c(X_0, \psi) = sint\psi_1 + 2cost\psi_2 + 100|\psi_1| + 300|\psi_2|$ .

### 3 Conclusion

The theorem on the existence of a unique solution of a differential equation with a generalized derivative with a delay and the theorem on the continuous dependence of this solution on the initial function are formulated and proved. A numerical algorithm for solving such equations is developed. The paper presents examples of this algorithm for different types of equations, different initial conditions, partitions, and delays.

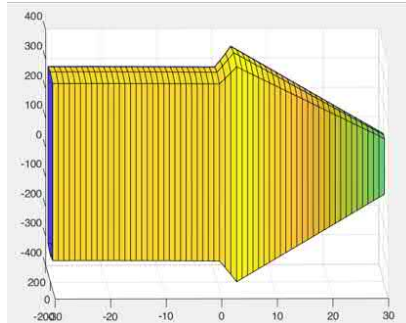


**Figure 5:** Equation (14) sol. graph for  $m = 30$ ,  $p = 30$ ,  $\Delta = 30$ ,  $T = 30$ , init. conditions (2).

### Acknowledgment

This research was partially supported by the German foreign exchange service DAAD in the frame of the east partnerships program.

### References

- [1] J.-P. Aubin, and A. Cellina. *Differential Inclusions. Set-valued Maps and Viability Theory*. Springer-Verlag, Berlin, New York, 1984.
- [2] H. T. Banks and M. Q. Jacobs. A differential calculus of multifunctions. *J. Math. Anal. Appl.* **29** (1970) 246–272.
- [3] B. Bede and S. G. Gal. Generalizations of the differentiability of fuzzy-number-valued functions with applications to fuzzy differential equations. *Fuzzy Sets and Systems* **151** (2005) 581–599.
- [4] T. F. Bridgland. Trajectory integrals of set valued functions. *Pacific J. Math.* **33** (1) (1970) 43–68.
- [5] H. Chouial and M. F. Yarou. Functional Differential Inclusions with Unbounded Right-hand Side in Banach Spaces. *Nonlinear Dynamics and Systems Theory* **22** (4) (2022) 355–366.
- [6] O. Carja, T. Donchev and A. I. Lazu Generalized Solutions of Semilinear Evolution Inclusions/ *SIAM Journal on Optimization*. **26** (2) (2016) 1365–1378.
- [7] K. Deimling. *Multivalued Differential Equations*. Berlin: Walter de Gruyter, 1992.
- [8] M. Hukuhara. Integration des applications mesurables dont la valeur est un compact convexe. *Func. Ekvacioj.* **10** (1967) 205–223.
- [9] V. Kisielewicz. *Differential inclusion and optimal control*. Warszawa: PWN, 1991.
- [10] M. Kisielewicz, B. Serafin and W. Sosulsk. Existence theorem for functional-differential equation with compact convex valued solutions. *Demonstratio math.* **13** (2) (1975) 229–237.
- [11] T. A. Komleva, A. V. Plotnikov, L. I. Plotnikova and N. V. Skripnik. Conditions for the existence of basic solutions of linear multivalued differential equations. *Ukr. Math. J.* **73** (5) (2021) 758–783.
- [12] A. Marchaud. Sur les champs de demi-cones et equations differentielles du premier order. *Bull. Soc. Math. France.* **62** (1934) 1–38.
- [13] A. Marchaud. Sur les champs continus de demi-cones convexes et leurs integrals. *Comput. Math.* **8** (1936) 89–127.

- [14] A. Marchaud. Sur les champs de demi-cones convexes. *Bull. Sci. Math.* **LXII** (2) (1938) 229–240.
- [15] A. A. Martynyuk. *Qualitative Analysis of Set-Valued Differential Equations*. Springer International Publishing, 2019.
- [16] Lopes Pinto, A. J. Brandão, F. S. De Blasi and F. Iervolino. Uniqueness and existence theorems for differential equations with compact convex valued solutions. *Boll. Un. Mat. Ital.* **4** (3) (1970) 47–54.
- [17] A. V. Plotnikov and N. V. Skripnik. Conditions for the Existence of Local Solutions of Set-Valued Differential Equations with Generalized Derivative. *Ukrainian Mathematical Journal.* **65** (2014) 1498–1513.
- [18] A. V. Plotnikov and N. V. Skripnik. *Differential equations with "clear" and fuzzy multivalued right-hand sides. Asymptotics Methods*. AstroPrint, Odessa, 2009. [Russian]
- [19] A. V. Plotnikov and N. V. Skripnik. Set-valued differential equations with generalized derivative. *J. Adv. Res. Pure Math.* **3** (1) (2011) 144–160, doi:10.5373/jarpm.475.062210.
- [20] A. V. Plotnikov and N. V. Skripnik. Existence and uniqueness theorems for generalized set differential equations. *Int. J. Control Sci. Eng.* **2** (1) (2012) 1-6. doi:10.5923/j.control.20120201.
- [21] A. V. Plotnikov and N. V. Skripnik. An Existence and uniqueness theorem to the Cauchy problem for generalized set differential equations. *J. Dynamics of Continuous, Discrete and Impulsive Systems. Series A.* **20** (2013) 433–445.
- [22] V. A. Plotnikov. *Averaging Method for Control Problems*. Kiev-Odessa: Lybid', 1992.[Russian]
- [23] V. A. Plotnikov, A. V. Plotnikov and A. N. Vitjuk. *Differential Equations with multivalued right hand side. Averaging Methods*. Odessa: AstroPrint, 1999.[Russian]
- [24] V. A. Plotnikov and P. I. Rashkov. Averaging in differential equations with Hukuhara derivative and delay. *Funct. Different. Equat.* (Israel) **8** (2001) 3–4.
- [25] L. Stefanini. *A generalization of Hukuhara difference. Soft Methods for Handling Variability and Imprecision*. Springer, Berlin, Heidelberg, 2008.
- [26] T. Wazewski. Systemes de comande et equations au contingent. *Bull. Pol. Acad. Sci. Ser. Sci. Math., astron. et phys.* **9** (3) (1961) 151–155.
- [27] T. Wazewski Sur une condition equivalente l'equation an contingent. *Bull. Pol. Acad. Sci. Ser. Sci. math., astr. et phys.* **9** (12) (1961) 865–867.
- [28] S. K. Zaremba Sur les equations au paratingent. *Bull. Sci. Math.* **LX** (2) (1936) 139–160.



# Chaos Anti-Synchronization between Fractional-Order Lesser Date Moth Chaotic System and Integer-Order Chaotic System by Nonlinear Control

M. Labid<sup>1</sup> and N. Hamri<sup>2\*</sup>

<sup>1</sup> *Department of Mathematics, University Center of Mila, Mila 43000, Algeria.*

<sup>2</sup> *Laboratory of Mathematics and Their Interactions,  
Department of Science and Technology, University Center of Mila, Mila 43000, Algeria.*

Received: February 4, 2023; Revised: April 7, 2023

**Abstract:** This paper investigates the phenomenon of chaos anti-synchronization between the fractional-order lesser date moth and the integer-order chaotic systems based on the Lyapunov stability theory and numerical differentiation. The nonlinear feedback control is the method used to achieve the anti-synchronization of chaotic systems addressed in this paper. Numerical examples are implemented to illustrate and validate the results.

**Keywords:** *chaos; anti-synchronization; nonlinear control; fractional-order chaotic system; integer-order chaotic system.*

**Mathematics Subject Classification (2010):** 34H10, 37N35, 93C10, 93C15, 93C95.

## 1 Introduction

Chaos is a fascinating nonlinear phenomenon that has received a lot of attention in recent years. During the previous two decades, the chaos theory proved to be effective in a wide range of areas such as data encryption [20], financial systems [18, 19], biology [23] and biomedical engineering [2], etc. Fractional-order chaotic dynamical systems have begun to attract a lot of attention in recent years and can be seen as a generalization of chaotic dynamic integer-order systems. The synchronization between a fractional-order chaotic system and an integer-order chaotic system is thoroughly a new domain which has begun

---

\* Corresponding author: <mailto:mes.laabid@centre-univ-mila.dz>

to attract much attention in recent years [9,21] because of its potential applications in secure communication and cryptography [11,12]. Obviously, the synchronization between a fractional-order chaotic system and an integer-order chaotic system is more difficult than the synchronization between a fractional-order chaotic system or an integer-order chaotic system for the different order of their error dynamical system. The synchronization between a fractional-order system and an integer-order system was first studied by Zhou et al. [21]. As a special case of generalized synchronization, anti-synchronization is achieved when the sum of the states of master and slave systems converge to zero asymptotically with time. In this research work, we apply nonlinear control theory to anti-synchronize two chaotic systems when a fractional-order system is chosen as the drive system and an integer-order system serves as the response system. The anti-synchronization capability of the approach is demonstrated using a fractional-order lesser date moth chaotic system and an integer-order chaotic system [15]. The paper is arranged in the following manner. In Section 2, we describe the problem formulation for a fractional-order and an integer-order chaotic system. In Section 3, we discuss the anti-synchronisation between a fractional-order lesser date moth chaotic system and an integer-order chaotic system using the nonlinear control. Section 4 gives a brief conclusion.

## 2 Problem Formulation for Fractional-Order and Integer-Order Chaotic System

Consider the following fractional-order chaotic system as a drive (master) system:

$$D^\alpha x_1 = Ax_1 + g(x_1), \quad (1)$$

where  $x_1 \in \mathbb{R}^n$  is the state vector,  $A \in \mathbb{R}^{n \times n}$  is the linear part,  $g(x_1)$  is a continuous nonlinear function, and  $D^\alpha$  is the Caputo fractional derivative. Also, the response system (slave) can be described as

$$\dot{x}_2 = Ax_2 + g(x_2) + u, \quad (2)$$

where  $x_2 \in \mathbb{R}^n$  is the state vector,  $A \in \mathbb{R}^{n \times n}$  is the linear part,  $g(x_2)$  is a continuous nonlinear function and  $u \in \mathbb{R}^n$  is the control.

Define the anti-synchronization errors as  $e = x_2 + x_1$ . The anti-synchronisation error system between the driving system (1) and the response system (2) can be expressed as

$$\dot{e} = \dot{x}_2 + \dot{x}_1,$$

where  $\dot{x}_2$  is obtained from the response system (2), while no exact expressions of  $\dot{x}_1$  can be obtained from the driving system (1). Therefore, a numerical differentiation method is used to obtain  $\dot{x}_1$ .

According to the definition of the derivative, the derivative is approximately expressed using the difference quotient as

$$g'(a) \approx \frac{g(a+h) - g(a)}{h}, \quad (3)$$

$$g'(a) \approx \frac{g(a) - g(a-h)}{h}, \quad (4)$$

where ( $h > 0$ ) is a small increment. Formulae (3) and (4) are called the pre-difference formula and the post-difference formula, respectively. The post-difference formula is used in this paper.

The global anti-synchronization problem is essentially to find a feedback controller  $u$  so as to stabilize the error dynamics for all initial conditions  $e(0) \in \mathbb{R}^n$  (i.e.,  $\lim_{t \rightarrow \infty} \|e(t)\| = 0$ ).

### 3 Anti-Synchronisation of Fractional-Order Lesser Date Moth Chaotic System and Integer-Order Chaotic System by Nonlinear Control

#### 3.1 Main results

In this section, to validate the nonlinear control method proposed in [5], we take the fractional-order lesser date moth chaotic system [15] as a drive system and the integer-order chaotic system as a response system.

Thus, the drive and response systems are as follows:

$$\begin{cases} D^\alpha x_1 = x_1(1 - x_1) - \frac{x_1 y_1}{\beta + x_1}, \\ D^\alpha y_1 = -\delta y_1 + \frac{\gamma x_1 y_1}{\beta + x_1} - y_1 z_1, \\ D^\alpha z_1 = -\eta z_1 + \sigma y_1 z_1, \end{cases} \quad (5)$$

and

$$\begin{cases} \dot{x}_2 = x_2(1 - x_2) - \frac{x_2 y_2}{\beta + x_2} + u_1, \\ \dot{y}_2 = -\delta y_2 + \frac{\gamma x_2 y_2}{\beta + x_2} - y_2 z_2 + u_2, \\ \dot{z}_2 = -\eta z_2 + \sigma y_2 z_2 + u_3, \end{cases} \quad (6)$$

where  $u_1, u_2, u_3$  are the nonlinear controller. It is reported that the fractional-order lesser date moth system (5) with the fractional order of  $\alpha = 0.95$  can behave chaotically [15]. The three-dimensional (3D) phase portraits of the lesser date moth chaotic system with fractional-order and integer-order, respectively, are shown in Figure 1 and Figure 2.

The anti-synchronization error  $e$  is defined by

$$\begin{cases} e_1 = x_1 + x_2, \\ e_2 = y_1 + y_2, \\ e_3 = z_1 + z_2. \end{cases} \quad (7)$$

The error dynamics is obtained as

$$\begin{cases} \dot{e}_1 = \dot{x}_1 + x_2(1 - x_2) - \frac{x_2 y_2}{\beta + x_2} + u_1, \\ \dot{e}_2 = \dot{y}_1 - \delta y_2 + \frac{\gamma x_2 y_2}{\beta + x_2} - y_2 z_2 + u_2, \\ \dot{e}_3 = \dot{z}_1 - \eta z_2 + \sigma y_2 z_2 + u_3. \end{cases} \quad (8)$$

We consider the nonlinear controller defined by

$$\begin{cases} u_1 = -\dot{x}_1 - x_2(1 - x_2) + \frac{x_2 y_2}{\beta + x_2} - e_1, \\ u_2 = -\dot{y}_1 - \delta y_2 + \frac{\gamma x_2 y_2}{\beta + x_2} + y_2 z_2, \\ u_3 = -\dot{z}_1 - \eta z_2 - \sigma y_2 z_2. \end{cases} \quad (9)$$

Substituting (9) into (8), we obtain the linear system

$$\begin{cases} \dot{e}_1 = -e_1, \\ \dot{e}_2 = -\delta e_2, \\ \dot{e}_3 = -\eta e_3. \end{cases} \quad (10)$$

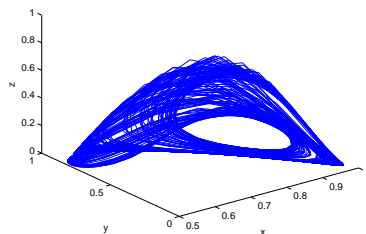


**Figure 1:** The 3D phase portrait of the fractional-order lesser date moth system.

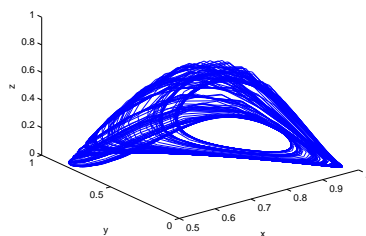


**Figure 2:** The 3D phase portrait of the integer-order lesser date moth system.

We consider the quadratic Lyapunov function defined by

$$V(e) = \frac{1}{2}e^T e = \frac{1}{2}(e_1^2 + e_2^2 + e_3^2), \quad (11)$$

which is a positive definite function on  $\mathbb{R}^3$ . A simple calculation gives

$$\dot{V}(e) = -e_1^2 - \delta e_2^2 - \eta e_3^2, \quad (12)$$

which is a negative definite function on  $\mathbb{R}^3$ .

Thus, by the Lyapunov stability theory [24], the error dynamics (10) is globally exponentially stable. Hence, we have proved the following result.

**Theorem 1** *The fractional-order lesser date moth chaotic system and the integer-order chaotic systems (5) and (6) are exponentially and globally anti-synchronized for any initial conditions with the nonlinear controller  $u$  defined by (9).*

### 3.2 Numerical results

For the numerical simulations, we use some documented data for some parameters like  $\gamma = 3$ ,  $\delta = \eta = 1$ ,  $\sigma = 3$ ,  $\beta = 1.15$ ,  $h = 0.85$ ,  $\alpha = 0.95$ , then we have  $(x_1, y_1, z_1) = (0.7, 0.3, 0.8)$  and  $(x_2, y_2, z_2) = (-0.68, -0.91, -0.65)$ . The simulation results are illustrated in Figure 3.

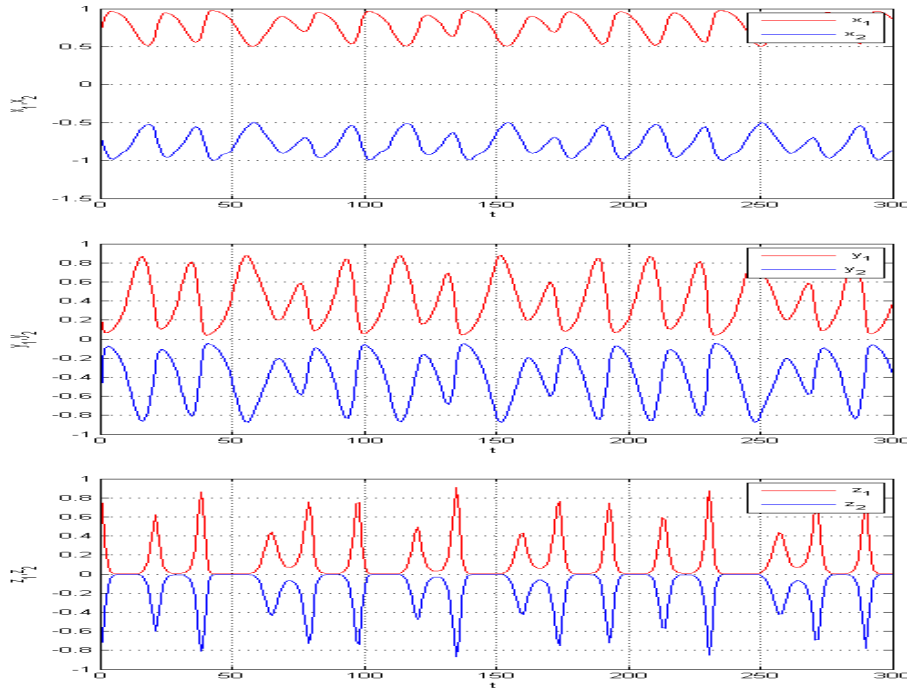


**Figure 3:** Anti-synchronization between response system (6) and drive system (5).

#### 4 Conclusion

Anti-synchronizing different chaotic systems have important applications in many physical and biological systems, as well as in secure communication using chaotic signals, where one cannot assume that the equations and parameters of the drive and response systems are identical. Furthermore, in the literature, few studies apply nonlinear control theory to anti-synchronize two chaotic systems when a fractional-order system is chosen as the drive system and an integer-order system is the response system. And there is no study regarding the anti-synchronization capability of the approach demonstrated using a fractional-order lesser date moth chaotic system and an integer-order chaotic system. Our goal in this paper was to study the phenomenon of chaos anti-synchronization between a fractional-order lesser date moth chaotic system and an integer-order chaotic system. Our findings show that chaos anti-synchronization can be performed between fractional-order chaotic systems and integer-order chaotic systems using nonlinear control techniques. The numerical outcomes are consistent with the theoretical analyses.

#### References

- [1] A. E. Matouk. Chaos, feedback control and synchronization of a fractional-order modified autonomous Van der Pol-Duffing circuit. *Commun Nonlinear Sci. Numer. Simulat.* **16** (2011) 975–986.

- [2] B. Zsolt. Chaos theory and power spectrum analysis in computerized cardiocography. *Eur. J. Obstet. Gynecol. Reprod. Biol.* **71** (2) (1997) 163–168.
- [3] D. Matignon. Stability result on fractional differential equations with applications to control processing. *Computational Engineering in Systems and Application multi-conference, IMACS. In: IEEE-SMC Proceedings.* Lille, France **2** (1996) 963–968.
- [4] D. Pazo, M. A. Zaks and J. Kurths. Role of unstable periodic orbit in phase and lag synchronization between coupled chaotic oscillators. *Chaos.* **13** (2003) 309–318.
- [5] E. W. Bai and K. E. Lonngren. Synchronization of two Lorenz systems using active control. *Chaos, Solitons and Fractals.* **9** (1998) 1555–1561.
- [6] G. Alvarez, S. Li, F. Montoya, G. Pastor and M. Romera. Breaking projective chaos synchronization secure communication using filtering and gneralized synchronization. *Chaos, Solutons and Fractals.* **24** (2005) 775–783.
- [7] G.M. Mahmoud, T. Bountis, G.M. AbdEl-Latif and Emad E. Mahmoud. Chaos synchronization of two different chaotic complex Chen and Lü systems. *Nonlinear Dynamics* **55** (2009) 43–53.
- [8] G. P. Jiang, K. S. Tang and G. Chen. A simple global synchronization criterion for coupled chaotic systems. *Chaos, Soliton and Fractals.* **15** (2003) 925–935.
- [9] G. Q. Si, Z. Y. Sun, and Y. B. Zhang. A general method for synchronizing an integer-order chaotic system and a fractionalorder chaotic system. *Chinese Physics B.* **20** (8) (2011), 080505.
- [10] H. Targhvafard and G. H. Enjace. Phase and anti-phase synchronization of fractional-order chaotic systems via active control. *Commun Nonlinear Sci. Numer. Simul.* **16** (2011) 4079–4408.
- [11] K. Murali and M. Lakshmanan. Secure communication using a compound signal from generalized synchronizable chaotic system. *Phys. Letters A* **241** (1998) 303–310.
- [12] L. Kocarev and U. Parlitz. General approach for chaotic synchronization with applications to communication. *Phys. Rev. Lett.* **74** (1995) 5028–5030.
- [13] L. X. Jia, H. Dai and M. Hui. Nonlinear feedback synchronisation control between fractional-order and integer-order chaotic systems. *Chinese Physics B.* **19** (11) (2010), Article ID 110509.
- [14] M. C. Ho, and Y. C. Hung. Synchronization of two different chaotic systems by using generalized active control. *Physics Letters A* **301** (2002) 424–428.
- [15] M. El-Shahed, Juan J. Nieto, A. M. Ahmed and I. M. E. Abdelstar. Fractional-order model for biocontrol of the lesser date moth in palm trees and its discretization. *Advance in Difference Equations* (2017) 2017–2295.
- [16] M. Labid and N. Hamri. Chaos Synchronization and Anti-Synchronization of two Fractional-Order Systems via Global Synchronization and Active Control. *Nonlinear Dynamics and Systems Theory* **19** (3) (2019) 416–426.
- [17] M. Labid and N. Hamri. Chaos Synchronization between Fractional-Order Lesser Date Moth Chaotic System and Integer-Order Chaotic System via Active Control. *Nonlinear Dynamics and Systems Theory* **22** (4) (2022) 407–413.
- [18] M. S. Abd-Elouhab, N. Hamri and J. Wang. Chaos Control of a Fractional-Order Financial System. *Mathamatical Problems in Engineering* (2010), Article ID270646, 18 pages, doi: 10.1155/2010/270646.
- [19] N. Laskin. Fractional market dynamics. *Physics A* **287** (2000) 482–492.
- [20] N. Zhou, Y. Wang, L. Gong, H. He and J. Wu. Novel single-channel color image encryption algorithm based on chaos and fractional Fourier transform. *Optics Communications* **284** (2011) 2789–2796.

- [21] P. Zhou, Y. M. Chen and F. Kuang. Synchronization between fractional-order chaotic systems and integer orders chaotic systems (fractional-order chaotic systems). *Chinese Physics B* **19** (9) (2010), 090503.
- [22] R. Mainieri and J. Rehacek. Projective synchronization in three dimensional chaotic systems. *Phys. Rev. Lett.* **82** (1999) 3042–3045.
- [23] S. Vaidyanathan. Lotka-Volterra two-species mutualistic biology models and their ecological monitoring. *Pharm Tech Research.* **8** (2015) 199–212.
- [24] W. Hahn. *The Stability of Motion*. Springer-Verlag, Berlin, 1967.
- [25] W. H. Deng and C. P. Li. Chaos synchronization of the fractional Lü system, *Physica A.* **353** (2005) 61–72.
- [26] Y. Zhang and J. Sun. Chaotic synchronization and anti-synchronization based on suitable separation. *Physics Letters A* **330** (2004) 442–447.



# A New Hidden Attractor Hyperchaotic System and Its Circuit Implementation, Adaptive Synchronization and FPGA Implementation

R. Rameshbabu \*, K. Kavitha, P. S. Gomathi and K. Kalaichelvi

*Department of Electronics and Communication Engineering, V.S.B. Engineering College,  
Tamilnadu, Karur, India*

Received: November 17, 2022; Revised: April 4, 2023

**Abstract:** In this paper, a new hyperchaotic system with no rest point is presented and its basic properties such as divergence and convergence, rest points and instability, Lypunov exponents, and bifurcation are analyzed in detail. In the proposed system, some special features such as position controllability and multistability in periodic state are observed. The analog circuit realization of the proposed hyperchaotic system is also presented to validate the present theoretical study of the system. Furthermore, the adaptive synchronization of the proposed hyperchaotic system is demonstrated using a novel anti-synchronization methodology. This paper also presents the Field Programmable Gate Array based digital circuit realization of adaptive anti-synchronization methodology for the proposed hyperchaotic system. The digital circuit implementation is achieved by generating the VHDL code for the FPGA implementation in Matlab and Xilinx. The experimental results are provided to verify the feasibility and effectiveness of our proposed scheme.

**Keywords:** *hidden attractor; hyperchaotic system; circuit implementation; adaptive synchronization; FPGA implementation.*

**Mathematics Subject Classification (2010):** 93-XX.

---

\* Corresponding author: <mailto:ramarrameshbabu@gmail.com>

## 1 Introduction

The hyperchaotic system is a nonlinear dynamical system with at least two positive Lyapunov exponents. The positive Lyapunov exponents indicate the complexity and unpredictable response of a dynamical system. Due to this complex nature, the hyperchaotic system is used in many engineering fields such as oscillators [1], image encryption [2] and secure communication [3] etc. Recently, many hyperchaotic systems with hidden attractors have been introduced [4–6] and their dynamic behaviors are discussed in detail.

In this paper, another hyperchaotic system with hidden attractor is proposed and its basic dynamic properties and bifurcation are studied in detail. The proposed system also exhibits some special features such as multistability and offset boosting property for various applications. Multistability is an important phenomenon by which the chaotic system generates various number of attractors for different initial conditions. The multistability feature is observed in a periodic state in the proposed system. The position of the proposed attractor is controllable by introducing a controller in one of the state variable and this is known as the offset boosting control. The proposed system has three nonlinear terms. It is exciting to observe that our proposed system has no rest point and hence, its attractor is masked. In order to verify the dynamical behavior of our proposed system, the electronic circuit realization is presented in this paper. The circuit realization is based on discrete components and Integrated Circuits (IC) and simulated using MULTISIM software.

The trajectory of a hyperchaotic signal highly depends on its initial points and the parameters of the system are uncertain in practice. Therefore, there is a need to design a controller function to synchronize the even identical hyperchaotic systems with unknown parameters. Recently, many chaos synchronization methodologies have been proposed in literature reviews [7–9]. In this research paper, an anti-synchronization scheme is chosen for the demonstration of adaptive synchronization of the proposed system.

The digital realization of an adaptive synchronization scheme for chaotic systems has predominant applications in many digital chaotic systems such as digital data transmission [10] etc. In order to expand the hyperchaos based real time applications, nowadays, researchers give more attention to the implementation of a hyperchaotic system in digital circuits such as Field Programmable Gate Array (FPGA) [11], [12]. Based on the literature survey, in this work, the proposed adaptive anti-synchronization scheme for the hyperchaotic system is realized in FPGA using MATLAB simulink and Xilinx system generator tools.

## 2 Modelling of New Hidden Attractor Hyperchaotic System

The new hyperchaotic system with hidden attractor is of the form

$$\begin{aligned}\dot{p} &= \alpha(q - p), \\ \dot{q} &= \beta q - pr + w, \\ \dot{r} &= pq - \gamma r, \\ \dot{w} &= w - pr.\end{aligned}\tag{1}$$

Here,  $p, q, r, w$  are the state variables and  $\alpha, \beta, \gamma$  are the non zero positive parameters of the system (1). The system parameter values are chosen as  $\alpha = 26$ ,  $\beta = 14$  and  $\gamma = 3$ . The behavior of the new dynamical system (1) never changes the polarity of the co-ordinates changes as  $(p, q, r, w) \rightarrow (-p, -q, r, -w)$  and the proposed system has

rotational symmetry about the  $r$ -axis. The divergence of the system (1) is given as  $\nabla f = \frac{\partial f_p}{\partial p} + \frac{\partial f_q}{\partial q} + \frac{\partial f_r}{\partial r} + \frac{\partial f_w}{\partial w} = -14.36$ , where  $f_p = \dot{p}$ ,  $f_q = \dot{q}$ ,  $f_r = \dot{r}$ ,  $f_w = \dot{w}$ . Since the divergence of (1) is negative for all positive values of  $\alpha, \beta, \gamma$ , we can conclude that the proposed system has a strange attractor. The rest points of the proposed system (1) can be computed numerically by equating the Equation (1) to zero as given in Equation (2),

$$\begin{aligned}\alpha(q - p) &= 0, \\ \beta q - pr + w &= 0, \\ pq - \gamma r &= 0, \\ w - pr &= 0.\end{aligned}\tag{2}$$

From Equation (2), the rest points of system (1) are computed as  $E\{0, 0, 0, 0\}$  and it is observed that the attractor of new dynamical system (1) is masked up somewhere in phase space. The Jacobian matrix of the system (1) is given as

$$J = \begin{pmatrix} -\alpha & \alpha & 0 & 0 \\ -r & \beta & -p & 1 \\ q & p & -\gamma & 0 \\ -r & 0 & -p & 1 \end{pmatrix}.\tag{3}$$

The eigenvalues of the Jacobian matrix (J) can be obtained as  $\lambda_1 = -26, \lambda_2 = 14, \lambda_3 = -3$  and  $\lambda_4 = 1$ . Since the set of eigenvalues has both positive and negative real values, the rest point  $E$  is an unstable point. The Lyapunov exponents of the new hyperchaotic dynamic system (1) are calculated using the Wolf algorithm as  $LE = [0.331891, 0.038063, 0, -14.314174]$  for the initial conditions  $p_0 = 1, q_0 = 2, r_0 = 1, w_0 = 3$ . The sum of Lyapunov exponents is  $-13.94422 < 0$  and hence, the proposed system (1) is dissipative. The Lyapunov dimension ( $D_L$ ) can be obtained as  $D_L = 3 + \frac{LE_1 + LE_2 + LE_3}{|LE_4|} = 3.019644$ , which indicates the fractional dimension of the proposed system (1).

### 3 Dynamic Analysis of Proposed System

The variations of state variables of the proposed hyperchaotic system (1) in 2D and 3D planes are given in Figure 1. The bifurcation diagrams and Lyapunov exponents of the proposed system (1), based on the parameters  $\alpha$  and  $\beta$  for the initial conditions  $\{0, 1, -1, 1\}$ , are shown in Figure 2. First, the parameter  $\alpha$  varies in the range of  $\alpha \in [22 - 27]$  and the remaining parameters are kept constant, as demonstrated in Figure 2a, which shows that the system (1) is in a period state in the range of  $\alpha \in [22 - 22.3]$ ,  $\alpha \in [24.3 - 25.5]$  and in chaos states in the range of  $\alpha \in [22.3 - 24.2]$ ,  $\alpha \in [25.5 - 27]$ . Second, the parameter  $\beta$  varies in the range of  $\beta \in [13 - 18]$  and the other parameters are kept constant as given in Figure 2b, which shows that there is the inverse doubling behavior. It is in a chaotic state in the range of  $\beta \in [13 - 14.5]$ , and in a period state in the range of nearly  $\beta \in [14.5 - 15.4]$  and  $\beta \in [17.5 - 18]$ . The Lyapunov spectrum versus the various parameters is also demonstrated in Figures 2c and 2d, in which  $LE_1, LE_2, LE_3$  and  $LE_4$  are represented in blue, red, green, and cyan, respectively.

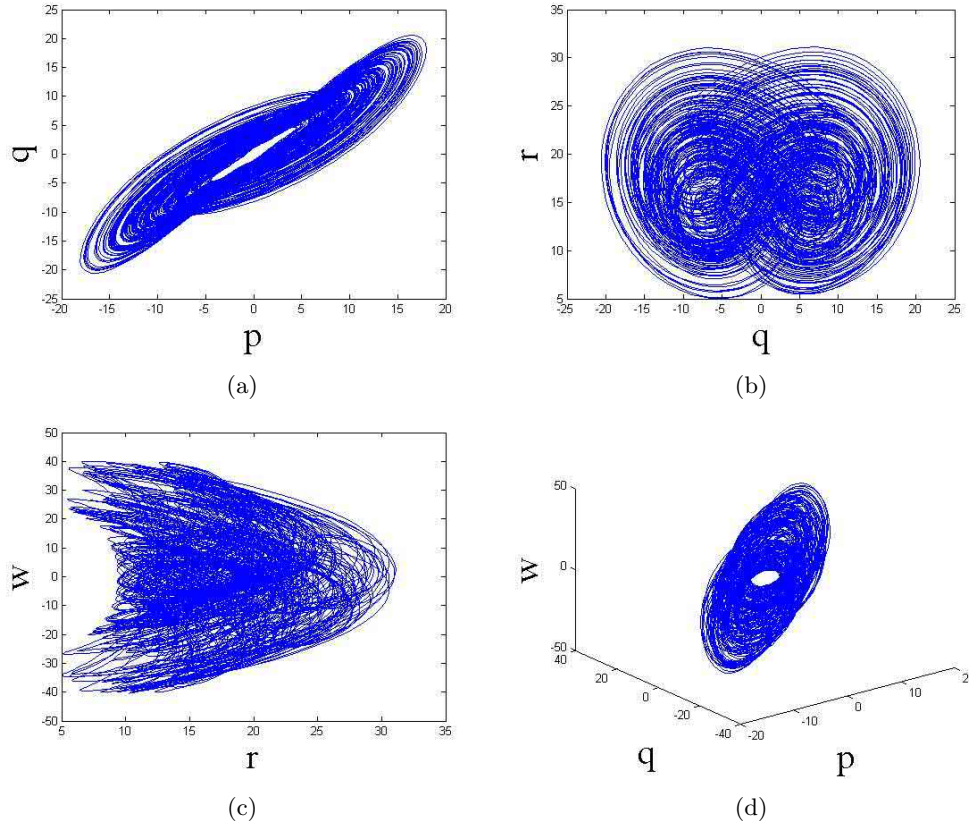


Figure 1: Attractors of the proposed hyperchaotic system.

#### 4 Controllability of Proposed Hyperchaotic System

The position of the proposed attractor is controllable by introducing a controller parameter  $\delta$  in the state variable  $w$  in the proposed system (1). The state variable  $w$  in the proposed system is replaced with  $w + \delta$  as given in (4). Figure 3a shows the position of the proposed controlled attractor in the  $r-w$  plane for  $\delta = 0$  (blue),  $\delta = -90$  (black) and  $\delta = 90$  (magenta). Figure 3b shows that the state variable  $w$  is converted from bipolar into unipolar by varying the controller value.

$$\begin{aligned}
 \dot{p} &= \alpha(q - p), \\
 \dot{q} &= \beta q - pr + (w + \delta), \\
 \dot{r} &= pq - \gamma r, \\
 \dot{w} &= (w + \delta) - pr.
 \end{aligned} \tag{4}$$

#### 5 Multistability of Proposed Hyperchaotic System

Multistability or a multiple attractor property is observed in the various periodic states of the proposed system. Figure 4a shows a bifurcation diagram for the parameter  $\beta$

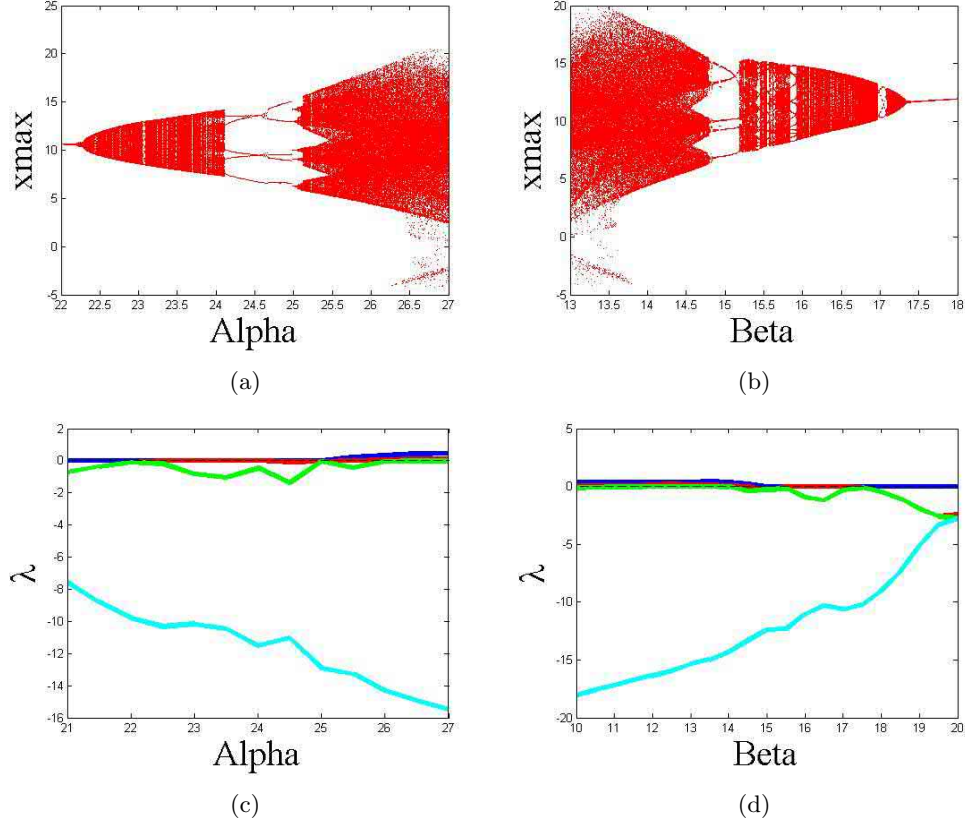


**Figure 2:** (a-b) Bifurcation diagram, (c-d) Lyapunov exponents plots of the proposed system.

under the initial conditions  $(0, 1, -1, 1)$  (red) and  $(1, 1, -1, 1)$  (black) and indicates that there is a multiple attractor in periodic states. Figure 4b shows the phase portraits of the proposed system when  $a = 26, b = 15, c = 3$  under the initial conditions  $(0, 1, -1, 1)$  (blue) and  $(1, 1, -1, 1)$  (magenta).

## 6 Electronic Circuit Implementation of Proposed Hyperchaotic System

In this section, an analog circuit is constructed to confirm the theoretical results of the proposed system (1) using electronic components such as resistors, capacitors, OPAMP 741, and multiplier. The time and amplitude scaling factors are chosen as  $T = 100t$  and  $A = 5$ , respectively, to realize the circuit parameters  $\alpha, \beta$  and  $\gamma$ . The system (1) can be written as (5),

$$\begin{aligned}
 \frac{dx}{dT} &= 100\alpha(y - x), \\
 \frac{dy}{dT} &= 100(\beta y - Axz + w), \\
 \frac{dz}{dT} &= 100(Axy - \gamma z), \\
 \frac{dw}{dT} &= 100(w - Axz).
 \end{aligned} \tag{5}$$

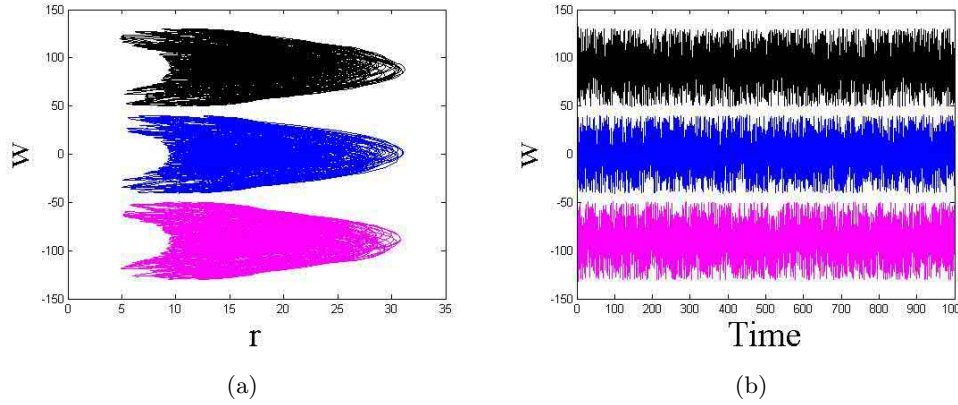


**Figure 3:** Position variation of the proposed attractor with  $\delta = 0$ (Blue),  $\delta = 90$ (Magenta),  $\delta = -90$ (Black). (a)  $r - w$  plane, (b) The time series of the state variable  $w$ .

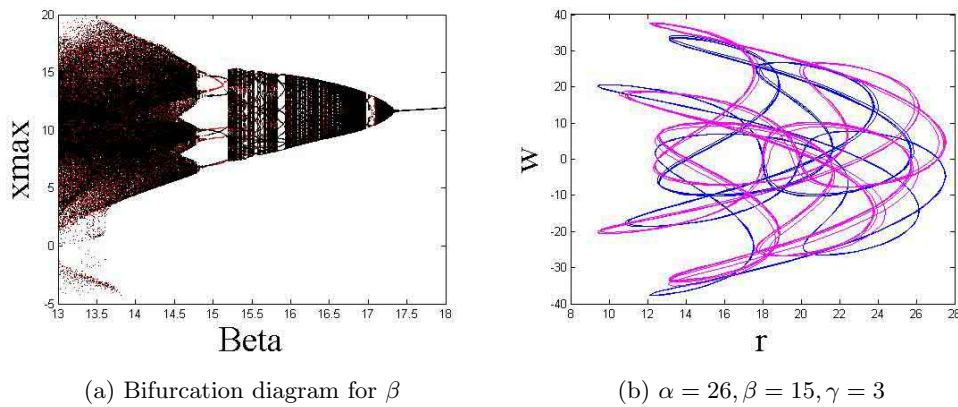


**Figure 4:** Multistability behaviour of the proposed system.

The equations for the proposed electronic circuit design can be given as in Equation (6),

$$\begin{aligned}
 \frac{dx}{dT} &= \frac{R_1}{R_2 R_3 C_1}(-y) - \frac{R_1}{R_2 R_4 C_1}(x), \\
 \frac{dy}{dT} &= \frac{R_5}{R_6 R_7 C_2}(-y) - \frac{R_5}{10 R_6 R_9 C_2}(xz) - \frac{R_5}{R_6 R_8 C_2}(-w), \\
 \frac{dz}{dT} &= \frac{R_{10}}{R_{11} R_{12} C_3}(-xy) - \frac{R_{10}}{R_{11} R_{13} C_3}(z), \\
 \frac{dw}{dT} &= \frac{R_{14}}{R_{15} R_{16} C_4}(-w) - \frac{R_{14}}{R_{15} R_{17} C_4}(-xz).
 \end{aligned}
 \tag{6}$$

The circuit realization of system (6) using Multisim software is shown in Figure 5. The electronic components are chosen as  $C_1 = C_2 = C_3 = C_4 = 10\text{nF}$ ,  $R_1 = R_5 = R_{10} = R_{14} = R_{18} = R_{19} = R_{20} = R_{21} = R_{22} = R_{23} = R_{24} = R_{25} = 100\Omega$ ,  $R_2 = R_6 = R_{11} = R_{15} = 50\text{k}\Omega$ ,  $R_3 = R_4 = 77\text{k}\Omega$ ,  $R_7 = 143\text{k}\Omega$ ,  $R_8 = R_{16} = 2000\text{k}\Omega$ ,  $R_9 = R_{12} = R_{17} = 40\text{k}\Omega$  and  $R_{13} = 595\text{k}\Omega$ . Circuit simulation results are shown in Figure 6. Note that the Multisim simulation results are agreeing with the Matlab results shown in Figure 1.

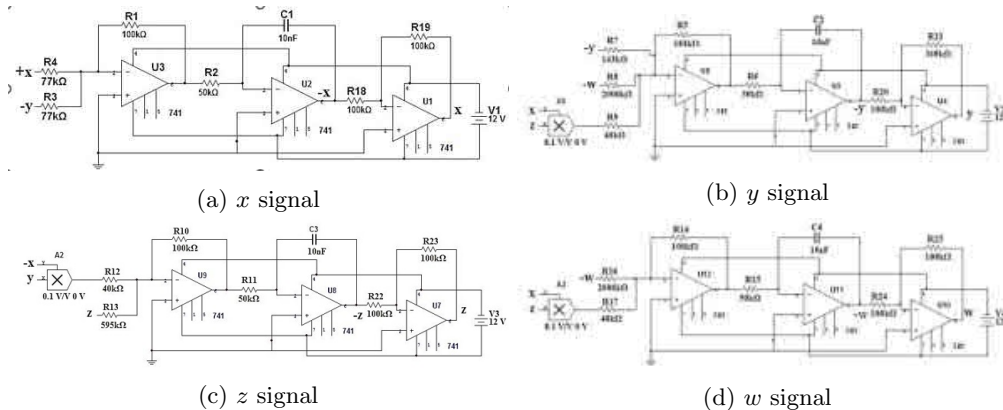


Figure 5: Circuit realization of the proposed system.

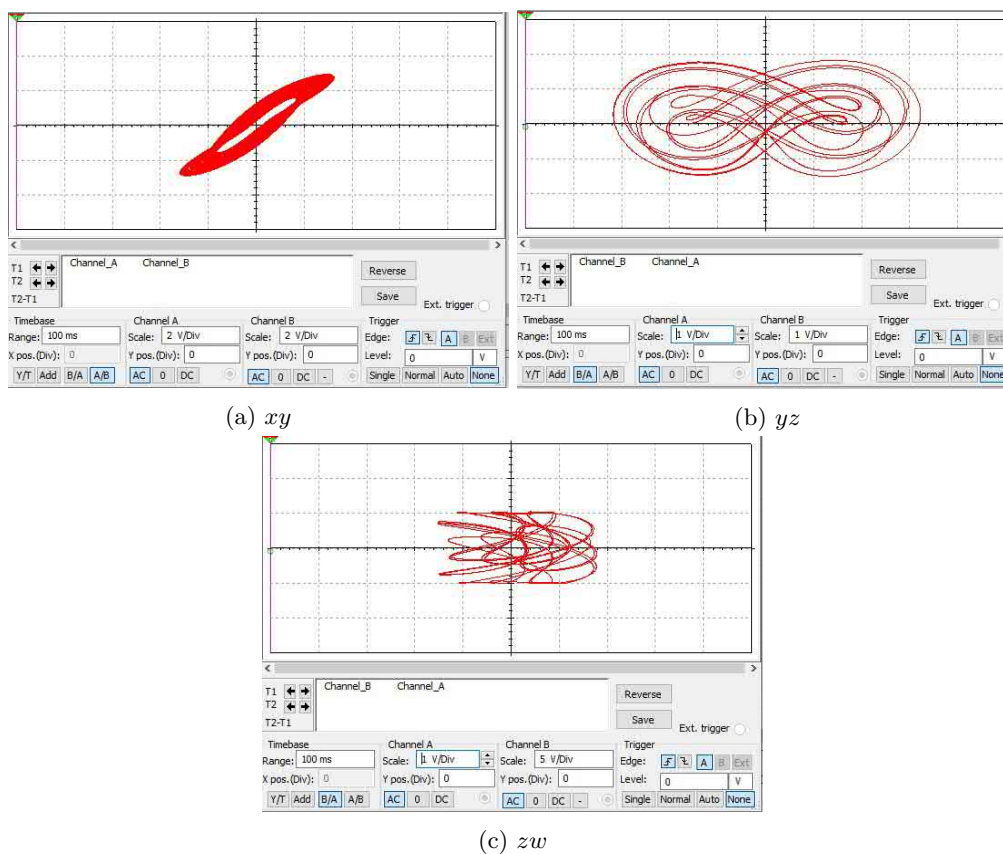


Figure 6: Electronic simulation result for the proposed system.

## 7 Adaptive Synchronization of Proposed Hyperchaotic System

In this section, the anti-synchronization of the proposed system (1) is established using an adaptive control method. In the last two decades, a variety of synchronization schemes such as fuzzy set based methods [13], observer-based methods [14], Lyapunov-based methods [15], sliding surface-based methods [16], PID control [17], and active method [18] were used. However, the synchronization schemes proposed in the literature review [13–18] have some limitations. The fuzzy set methods need the states of the system for the calculations of membership and non-membership functions and building a regressor vector. The observer-based synchronization scheme is restricted to synchronize different systems since the structure of the slave system is defined by the master system. In backstepping, synchronization is a Lyapunov-based synchronization method in which the calculation of the Lyapunov exponent is required for the entire system. The sliding mode control method requires the design of a sliding surface in which the states of the system sliding on the sliding surface and the dynamic behavior of the system depend on the sliding surface equations. The chattering problem is the main drawback of the sliding mode controller. The Proportional Integral Derivative (PID) controller has low robustness and suitability for linear systems. The active control method is not suitable for practical situations since the initial conditions and the system parameters are unknown in practice. The literature review on chaos synchronization pinpoints that compared to any other method, the adaptive feedback control method is a simple, convenient, and efficient methodology for implementing the chaos synchronization. The master and the slave system are given as in (1) and (7), respectively,

$$\begin{aligned} \dot{p}_1 &= \alpha(q_1 - p_1) + u_1, \\ \dot{q}_1 &= \beta q_1 - p_1 r_1 + w_1 + u_2, \\ \dot{r}_1 &= p_1 q_1 - \gamma r_1 + u_3, \\ \dot{w}_1 &= w_1 - p_1 r_1 + u_4. \end{aligned} \quad (7)$$

Here,  $p_1, q_1, r_1$  and  $w_1$  are the state variables of the slave system,  $u_1, u_2, u_3$  and  $u_4$  are the adaptive controllers used to synchronize the master and the slave system,  $\alpha = 26, \beta = 14, \gamma = 3$  are the system parameters. The anti-synchronization error between the master and the slave system can be written as (8),

$$\begin{aligned} e_1 &= p_1 + p, \\ e_2 &= q_1 + q, \\ e_3 &= r_1 + r, \\ e_4 &= w_1 + w. \end{aligned} \quad (8)$$

Based on adaptive control theory, the adaptive controllers can be derived as (9),

$$\begin{aligned} \dot{u}_1 &= -\hat{\alpha}(e_2 - e_1) - g_1 e_1, \\ \dot{u}_2 &= -\hat{\beta} e_2 + e_4 + p_1 r_1 + p r - g_2 e_2, \\ \dot{u}_3 &= \hat{\gamma} e_3 - p_1 q_1 - p q - g_3 e_3, \\ \dot{u}_4 &= -e_4 + p_1 r_1 + p r - g_4 e_4. \end{aligned} \quad (9)$$

Here,  $\hat{\alpha}, \hat{\beta}, \hat{\gamma}$  are the estimate values of the unknown parameters  $\alpha, \beta, \gamma$ , respectively.  $g_1, g_2, g_3, g_4$  are the gain of the controllers. Consider a Lyapunov function candidate as

$$\begin{aligned} V &= e_1 \dot{e}_1 + e_2 \dot{e}_2 + e_3 \dot{e}_3 + e_4 \dot{e}_4 + e_a \dot{e}_a + e_b \dot{e}_b + e_c \dot{e}_c \\ &= e_a [e_1(e_2 - e_1) - \hat{\alpha}] + e_b [e_2^2 - \hat{\beta}] + e_c [-e_3^2 - \hat{\gamma}] - g_1 e_1^2 - g_2 e_2^2 - g_3 e_3^2 - g_4 e_4^2. \end{aligned} \quad (10)$$

By choosing the dynamics of unknown parameter values as  $\dot{\hat{\alpha}} = e_1(e_2 - e_1)$ ,  $\dot{\hat{\beta}} = e_2^2$  and  $\dot{\hat{\gamma}} = -e_3^2$ , Equation (10) becomes Equation (11) which indicates the negative Lyapunov function, the anti-synchronization error signals and the parameter error signals exponentially reach zero, which means that both the master and the slave system are synchronized together.

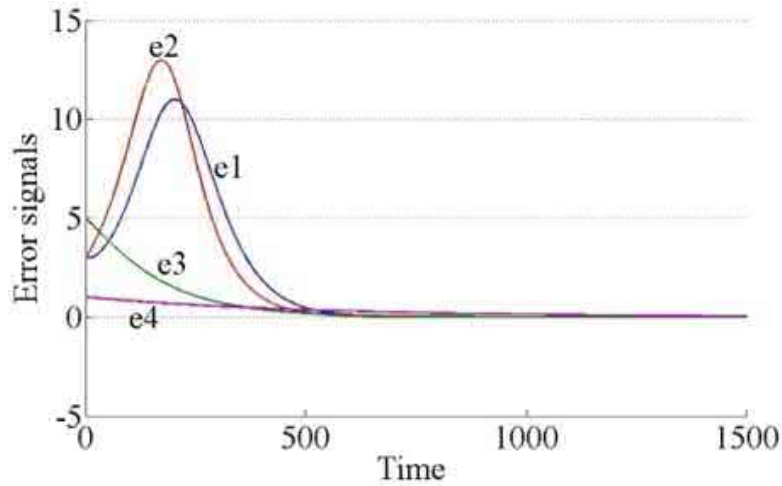
$$V = -(g_1 e_1^2 + g_2 e_2^2 + g_3 e_3^2 + g_4 e_4^2) < 0. \quad (11)$$

To demonstrate the adaptive synchronization of the proposed system, different initial conditions are chosen for the master and the slave system separately such as  $X_m = (3, -7, 1.5, 6)$  and  $X_s = (2, 3, 4, 1)$ . The initial conditions for the positive parameters  $\alpha, \beta, \gamma$  are, respectively, taken for demonstration as  $(0.5, 0.2, 0.7)$ . The gain of the adaptive controllers is also chosen for the demonstration purpose as  $g_i = 1$ , where  $i = 1, 2, 3, 4$ . Figure 7a shows that the anti-synchronization errors  $e_1, e_2, e_3$  and  $e_4$  become zero when both the master and the slave system are synchronized together. Figure 7b represents the synchronized state variables for the simulation time 1500s. The dotted line represents the master system and the solid line represents the controlled slave system  $p - p_1$  (Blue),  $q - q_1$  (Brown),  $r - r_1$  (Magenta) and  $w - w_1$  (Red).

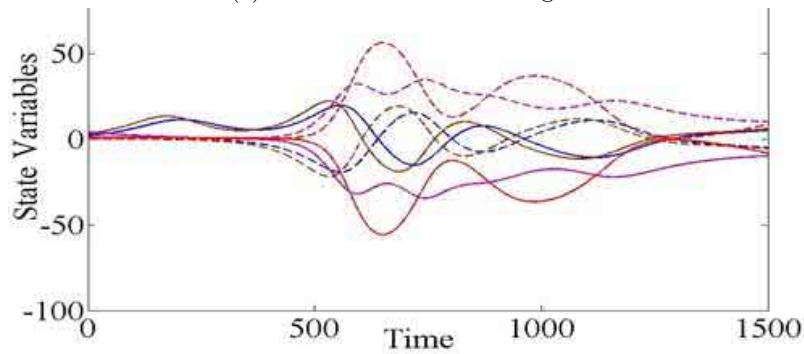
## 8 FPGA Implementation of Adaptive Synchronization of Proposed Hyperchaotic System

In this section, an FPGA-based digital circuit realization of the proposed adaptive synchronization methodology for a new hyperchaotic system is presented. The digital realization of the synchronized hyperchaotic system is achieved in the MATLAB and Xilinx environments. In this methodology, initially, Equations (1) and (7) to (9) are constructed in MATLAB simulink using Xilinx system generator tools to generate the VHDL code. Then, the generated VHDL code is simulated and synthesized in Xilinx software. Figure 8 shows the digital circuit realization of the proposed hyperchaotic system. The initial conditions for the master and the slave system are chosen for the FPGA implementation of the synchronization methodology as  $(p(0), q(0), r(0), w(0)) = (5, 2, 3, 1)$  and  $(p_1(0), q_1(0), r_1(0), w_1(0)) = (20, 30, 25, 15)$ , respectively. Hence, the initial conditions for the anti-synchronization error signal can be from Equation (8):  $(e_1(0), e_2(0), e_3(0), e_4(0)) = (25, 32, 28, 16)$ . The model of the proposed anti-synchronization methodology is shown in Figure 9, which shows the coupling between Equations (1) and (7) to (9). In Figure 9,  $p_0$  and  $q_0$  are the initial conditions for the master and the slave system,  $p_i \text{ outnet} [31 : 0]$  is the 32-bit state signal of the master system and  $q_i \text{ outnet} [31 : 0]$  is the 32-bit state signal of the slave system.  $\alpha_0, \beta_0$ , and  $\gamma_0$  are the initial conditions for the parameters  $\alpha, \beta$ , and  $\gamma$ , respectively. The master block is shown in Figure 8, the controller block contains Equation (10), parameter and error signal block generate the anti-synchronization error signals, and the initial conditions are fed in the master and slave system block. The VHDL code for the proposed synchronization methodology is generated for the FPGA device virtex-xc6vsx315t3ff1156. After that, the generated code is simulated in Xilinx software using ISE simulator.

As a result of simulation, a small portion of discrete waveform for the proposed anti-synchronization methodology is obtained as given in Figure 11, in which the signals  $x_1 \text{ outnet} [31 : 0]$  to  $x_4 \text{ outnet} [31 : 0]$  represent the signals from the master system, the signals  $y_1 \text{ outnet} [31 : 0]$  to  $y_4 \text{ outnet} [31 : 0]$  represent the signals from the slave system, and  $e_1 \text{ outnet} [31 : 0]$  to  $e_4 \text{ outnet} [31 : 0]$  are the error signals. For instance,



(a) Time variation of error signals.



(b) Synchronized master and slave system.

**Figure 7:** Simulation result for the adaptive synchronization of the proposed system.

$x_1 \text{ outnet} [31 : 0]$  has the value 000000000000101, which is equivalent to  $x_1(0) = 5$ , and  $y_1 \text{ outnet} [31 : 0]$  has the value 000000000010100, which is equivalent to  $y_1(0) = 20$ , and the anti-synchronization error  $e_1 \text{ outnet} [31 : 0]$  has the value 000000000011001, which is equivalent to  $e_1(0) = 25$ . Thus, we can conclude that the VHDL code simulation result agrees with the theoretical model developed for the adaptive anti-synchronization methodology in Section 7.

The resource utilization for virtex-xc6vsx315t3ff1156 is given in Table 1, which shows that the proposed synchronization methodology utilizes a very small amount of the available source.

## 9 Conclusion

A new hyperchaotic system with no rest point or hidden attractors is investigated, and numerical and analytical studies are carried out on its basic properties. The new system has two positive, 4-dimensional Lyapunov exponents, no rest points, and is unstable,

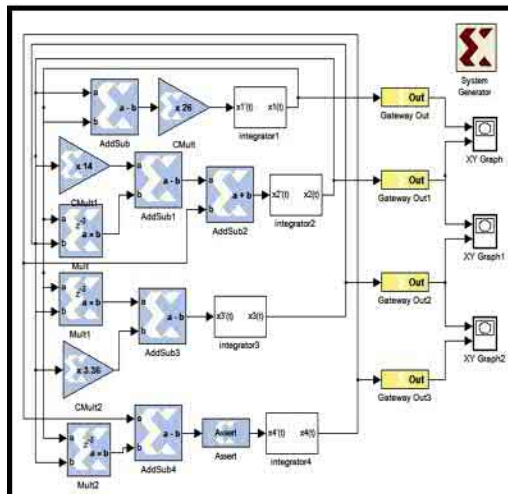


Figure 8: Digital realization of the proposed hyperchaotic system.

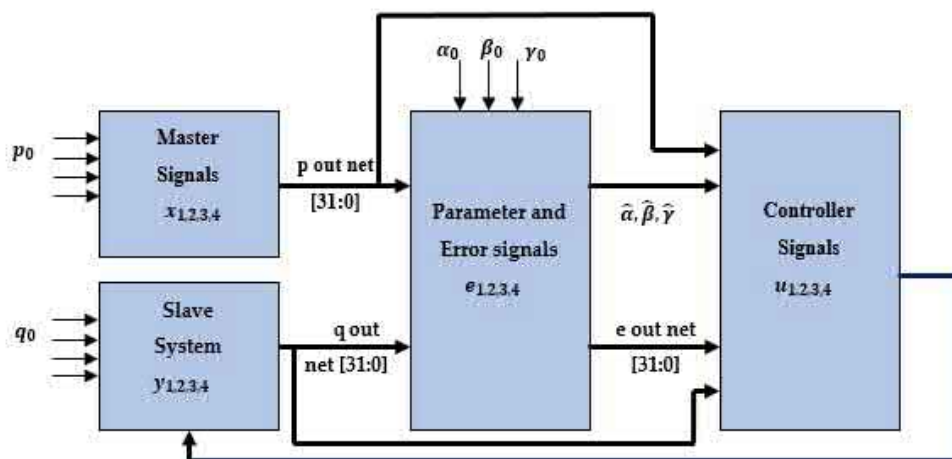


Figure 9: Coupling between the master and the slave hyperchaotic system.

which means that the proposed system has a hyperchaotic nature. The dynamical analysis of the proposed system is conducted using a bifurcation diagram and a Lyapunov exponents spectrum. An analog circuit for the new hyperchaotic system is constructed and simulated in Multisim and the simulation results show the viability of the proposed theoretical modeling of the new system. By using the adaptive control methodology, the anti-synchronization of a new, identical hyperchaotic system is studied. The Matlab simulation results for the adaptive anti-synchronization are demonstrated with different initial conditions to verify the theoretical analysis of the designed controllers. In order to digitize the synchronization methodology, FPGA implementation of the new synchronized hyperchaotic system with hidden attractors is designed. The simulation results and FPGA outputs demonstrate the efficiency of the proposed digitization methodology

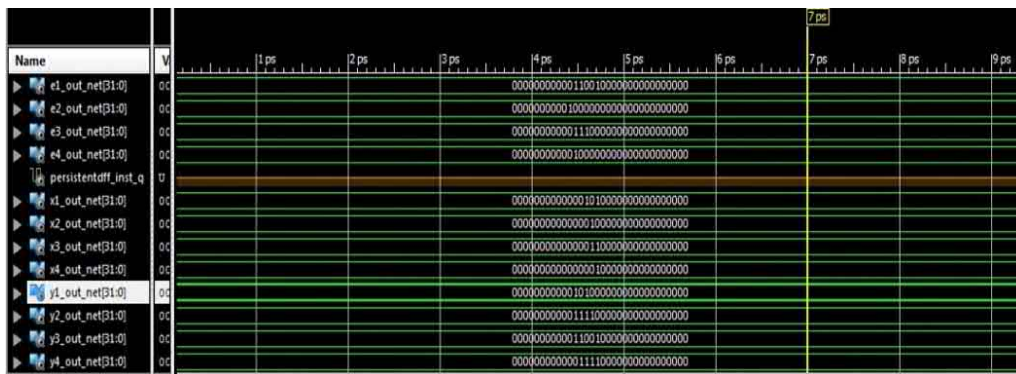


Figure 10: Simulation result of VHDL code for the proposed anti - synchronized hyperchaotic system.

	Used Sources	Available Sources	Percentage
Number of Slice Registers	2502	393,600	1
Number of Slice LUTs	4775	196,800	2
Number of Occupied Slices	1466	49,200	2
Number of Bonded IOBs	193	600	32
Number of BUFG/BUFGCTRLs	1	32	0.3

Table 1: Utilization of resources for virtex-xc6vsx315t3ff1156.

for the adaptive anti-synchronization scheme for a new hyperchaotic system with hidden attractors.

References

- [1] T. Fozin Fozin, P. Megavarna Ezhilarasu, Z. Njitacke Tabekoueng, G.D. Leutcho, J. Kengne, K. Thamilmaran, A. B. Mezatio and F. B. Pelab. On the dynamics of a simplified canonical Chua’s oscillator with smooth hyperbolic sine nonlinearity: Hyperchaos, multi-stability and multistability control. *Chaos Interdisciplinary Journal of Nonlinear Science* **29** (2019) 11315.
- [2] A. Arab, M.J. Rostami and B. Ghavami. An image encryption method based on chaos system and AES algorithm. *Journal of Super computing* **75** (2019) 6663–6682.
- [3] J. P. Singh, K. Lochan and B. K. Roy. Secure communication using new hyperchaotic system with hidden attractors. In: *Lecture Notes in Electrical Engineering* (Eds.: C. Shreesha and R. Gudi). Springer, Singapore, 2020, 67–69.
- [4] A. Al-khedhairi, A. Elsonbaty, A. H. Abdel kader, and A. A. Elsadany. Dynamic analysis and circuit implementation of new 4D Lorenz type hyperchaotic system. *Mathematical Problems* **2019** (2019) 6581586.
- [5] X. Zhang and C. Wang. Multi scroll hyperchaotic system with hidden attractors and its circuit implementation. *International Journal of Bifurcation and Chaos* **29** (2019) 1950117.
- [6] L. G. Dolvis, S. Vaidhyanathan, K. Jacques, A. Sambas and M. Mamat. A new 4 D hyperchaotic system with four scroll hidden attractor, its properties and bifurcation analysis. *International Journal of Bifurcation and Chaos* **29** (2019) 1950117.

- [7] S. Sajjadi, D. Baleanu, A. Jajarmi and H. M. Pirouz. A new adaptive synchronization and hyperchaos control of a biological snap oscillator. *Chaos, Solitons and Fractals* **138** (2020) 109919.
- [8] A. Jajarmi, M. Hajipour and D. Baleanu. New aspects of the adaptive synchronization and hyperchaos suppression of a financial model. *Chaos, Solitons and Fractals* **99** (2017) 285–296.
- [9] T. Khan and H. Chaudhary. Adaptive controllability of microscopic chaos generated in chemical reactor system using anti-synchronization strategy. *Number Algebra, Control and Optimization* **12** (2021) 611–620.
- [10] G. Kaddoum. Wireless Chaos-Based Communication Systems: A Comprehensive Survey. *IEEE Access* **4** (2016) 2621–2648.
- [11] R. Rameshbabu, and G. R. Suresh. Design of adaptive feedback control for new 3D chaotic system and its digital implementation on FPGA. *Indian Journal of Science and Technology* **13** (2020) 1977–1990.
- [12] R. Karthikeyan, A. Prasina, R. Babu, and S. Raghavendran. FPGA implementation of novel synchronization methodology for new chaotic system. *Indian Journal of Science and Technology* **8** (2015) 47901.
- [13] S. Helmy, M. Magdy, and M. Hamdy. Control in the loop for synchronization of nonlinear chaotic systems via adaptive intuitionistic neuro-fuzzy: A comparative study. *Complex and Intelligent Systems* **8** (2022) 3437–3450.
- [14] S. Kaouache, N. E. Hamri, A. S. Hecinliyan, E. Kandiran, B. Druni and A. C. Keles. Increased Order Generalized Combination Synchronization of Non-Identical Dimensional Fractional-Order Systems by Introducing Different Observable Variable Functions. *Nonlinear Dynamics and System Theory* **20** (2020) (3) 307–315.
- [15] M. K. Shukla, and B. B. Sharma. Backstepping based stabilization and synchronization of a class of fractional order chaotic systems. *Chaos, Solitons and Fractals* **102** (2022) 274–284.
- [16] L. M. Wang. Model-free adaptive sliding mode controller design for generalized projective synchronization of the fractional-order chaotic system via radial basis function neural networks. *Pramana Journal of Physics* **89** (2017) 38.
- [17] M. M. Zirkohi. Chaos synchronization using higher-order adaptive PID controller. *AEU International Journal of Electronics and Communication* **94** (2018) 157–167.
- [18] M. Labid, and N. Hamri. A Chaos Synchronization between Fractional-Order Lesser Date Moth Chaotic System and Integer-Order Chaotic System via Active Control. *Nonlinear Dynamics and System Theory* **22** (4) (2022) 407–413.



## Nonlinear Damped Oscillator with Varying Coefficients and Periodic External Forces

M. Alhaz Uddin<sup>1\*</sup>, Mahmuda Akhter Nishu<sup>1</sup> and M. Wali Ullah<sup>2</sup>

<sup>1</sup> *Department of Mathematics, Khulna University of Engineering & Technology,  
Khulna-9203, Bangladesh.*

<sup>2</sup> *Department of Computer Science & Engineering, Northern University of Business and  
Technology, Khulna, Bangladesh.*

Received: January 6, 2023; Revised: March 4, 2023

**Abstract:** A modified harmonic balance method (MHBM) has been exhibited for operating the damped Duffing oscillator with varying coefficients and periodic external forces. The mentioned technique is able to convert a set of nonlinear algebraic equations into a set of linear algebraic equations using only a nonlinear algebraic equation and it makes the simplest form of the system and requires less computational effort than the classic harmonic balance method (HBM). On the contrary, a set of nonlinear algebraic equations is required to solve by the numerical technique in classic HBM. As a result, it needs a heavy computational attempt. The obtained results have been compared with the numerical solutions attained by the fourth order Runge-Kutta method in the Figures and Table. It is mentioned that the obtained results display a strong similarity with the corresponding numerical results.

**Keywords:** *harmonic balance method; nonlinear oscillators; varying coefficients and periodic forcing term.*

**Mathematics Subject Classification (2010):** 34E05, 34E10, 34M10.

---

\* Corresponding author: <mailto:alhazuddin@math.kuet.ac.bd>

## 1 Introduction

Differential equations are a very important branch of science and engineering. They are linear or nonlinear differential equations. Actually, a greater portion of the real life physical and engineering problems are related to nonlinear differential equations. Solutions of differential equations provide a detailed information regarding the behavior of the systems. In this regard, nonlinear oscillators are very important in all areas of science and engineering. The appropriate solutions of these nonlinear oscillators are rarely obtained. Therefore, many researchers and scientists have focused their attention on developing numerical techniques as well as analytical methods. Numerical techniques are procedures for determining the true values for a set of discrete points. The true values are attained by the process of incremental steps. The proper initial guess values are required to perform the numerical techniques. Commonly, these techniques are comparatively simple but sometimes they need massive computational attempts and appropriate primary approximate values to achieve the desired solutions. Also, the numerical techniques are unable to provide overall feature of the nonlinear dynamical systems. It is also not possible to know the amplitude and phase by the numerical techniques. In contrast, analytical approximation methods have become more interesting to the scientists, physicists, engineers and applied mathematicians because of their analytical expression and suitability for parametric study. Many analytical approximation methods have been investigated for handling nonlinear dynamical systems, for example, the perturbation method [1- 10], homotopy analysis technique [11,12], homotopy perturbation technique [13-16], variational iteration technique [17,18], harmonic balance method (HBM) [19-28], modified multi-level residue harmonic balance method [25- 27], modified harmonic balance method (HBM) [28-33], etc. The perturbation methods [1- 10] are broadly used techniques for dealing with weakly nonlinear dynamical systems. Jones [8] investigated a technique to improve the scope of precision of the classical perturbation technique for large as well as small parameters. Cheung et al.[9] modified the Lindstedt–Poincare technique based on the idea of Jones [8]. Alam et al.[10] developed a modified Lindstedt–Poincare method to control oscillators with strong nonlinearities. The HBM and MHBM are also impressive methods for obtaining periodic solutions of nonlinear oscillators. In this method, the truncated Fourier series is selected as the trial solution of the nonlinear oscillators. According to the classical HBM, a set of nonlinear algebraic equations is handled by a numerical technique to find the values of the unknown coefficients. This method has been revised by some authors [18-28]. Rahman et al.[20] applied the HBM to study the Van der Pol equation. Wagner and Lentz [21] investigated the HBM for detecting the solutions to nonlinear oscillators. Wu [22] presented the HBM for the Yao-Cheng oscillator. Yeasmin et al. [24] presented an analytical technique to solve the free vibration problems with quadratic nonlinearity based on the HBM. Rahman and Lee [25] and Rahman et al. [26] exhibited a modified multi-level residue HBM. Hasan et al.[27] developed a multi-level residue harmonic balance solution for the nonlinear natural frequency of axially loaded beams with an internal hinge. Lee [28] presented an analytical solution for nonlinear multimode beam vibration using a modified harmonic balance approach and Vieta's substitution. Ullah et al. [29] exhibited MHBM to solve forced vibration problems with strong cubic and quadratic nonlinearities. Ullah et al.[30] extended this method to forced vibration problems with generalized nonlinearities. Further, Ullah et al.[31] exhibited the MHBM for the forced Van der Pol vibration equation. Recently, Ullah et al. [32] have exhibited the MHBM for free vibration analysis of non-

linear axially loaded beams. Ullah et al.[33] have handled a modified forced Van der Pol vibration equation using a modified harmonic balance method. Kandil et al.[35] have exhibited a HBM to obtain the steady-state solutions of the nonlinear problems. Alam et al. [36] have solved some strongly nonlinear oscillators with a combination of the modified Lindstedt-Poincare and the homotopy perturbation methods. Uddin and Sattar [34] developed an analytical procedure to solve the damped Duffing equation with varying coefficients without periodic external force combining KBM and homotopy perturbation methods. It is observed that MHBM has been remaining untouched for the controlling forced Duffing equation with varying coefficients and damping with strong nonlinearity. To fulfill this gap, a MHBM has been proposed to control the damped Duffing oscillator with varying coefficients and periodic external forces. The proposed technique reduces the heavy computational effort that cannot be avoided in the classical HBM.

**2 Method**

We guess a damped nonlinear oscillator [29-33, 34] with varying coefficients and periodic external force

$$\ddot{x} + 2k \dot{x} + e^{-\tau} x + \epsilon f(x) = F \cos(\omega t), \tag{1}$$

where the dots above denote differentiation with respect to time  $t$ ,  $2k$  is the coefficient of viscous damping,  $f(x)$  is a certain nonlinear function,  $\epsilon$  is a positive parameter which is not necessarily small,  $\tau = \epsilon t$  is the slow varying time,  $F$  and  $\omega$  represent the amplitude and frequency of excitation, respectively. All of the parameters are positive. According to the proposed method, the approximate solution of Eq.(1) is assumed [29-33]to be of the following form:

$$x = c_1 \cos(\omega t) + d_1 \sin(\omega t) + c_3 \cos(3\omega t) + d_3 \sin(3\omega t) + \dots, \tag{2}$$

where  $c_1, d_1, c_3, d_3...$  are unknown coefficients in the Fourier series. Now, differentiating Eq.(2) twice with respect to  $t$  and then putting into Eq.(1) and expanding  $f(x)$  as a truncated Fourier series expansion and then comparing similar harmonics, we accomplish the following set of algebraic equations

$$c_1(-\omega^2 + e^{-\tau}) + 2d_1k\omega + \epsilon A_1(c_1, d_1, c_3, d_3, \dots) = F, \tag{3a}$$

$$d_1(-\omega^2 + e^{-\tau}) - 2c_1k\omega + \epsilon B_1(c_1, d_1, c_3, d_3, \dots) = 0, \tag{3b}$$

$$c_3(-9\omega^2 + e^{-\tau}) + 6d_3k\omega + \epsilon A_3(c_1, d_1, c_3, d_3, \dots) = 0, \tag{3c}$$

$$d_3(-9\omega^2 + e^{-\tau}) - 6c_3k\omega + \epsilon B_3(c_1, d_1, c_3, d_3, \dots) = 0. \tag{3d}$$

Deducting  $\omega^2$  from the Eqs.(3b)-(3d), utilizing Eq.(3a), and removing the terms whose responses are small, we get Eqs.(3a)-(3d) in the form

$$\omega^2 = e^{-\tau} + 2d_1k\omega/c_1 + \epsilon A_1(c_1, d_1, c_3, d_3, \dots) - F/c_1, \tag{4a}$$

$$- 2c_1k\omega - 2d_1^2k\omega/c_1 - \epsilon A_1(c_1, d_1, c_3, d_3, \dots) + \epsilon B_1(c_1, d_1, c_3, d_3, \dots) + d_1F/c_1 = 0, \tag{4b}$$

$$- 8c_3e^{-\tau} - 18c_3d_1k\omega/c_1 + 6d_3k\omega - \epsilon A_1(c_1, d_1, c_3, d_3, \dots) + \epsilon A_3(c_1, d_1, c_3, d_3, \dots) - 9c_3F/c_1 = 0, \tag{4c}$$

$$- 8d_3e^{-\tau} - 18d_1d_3k\omega/c_1 + 6c_3k\omega - \epsilon A_1(c_1, d_1, c_3, d_3, \dots) + \epsilon B_3(c_1, d_1, c_3, d_3, \dots) + 9d_3F/c_1 = 0. \tag{4d}$$

Utilizing Eq.(4b), terminating  $\omega$  from the Eqs.(4c)-(4d) and taking into account only the linear terms of  $c_3$ ,  $d_3$ , a set of linear algebraic equations of  $c_3$ ,  $d_3$  is achieved. After simplifying,  $c_3$ ,  $d_3$  are acquired in terms of  $c_1, d_1$ . Finally, inserting  $c_3$ ,  $d_3$  in Eq.(4b), and expanding  $d_1$  into a power series of  $\lambda(k, \omega, F)$ , we acquire

$$d_1 = l_0 + l_1\lambda + l_2\lambda^2 + l_3\lambda^3 + \dots, \quad (5)$$

where  $l_0, l_1, l_2, \dots$  are the functions of  $c_1$  and  $\lambda$  is a small parameter. After inserting  $c_3$ ,  $d_3$  and  $d_1$  in Eq.(4a) and solving,  $c_1$  is obtained. Systematically,  $d_1$ ,  $c_3$  and  $d_3$  are obtained.

### 3 Example

Consider a nonlinear damped oscillator having varying coefficients with periodic external force [29-33, 34] of the following form:

$$\ddot{x} + 2k \dot{x} + e^{-\tau} x + \epsilon x^3 = F \cos(\omega t). \quad (6)$$

The solution of Eq.(6) is supposed as [29-33]

$$x(t) = c_1 \cos(\omega t) + d_1 \sin(\omega t) + c_3 \cos(3\omega t) + d_3 \sin(3\omega t). \quad (7)$$

Eq.(7) is treated as the truncated Fourier series. The unknown constants  $c_1$ ,  $d_1$ ,  $c_3$  and  $d_3$  are to be found to get the desired results. Putting Eq.(7) in Eq.(6) and then comparing the coefficients of similar harmonics and removing the terms whose effects are negligible, we carry out

$$c_1 e^{-\tau} - c_1 \omega^2 + 3\epsilon c_1^3/4 + 3\epsilon c_1^2 c_3/4 + 3\epsilon c_1 c_3^2/2 + 2k\omega d_1 + 3\epsilon c_1 d_1^2/4 - 3\epsilon c_3 d_1^2/4 + 3\epsilon c_1 d_1 d_3/2 + 3\epsilon c_1 d_3^2/2 = F, \quad (8a)$$

$$-2k\omega c_1 + d_1 e^{-\tau} - d_1 \omega^2 + 3\epsilon c_1^2 d_1/4 - 3\epsilon c_1 c_3 d_1/2 + 3\epsilon c_3^2 d_1/2 + 3\epsilon d_1^3/4 + 3\epsilon c_1^2 d_3/4 - 3\epsilon d_1^2 d_3/4 + 3\epsilon d_1 d_3^2/2 = 0, \quad (8b)$$

$$\epsilon c_1^3/4 + c_3 e^{-\tau} - 9c_3 \omega^2 + 3\epsilon c_1^2 c_3/2 + 3\epsilon c_3^3/4 - 3\epsilon c_1 d_1^2/4 + 3\epsilon c_3 d_1^2/2 + 6k\omega d_3 + 3\epsilon c_3 d_3^2/4 = 0, \quad (8c)$$

$$-6k\omega c_3 + 3\epsilon c_1^2 d_1/4 - \epsilon d_1^3/4 + d_3 e^{-\tau} - 9d_3 \omega^2 + 3\epsilon c_1^2 d_3/2 + 3\epsilon c_3^2 d_3/4 + 3\epsilon d_1^2 d_3/2 + 3\epsilon d_3^3/4 = 0. \quad (8d)$$

Deducting  $\omega^2$  from the Eqs.(8b)-(8d), utilizing Eq.(8a), and removing the terms whose responses are small, we receive

$$-8k\omega c_1^2 + 4Fd_1 - 9\epsilon c_1^2 c_3 d_1 - 8k\omega d_1^2 + 3\epsilon c_3 d_1^3 + 3\epsilon c_1^3 d_3 - 9\epsilon c_1 d_1^2 d_3 = 0, \quad (9a)$$

$$\epsilon c_1^4 + 36Fc_3 - 32c_1 c_3 e^{-\tau} - 21\epsilon c_1^3 c_3 - 72k\omega c_3 d_1 - 3\epsilon c_1^2 d_1^2 - 21\epsilon c_1 c_3 d_1^2 + 24k\omega c_1 d_3 = 0, \quad (9b)$$

$$-24k\omega c_1 c_3 + 3\epsilon c_1^3 d_1 - \epsilon c_1 d_1^3 + 36Fd_3 - 32c_1 d_3 e^{-\tau} - 21\epsilon c_1^3 d_3 - 72k\omega d_1 d_3 - 21\epsilon c_1 d_1^2 d_3 = 0. \quad (9c)$$

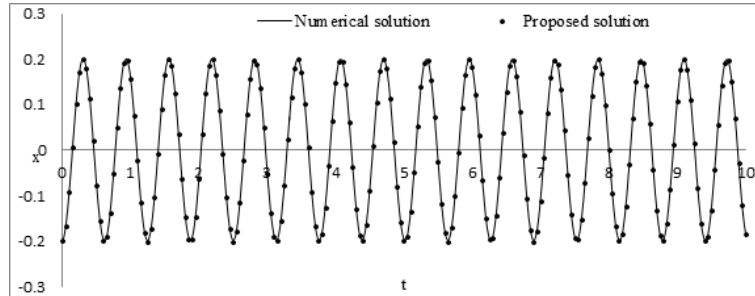


**Figure 1:** Comparison between the outcomes attained by the mentioned technique and the numerical technique of Eq.(6) for  $\omega = 10, \epsilon = 0.5, k = 0.5, F = 20$ .

Utilizing Eq.(9a), terminating  $\omega$  from the Eqs.(9b) and (9c) and taking into account only the linear expressions of  $c_3, d_3$  and omitting the expressions whose effects are insignificant, we obtain

$$8\epsilon kc_1^6 + 288kFc_1^2c_3 - 256kc_1^5c_3e^{-\tau} - 168\epsilon kC_1^3c_3 - 16\epsilon kc_1^4d_1^2 - 256kc_1c_3d_1^2e^{-\tau} - 16\epsilon kc_1^4d_1^2 - 256kc_1c_3d_1^2e^{-\tau} - 336\epsilon kc_1^3c_3d_1^2 - 24\epsilon kc_1^2d_4 - 168\epsilon kc_1c_3d_1^4 = 0, \tag{10a}$$

$$24\epsilon kc_1^5d_1 + 16\epsilon kc_1^3d_1^3 - 8\epsilon kc_1d_1^5 + 288kFc_1^2d_3 - 256kc_1^3d_3e^{-\tau} - 168\epsilon kc_1^5d_3 - 256kc_1d_1^2d_3e^{-\tau} - 336\epsilon kc_1^3d_1^2d_3 - 168\epsilon kc_1d_1^4d_3 = 0. \tag{10b}$$

By simplifying Eqs.(10a) and (10b),  $c_3$  and  $d_3$  are obtained as follows:

$$c_3 = \epsilon c_1(c_1^4 - 2c_1^2d_1^2 - 3d_1^4)e^{-\tau} / (-36Fc_1e^\tau + 32c_1^2 + 21\epsilon c_1^4e^\tau + 32d_1^2 + 42\epsilon c_1^2d_1^2e^\tau + 21\epsilon d_1^4e^\tau), \tag{11a}$$

$$d_3 = \epsilon d_1(-c_1^4 - 2c_1^2d_1^2 + d_1^4)e^\tau / (36Fc_1e^\tau - 32c_1^2 - 21\epsilon c_1^4e^\tau - 32d_1^2 - 42\epsilon c_1^2d_1^2e^\tau - 21\epsilon d_1^4e^\tau). \tag{11b}$$

Inserting  $c_3$  and  $d_3$  in Eq.(9a) and expanding  $d_1$  into a power series of  $\lambda$ , we acquire

$$d_1 = l_0 + l_1\lambda + l_2\lambda^2 + l_3\lambda^3 + \dots, \tag{12}$$

where  $\lambda = 2k\omega/E, l_0 = 2c_1^2k\omega/F, l_1 = 16c_1^4k^2\omega^2/F^2, l_2 = 16c_1^6k^3\omega^3/F^3, l_3 = 80c_1^8k^4\omega^4/F^4$ . Finally, after inserting  $c_3, d_3$  and  $d_1$  into Eq.(8a) and solving,  $c_1$  is obtained. Systematically,  $d_1, c_3$  and  $d_3$  are obtained.

#### 4 Results and Discussion

The proposed method is easy and straightforward. We have successfully applied this technique to solve the strongly nonlinear forced dynamical damped problems with varying coefficients and cubic nonlinearity. The solutions have been assimilated with the corresponding numerical outcomes to rationalize the precision and the correctness of the mentioned scheme. Comparisons between the solutions acquired by the mentioned scheme and the numerical technique have been displayed in Figs. 1–5 for nonlinear forced

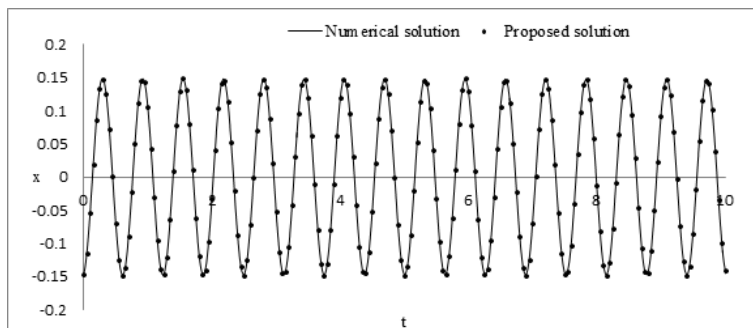


**Figure 2:** Comparison between the outcomes attained by the mentioned technique and the numerical technique of Eq.(6) for  $\omega = 10, \epsilon = 1.0, k = 1.0, F = 15$ .

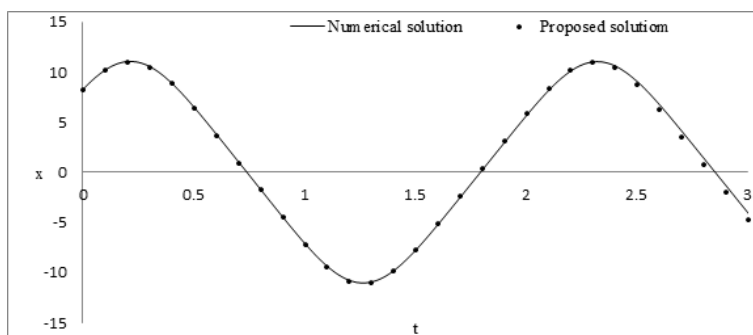


**Figure 3:** Comparison between the outcomes attained by the mentioned technique and the numerical technique of Eq.(6) for  $\omega = 3, \epsilon = 0.1, k = 0.1, F = 10$ .

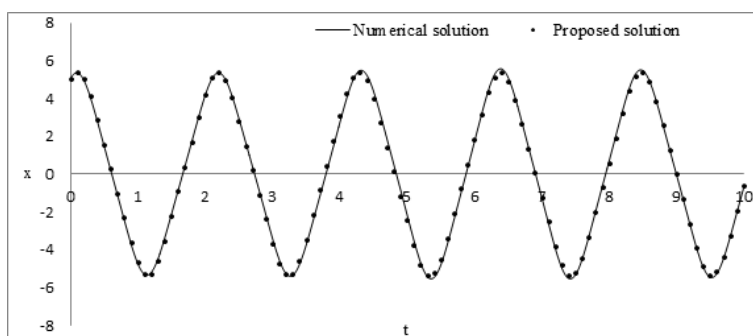


**Figure 4:** Comparison between the outcomes attained by the mentioned technique and the numerical technique of Eq.(6) for  $\omega = 3, \epsilon = 0.5, k = 0.2, F = 10$ .

vibration problems with varying coefficients for various damping. Moreover, the phase planes have been traced for different values in Figs. 6 and 7.

Geometrical representation is very important to visualize the behavior of the physical

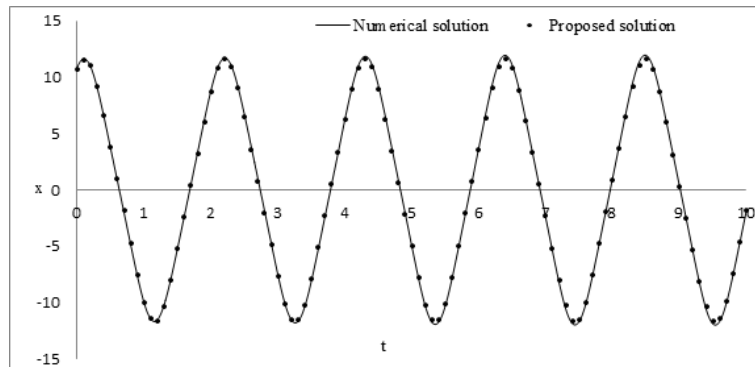


**Figure 5:** Comparison between the outcomes attained by the mentioned technique and the numerical technique of Eq.(6) for  $\omega = 3, \epsilon = 0.1, k = 0.1, F = 20$ .

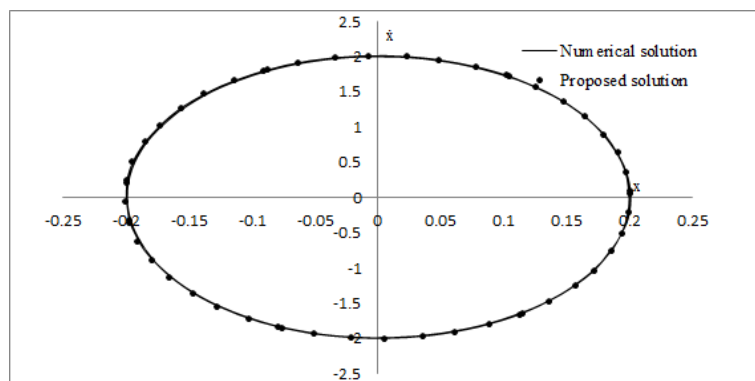


**Figure 6:** Comparison between the outcomes attained by the mentioned technique and the numerical technique of Eq.(6) in the phase plane when  $\omega = 10, \epsilon = 0.5, k = 0.5, F = 20$ .

systems since it provides an overall view of the behavior of the nonlinear dynamical systems. The approximate methods have become more interesting to the scientists, physicists, engineers and applied mathematicians because of their analytical expression and suitability for parametric study. From the figures presented, it is noticed that the obtained results have agreed nicely with the numerical results determined by the fourth order Runge-Kutta method. In Table 1, a comparison between the results obtained by the proposed method and the numerical method is given. From the figures and table, it is observed that the acquired outcomes comply almost accurately with the numerical outcomes acquired by the fourth order Runge-Kutta technique.

### 5 Conclusion

A MHBM is exhibited for managing nonlinear forced dynamical equations with varying coefficients and damping. The convenience of the mentioned scheme is that only one nonlinear equation is requisite to handle instead of a set of nonlinear algebraic equations.

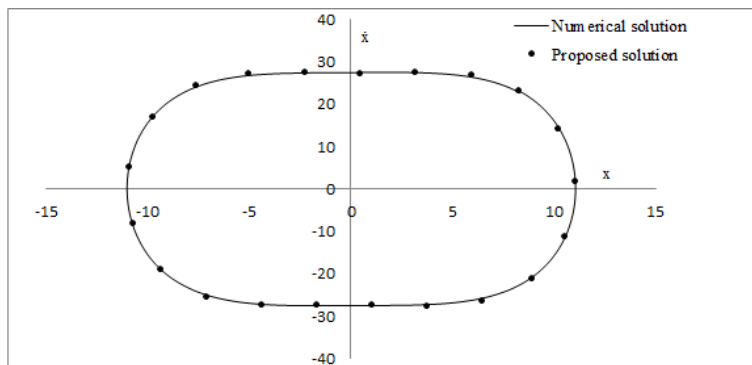


**Figure 7:** Comparison between the outcomes attained by the mentioned technique and the numerical technique of Eq.(6) in the phase plane when  $\omega = 3, \epsilon = 0.1, k = 0.1, F = 10$ .

**Table 1:** Comparison between the outcomes achieved by the mentioned and the numerical techniques.

Time, $t$	$E = 15, \omega = 10,$ $\epsilon = 0.1, k = 0.1$		$E = 20, \omega = 10,$ $\epsilon = 0.5, k = 0.5$	
	Analytical Solution, $x_{app}$	Numerical Solution, $x_{nu}$	Analytical Solution, $x_{app}$	Numerical Solution, $x_{nu}$
0	-0.151	-0.151	-0.2	-0.2
0.5	-0.046	-0.046	-0.076	-0.076
1	0.125	0.125	0.157	0.157
1.5	0.117	0.117	0.165	0.165
2	-0.059	-0.059	-0.063	-0.061
2.5	-0.151	-0.15	-0.201	-0.89
3	-0.026	-0.026	-0.051	-0.051
3.5	0.136	0.134	0.172	0.17
4	0.103	0.103	0.148	0.148
4.5	-0.077	-0.077	-0.088	-0.085
5	-0.147	-0.146	-0.88	-0.86

It requires less computational effort than the harmonic balance method. The outcomes acquired by the mentioned technique show a nice similarity with the numerical outcomes in the figures and table. The mentioned scheme may play an important role for tackling the forced dynamical systems with varying coefficients and damping.

### Acknowledgment

The authors are grateful to the unknown reviewers for their comments in preparing this research document. The authors are also grateful to Dr. Md. Abu Hanif Shaikh, BISI Research group, Vrije University Brussel, Belgium in preparing this research document in LATEX.

## References

- [1] J. A. Wickert. Non-linear vibration of a traveling tensioned beam. *International Journal of Non-Linear Mechanics* **27** (1992) 503–517.
- [2] A. H. Nayfeh. *Perturbation Method*. John Wiley and Sons, New York, 1973.
- [3] A. H. Nayfeh. *Introduction to Perturbation Techniques*. Wiley, New York, 1981.
- [4] A. H. Nayfeh and D.T. Mook. *Nonlinear Oscillations*. John Wiley and Sons, New York, 1979.
- [5] N. N. Krylov and N. N. Bogoliubov. *Introduction to Nonlinear Mechanics*. Princeton University Press, New Jersey, 1947.
- [6] M. S. Alam. A unified Krylov-Bogoliubov-Mitropolskii method for solving n-th order nonlinear systems. *Journal of the Franklin Institute* **399** (2) (2002) 239–248.
- [7] M. S. Alam, M. A. K. Azad and M. A. Hoque. A general Struble’s technique for solving an  $n - th$  order weakly nonlinear differential system with damping. *International Journal of Nonlinear Mechanics* **41** (2006) 905–918.
- [8] S. E. Jones. Remarks on the perturbation process for certain conservative systems. *International Journal of Non-Linear Mechanics* **13** (1978) 125–128.
- [9] Y. K. Cheung, S.H. Chen and S.L. Lau. A modified Lindstedt-Poincare method for certain strongly nonlinear oscillators *International Journal of Non-Linear Mechanics* **26** (1991) 367–378.
- [10] M. S. Alam, I. A. Yeasmin and M. S. Ahamed. Generalization of the modified Lindstedt-Poincare method for solving some strongly nonlinear oscillators. *Ain Shams Engineering Journal* **10**(1) (2019) 195–201.
- [11] M. Fooladi, S.R. Abaspour, A. Kimiaefar and M. Rahimpour. On the analytical solution of Kirchhoff simplified Model for beam by using of homotopy analysis method. *World Applied Sciences Journal* **6** (2009) 297–302.
- [12] S.J. Liao. *The proposed homotopy analysis technique for the solution of nonlinear problems*. Ph.D. Thesis, Shanghai Jiao Tong University, 1992.
- [13] Y.Wu and J.H. He. Homotopy perturbation method for nonlinear oscillators with coordinate dependent mass. *Results in Physics* **10** (2018) 270–271.
- [14] M. A. Uddin, M. A. Alom and M. W. Ullah. An analytical approximate technique for solving a certain type of fourth order strongly nonlinear oscillatory differential system with small damping. *Far East Journal of Mathematical Sciences* **67** (1) (2012) 59–72.
- [15] M.A. Uddin, M. A., Sattar and M. S. Alam. An approximate technique for solving strongly nonlinear differential systems with damping effects. *Indian Journal of Mathematics* **53** (1) (2011) 83–98.
- [16] C. U. Ghosh and M. A. Uddin. Analytical technique for damped nonlinear oscillators having generalized rational power restoring force. *Far East Journal of Mathematical Sciences* **130** (1) (2021) 25–41.
- [17] M. A. Wazwaz. The variational iteration method: A reliable analytic tool for solving linear and nonlinear wave equations. *Computers and Mathematics with Applications* **54** (2007) 926–932.
- [18] J. H. He. Some asymptotic methods for strongly nonlinear equations. *International Journal of Modern Physics B* **20** (2006) 1141–1199.
- [19] R. E. Mickens. A generalization of the method of harmonic balance. *Journal of Sound and Vibration* **111** (1986) 515–518.

- [20] M. S. Rahman, M. E. Haque and S.S. Shanta. Harmonic balance solution of nonlinear differential equation (non-conservative). *Journal of Advances in Vibration Engineering* **9** (4) (2010) 345–356.
- [21] U.V. Wagner and L. Lentz. On the detection of artifacts in harmonic balance solutions of nonlinear oscillators. *Applied Mathematical Modeling* **65** (2019) 408–414.
- [22] Y. Wu. The harmonic balance method for Yao-Cheng oscillator, *Journal of Low Frequency Noise Vibration and Active Control* **38** (2019) 1716–1718.
- [23] M. S. Rahman and Y.Y. Lee. New modified multi-level residue harmonic balance method for solving nonlinearly vibrating double-beam problem. *Journal of Sound and Vibration* **6** (2017) 295–327.
- [24] I. A. Yeasmin, N. Sharif, M. S. Rahman and M. S. Alam. Analytical technique for solving the quadratic nonlinear oscillator. *Results in Physics* **18** (2020) Article No. 103303.
- [25] M. S. Rahman, and Y. Y. Lee. New modified multi-level residue harmonic balance method for solving nonlinearly vibrating double-beam problem. *Journal of Sound and Vibration* **06** (2017) 295–327.
- [26] M. S. Rahman, A. S. M. Z. Hasan and I. A. Yeasmin. Modified multi-level residue harmonic balance method for solving nonlinear vibration problem of beam resting on nonlinear elastic foundation. *Journal of Applied and Computational Mechanics* **5** (4) (2019) 627–638.
- [27] A. S. M. Z. Hasan, M. S. Rahman, Y.Y. Lee and A.Y.T. Leung. Multi-level residue harmonic balance solution for the nonlinear natural frequency of axially loaded beams with an internal hinge. *Mechanics of Advanced Materials and Structures* **24(13)** (2017) 1074–1085.
- [28] Y.Y. Lee. Analytic solution for nonlinear multimode beam vibration using a modified harmonic balance approach and Vieta’s substitution. *Shock and Vibration* (2016) Article ID: 3462643.
- [29] M.W. Ullah, M. S. Rahman and M. A. Uddin. A modified harmonic balance method for solving forced vibration problems with strong nonlinearity. *Journal of Low Frequency Noise, Vibration and Active Control* **40** (2) (2021) 1096–1104.
- [30] M.W. Ullah, M. A. Uddin and M. S. Rahman. A modified harmonic balance method for solving strongly generalized nonlinear damped forced vibration systems. *Nonlinear Dynamics and Systems Theory* **21** (5) (2021) 544–552.
- [31] M.W. Ullah, M. A. Uddin and M. S. Rahman. An analytical technique for handling forced Van der Pol vibration equation. *J. of Bangladesh Academic of Sciences* **45** (2) (2021) 231–240.
- [32] M.W. Ullah, M. S. Rahman and M. A. Uddin. Free vibration analysis of nonlinear axially loaded beams using modified harmonic balance method. *Partial Differential Equations in Applied Mathematics* **6** (December 2022), 100414.
- [33] M.W. Ullah, M. A. Uddin and M. S. Rahman. Analytical solution of modified forced Van der Pol vibration equation using modified harmonic balance method. In: *Khulna University Studies Special Issue ICSTEM4IR*, Khulna University, Khulna, (2022) 892–903. <https://doi.org/10.53808/KUS.2022>.
- [34] M. A. Uddin and M. A. Sattar. An approximate technique to Duffing’s equation with small damping and slowly varying coefficients. *J. of Mechanics of Continua and Mathematical Sciences* **5** (2) (2011) 627–642.
- [35] A. Kandil, Y. S. Hamed and J. Awrejcewicz. Harmonic balance method to analyze the steady-state response of a controlled mass-damper-spring model. *Symmetry* **14** (2022) 1247. <https://doi.org/10.3390/sym1406124>.
- [36] M. S. Alam, N. Sharif and M. H. U. Molla. Combination of modified Lindstedt-Poincare and homotopy perturbation methods. *Journal of Low Frequency Noise, Vibration and Active Control* (2022) 1–12. <https://doi.org/10.1177/14613484221148049>.